Lehigh University
Lehigh Preserve

Theses and Dissertations

1-1-1984

The Petrological Evolution of Garnet-Rich Meta-Igneous Bodies in the Southeastern Adirondack Mountains, New York.

John Herbert Weakliem

Follow this and additional works at: http://preserve.lehigh.edu/etd

 Part of the Geology Commons

Recommended Citation
Weakliem, John Herbert, "The Petrological Evolution of Garnet-Rich Meta-Igneous Bodies in the Southeastern Adirondack Mountains, New York." (1984). *Theses and Dissertations*. Paper 2208.

This Thesis is brought to you for free and open access by Lehigh Preserve. It has been accepted for inclusion in Theses and Dissertations by an authorized administrator of Lehigh Preserve. For more information, please contact preserve@lehigh.edu.

The Petrological Evolution

of

Garnet-Rich Meta-Igneous Bodies

in the

Southeastern Adirondack Mountains,

New York

by

John Herbert Weakliem

A Thesis

Presented to the Graduate Committee

of Lehigh University

in Candidacy for the Degree of

Master of Science

in

Geology

Lehigh University

1984

ProQuest Number: EP76481

All rights reserved

INFORMATION TO ALL USERS
The quality of this reproduction is dependent upon the quality of the copy submitted.

In the unlikely event that the author did not send a complete manuscript
and there are missing pages, these will be noted. Also, if material had to be removed,
a note will indicate the deletion.

ProQuest EP76481

Published by ProQuest LLC (2015). Copyright of the Dissertation is held by the Author.

All rights reserved.
This work is protected against unauthorized copying under Title 17, United States Code
Microform Edition © ProQuest LLC.

ProQuest LLC.
789 East Eisenhower Parkway
P.O. Box 1346
Ann Arbor, MI 48106 - 1346

This thesis is accepted and approved in partial fulfillment of the requirements for the degree of Master of Science.

May 17/1984
(date)

Professor in Charge

Chairman of Department

Acknowledgements

The writer would like to thank his committee chairman, Dr. Charles B. Sclar, for introducing the writer to the problem, and for his lengthly review and comments upon the manuscript. The other members of the committee, Dr. Paul B. Myers of Lehigh University and Dr. Philip R. Whitney of the New York State Geological Survey, reviewed and commented upon it. Dr. Terry L. Pavlis of Lehigh University offered advice and suggestions. The Barton Mines Corporation granted permission to carry out the studies upon their property, and assisted in logistics. Mr. Gordon Hersey, and indeed, all of the employees of the Barton Mines Corporation were of great assistance to the writer. Dr. F. Bentel and Mr. F. Gramlich both permitted the writer to study outcrops upon their property. Dr. Roger H. Hewins of Rutgers University instructed the writer on data acquisition on the electron microprobe. Finally, Mr. James Kerner of the Department of Metallurgy and Materials Science, Lehigh University taught the writer the intricacies of operating the microprobe. I would also like to thank my parents, Mr. and Mrs. Herbert Weakliem, who made this possible.

Financial aid in support of this project was provided by grants from the Barton Mines Corporation, the Sun Oil Corporation, the Department of Geological Sciences, Lehigh University, and a grant-in-aid of research by Sigma Xi, the Scientific Research Society.

TABLE OF CONTENTS

Table of Contents (continued)

Table of Contents (Continued)

List of Tables

List of Figures

List of Figures (Continued)

List of Figures (Continued)

ABSTRACT

This study was undertaken in order to compare and contrast some of the smaller garnetiferous meta-igneous bodies with the previously studied Gore Mountain metagabbro and Ruby Mountain meta-anorthosite. In this study, a metagabbro layer below the Ruby Mountain anorthosite and a metagabbro just north of Speculator NY were examined using petrographic techniques, the electron microprobe, and X-ray fluoresence analysis. In addition, a small body of garnet amphibolite (the Old Hooper mine) and a small streaked garnetiferous anorthositic gneiss (the North River Garnet Company mine) were examined in less detail.

The Ruby Mountain metagabbro is lower in Ca, Mg, and Al, and higher in Fe and Ti than the Ruby Mountain anorthosite, but is otherwise similar. These trends suggest that the metagabbro is related to the overlying anorthosite. PH_2O was variable in the metagabbro, as it was in the anorthosite. The fO_2 was lower in the metagabbro than in the anorthosite, inasmuch as only olive green (but Ti-rich) hornblende is present in the metagabbro.

Hornblendes in the metagabbro which are closely related to clinopyroxenes contain more Fe than hornblende grains which are associated with garnet porphyroblasts. This is probably due to progressive metamorphism of the metagabbro, with the hornblendes closely associated with the clinopyroxenes representing the initial formation of hornblende from clinopyroxene which has been preserved

due to locally low PH_2O, and the more magnesian hornblendes in other parts of the body representing hornblende of higher grade. Garnets show chemical variations which are identical with those observed in the anorthosite by Novillo (1981). The smaller garnets show very weak zoning trends, with Fe and Mn decreasing and Mg increasing from core to rim of the grain. Larger grains however, do not exhibit any zoning and are richer in Mg. These trends in garnets within the anorthosite were ascribed by Novillo (1981) to the fractionation-depletion model of Hollister (1966). The garnet evidently formed during prograde metamorphism by the reaction:

plagioclase + hornblende + clinopyroxene + orthopyroxene

$\rightarrow$

garnet + quartz

Later, a garnet-consuming reaction occurred which produced biotite and plagioclase from garnet and hornblende.

The Speculator metagabbro is an olivine-normative metagabbro which contains relict igneous layering, and pegmatitic bodies which may be younger intrusives. In most of the metagabbro, garnet occurs as small porphyroblasts, or as xenoblastic grains associated with ferromagnesian minerals. Large porphyroblasts occur in a zone within the interior of the metagabbro. These occur scatttered throughout a granoblastic matrix of plagioclase and clinopyroxene, and do not possess monomineralic rims. Hornblende is present in this zone only in the neighborhood of the porphyroblasts. Fe-Ti oxides are not present.

Microprobe analyses reveal that the clinopyroxene, hornblende, and garnet are all richer in Mg in the large-garnet zone than elsewhere in the metagabbro. Further, the garnet porphyroblasts in the large-garnet zone are unzoned, whereas garnets in the remainder of the metagabbro show weak zoning, with Mg decreasing, and Fe increasing from core to rim. The reaction which formed the garnet was:

plagioclase + hornblende + clinopyroxene + orthopyroxene

$\rightarrow$

garnet + sodic plagioclase

Experimental studies of hornblende reactions by other workers show that the breakdown of Fe-rich hornblendes commonly produces garnet, whereas Mg-rich hornblendes produce forsterite or spinel. As noted, the hornblendes in the large-garnet zone are more Mg-rich relative to those in the remainder of the metagabbro. This might lead to fewer nucleation sites for garnet in the large-garnet zone than elsewhere. These garnets might have grown to a larger size, because of a lack of competition with other garnet crystals for reactants. The zoning trends within the garnets in the normal metagabbro indicate that these garnets probably grew during a period of slowly falling temperature. A garnet consuming reaction occurred later which produced hornblende and plagioclase from garnet and hornblende or clinopyroxene.

The smaller bodies studied, namely, the Old Hooper mine and the North River Garnet Company mine are, respectively, a smaller

equivalent of the Gore Mountain metagabbro, and a drier equivalent of the Ruby Mountain anorthosite.

Variations in garnet chemistry between the various metagabbro bodies are evidently due to differences in bulk chemistry of the igneous progenitor. P_{H_2O} evidently has an important effect not only on the size of the garnets produced, but on the nature of the garnet-forming reaction which occurs.

INTRODUCTION

The Adirondack Highlands are noted for the occurrence of garnetiferous meta-igneous bodies which are variable both in size and in the percentage and size of the garnet crystals contained within them. These bodies are typically developed from either gabbroic anorthosite or gabbro. The largest known bodies are the Gore Mountain and Ruby Mountain garnet deposits of the Barton Mines Corporation, which are rich enough in garnet to warrant mining them for the garnet, which is used as an industrial abrasive. In the same area, there are smaller garnetiferous bodies, some of which have been mined intermittently.

Much of the work on the development of garnet in the Adirondack Highlands has been focused either on the largest bodies or on more general aspects of garnet formation in the Adirondack dome as a whole. The smaller garnetiferous bodies in the Southeastern Adirondacks have not been studied by modern methods. Thus, it is not known how they relate to the formation of garnet in either of the two largest bodies cited above or to the history of the Adirondack dome as a whole.

FIELD AND ANALYTICAL METHODS

The area studied is located in the southeastern part of the Adirondack Mountains, and is part of the Thirteenth Lake and Indian Lake Quadrangles, which cover parts of Warren and Hamilton Counties, New York (Figure 1). Field work was carried out at two small garnetiferous bodies in the area, namely, a metagabbro layer below the Ruby Mountain anorthosite and the Speculator metagabbro. In addition, the abandoned North River Garnet Company open-pit mine on Garnet Hill and the Old Hooper mine pit were examined (Figure 2). Samples were collected for detailed petrological and geochemical study, and, where possible, structural observations were made.

Thin sections of the samples were studied using standard petrographic methods. The resultant textural and mineralogical data provided the basis for determining what reactions occurred, and their relative timing. These thin sections were also used in order to determine which specimens deserved further geochemical study.

Electron microprobe analysis of major phases was carried out on polished thin sections using a JEOL 733 Superprobe at the Department of Metallurgy and Materials Science, Lehigh University. Operating conditions were: accelerating voltage 15 Kv, sample current 10 nanoamperes, takeoff angle 40°. The data was corrected for matrix and interelement effects by the method of Bence and Albee (1971). The standards used are listed in Table 1. Fe^{3+}/Fe^{2+} ratios in

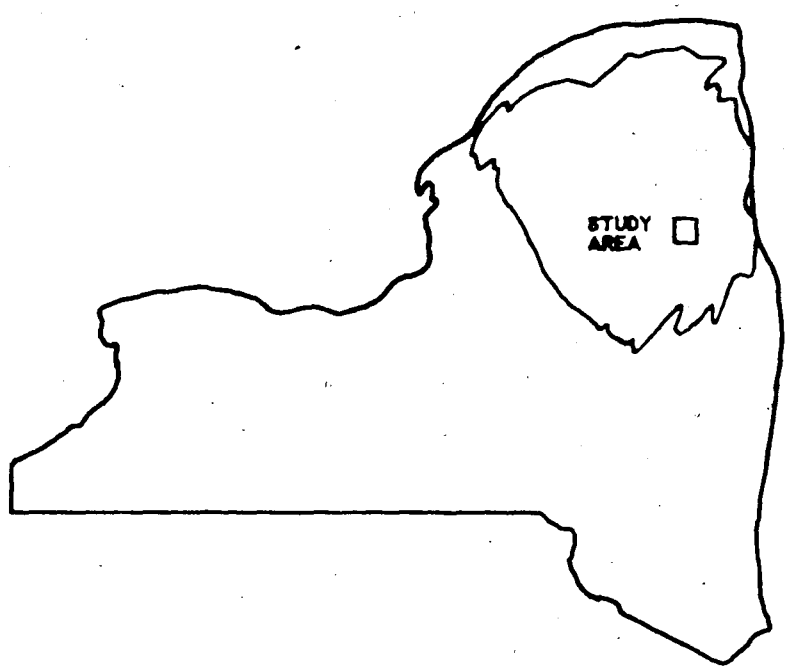

Figure 1. Index map showing location of the Thirteenth Lake and Indian Lake quadrangles in New York State.

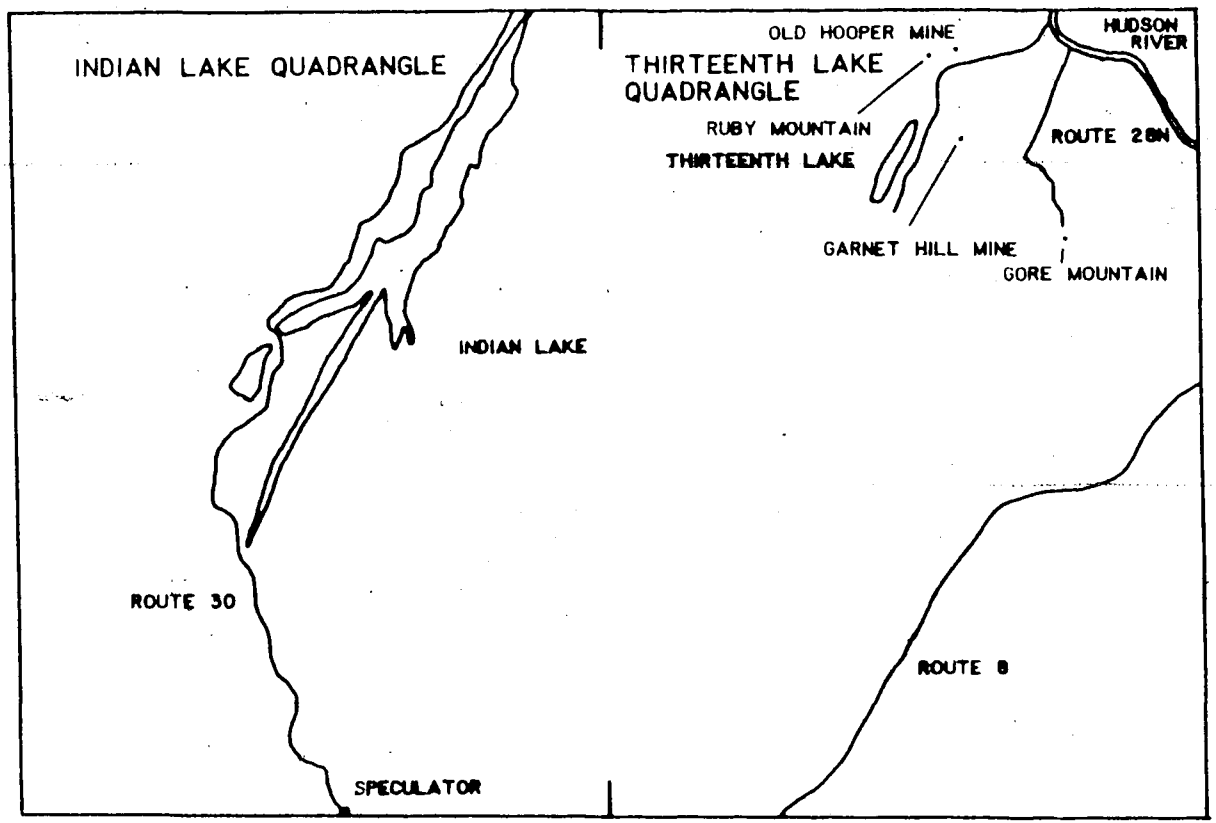

Figure 2. Index map showing the locations of the garnet-bearing meta-igneous bodies which were examined in this study.

Table 1

Standards Used for Microprobe Analysis

Mineral	Elements	Standard
Plagioclase	Na, Si	Synthetic glass, $An_{50}Ab_{50}$
	K	Natural orthoclase (Jarosewich et al, 1979)
	Ca, Al	Synthetic glass, $An_{100}Ab_{0}$
Hornblende, Clinopyroxene, Orthopyroxene	K, Na, Mg, Mn, Ti, Al, Si	Kakanui Hornblende (Jarosewich et al, 1979)
	Fe	Johnstown hypersthene (Jarosewich et al, 1979)
	Ca	Kakanui omphacite (Jarosewich et al, 1979)
Garnet	Ca, Mg, Mn, Fe	Gore Mountain garnet*
	Al, Si	Kakanui pyrope (Jarosewich et al, 1979)

* Wet chemical analysis, Battelle Memorial Institute

SiO_2	38.84
Al_2O_3	22.22
Fe_2O_3	1.23
FeO	21.0
MnO	0.62
MgO	8.80
CaO	6.73

hornblende were estimated using the procedure outlined in Robinson et al. (1982). Briefly, this procedure involves the normalization of the microprobe analysis to a certain number of cations, based upon crystal-chemical limits on cation substitution. This number is chosen by the analyst, depending upon the particular amphibole being analyzed. From this number, the total charge is calculated and a quantity of FeO sufficient to balance the charge is converted to Fe_2O_3. The recalculation is checked in order to see if it makes a reasonable amphibole, according to the crystal-chemical limits on cation substitution. In this study, hornblende analyses were all normalized to 13 cations, exclusive of Ca, Na, K. This gave reasonable amphibole formulas in most cases.

X-ray fluorescence analysis for Si, Al, Ti, Fe, Mn, Mg, Ca, Na, K, and P were carried out on a Philips AXS automated X-Ray spectrometer. Standards were: BCR-1, G-2, GSP-1, AGV-1, PCC-1, DTS-1 (all USGS standards). The samples were ground in a Spex Mill to pass a 200 μm mesh sieve, mixed with lithium tetraborate flux in a 6:1 ratio, and fused in a Pt crucible in a furnace for 20 minutes. The melt was then quenched to a glass disc, which was used for XRF analysis.

REGIONAL GEOLOGY

The Adirondack Highlands consist of multiply deformed Precambrian meta-igneous and meta-sedimentary rocks. The area is underlain by large domes of anorthosite and related anorthositic gabbros, gabbroic anorthosites, and norites, all of which are silica saturated. These rocks are sometimes referred to as the anorthositic series. The domes are surrounded by rocks that have been variously referred to as syenites, quartz syenites, charnockites, mangerites, jotunites, and syenitic granulites (Novillo, 1981). In this study, the descriptive non-genetic term syenitic granulite is used. Foliation in the syenitic granulites is comformable with the foliation in the anorthositic series. Located within the syenitic granulites are smaller bodies of anorthositic gneiss and olivine metagabbro. This association of syenitic granulite (charnockite) with anorthosite massifs has been reported worldwide (Buddington, 1969). The Highlands also contain granitic and alaskitic gneisses generally referred to as the younger granites, metasedimentary rocks of the Grenville series, and units of interlayered syenitic granulite, granitic gneiss and meta-sediments, in part migmatitic (Buddington, 1939).

The anorthosite is generally considered to be meta-igneous. It is divided into two facies, namely, the leucocratic Marcy facies, which occurs in the interior of the domes, and the Whiteface facies, which approximates gabbroic anorthosite in composition, and occurs

along the borders of the anorthosite massifs. Whiteface facies anorthosite also occurrs as small satellitic bodies within the syenitic granulite, some of which are sills (Husch et al., 1975). In addition, this facies may contain gabbroic segregations. Both facies contain sodic plagioclase, augite, hypersthene, hornblende, quartz, biotite, and garnet in variable proportions. It is generally thought that the anorthosite magma which was intruded contained a high percentage of phenocrysts (Balk, 1932; Buddington, 1939, 1969), and that the two facies originated through large scale flowage differentiation. Ashwal (1982) concluded that after magma movement ceased, cumulate processes dominated, and formed the mafic layers.

The syenitic granulites have been the center of much controversy. They have generally been considered to be meta-igneous. Their mineralogy is quartz, micro-perthite, oligoclase, hypersthene, augite, magnetite, and small amounts of garnet (Buddington, 1939). One school of thought, led by Balk (1932) considered them to be comagmatic with the anorthosites, a "mother liquor" squeezed out from the solidifying anorthosite along shear zones. The other school, led by Buddington (1939, 1969) believed the two to be unrelated intrusives, with the syenitic granulites being the younger. In addition, he noted that there were several series of syenitic granulites, not all of which were associated with anorthosites. Ashwal and Seifert (1980) concluded, based on the rare-earth element geochemistry of the syenitic granulites and the

anorthosites, that the two series were unrelated. McLelland and Isachsen (1980) contend that many of the syenitic granulites are actually metasedimentary. In the Southeastern Adirondacks, they have traced a consistent stratigraphy within the syenitic granulites and granitic gneisses. They believe that the only unquestionably igneous rocks are the anorthosites and anorthositic gabbros, the olivine gabbros, and the immediately adjacent charnockitic and mangeritic gneisses which contain xenoliths and xenocrysts from the anorthosite. They interpret these rocks to be of contact anatectic origin. These have been termed "hybrid rocks" by other workers (Letteney, 1969; DeWaard and Romey, 1969). They note that these syenitic granulites are intruded into and mixed with anorthosite-norite series rocks.

The olivine gabbros form a separate igneous series. They are generally small, oval shaped bodies in plan, probably lenses or sheet-like forms which have since been deformed (Buddington, 1939) or stocks (McLelland and Isachsen, 1980). Many of them still exhibit ophitic to subophitic textures in the interior, and their margins are often converted to foliated garnet amphibolite (Kreiger, 1937; Luther, 1976). They contain spinel-clouded plagioclase, clinopyroxene, olivine, magnetite and minor orthopyroxene as relict igneous minerals. Garnet, hornblende, orthopyroxene and minor clinopyroxene have developed as metamorphic products, often in a wide variety of corona structures (Luther, 1976; Whitney and McLelland, 1973, 1983; McLelland and Whitney, 1977, 1980).

The age relationships between the rock units discussed above are uncertain. Buddington (1939) believed that the Grenville Series represented the oldest rocks. They were intruded by anorthosites, then by olivine gabbros, later by syenites, and then intensely deformed and highly metamorphosed. Walton and DeWaard (1967) suggested that the anorthositic rocks formed an original basement, upon which the sedimentary protoliths of the syenitic granulites were deposited, followed by intrusion of the olivine gabbros. The sequence was then deformed and metamorphosed during the Grenville Orogeny. This interpretation ignores the reported occurrence of anorthositic sills in the syenitic granulite. McLelland and Isachsen (1980) believe the syenitic granulites represent metasedimentary rocks and large concordant intrusives into which were intruded anorthosite masses and stocks and sheets of olivine gabbro. As noted above, they attribute the apophyses of syenitic granulite to contact anatexis of the granulites by the anorthosite. Luther (1976) discovered a xenolith of deformed anorthosite within the Gore Mountain gabbro, thus indicating that the gabbros postdate the anorthosite and at least one deformational episode. No definitive relationships between the olivine gabbro and the syenitic granulite have been observed. McLelland and Isachsen (1980) contend that the syenitic granulites show evidences of partial melting adjacent to metagabbros, such as apophyses into the gabbro, and possible assimilated xenoliths of metagabbro within the syenitic granulite. However, these relationships permit various

interpretations, as is true of other contact relationships in the area.

The metamorphic grade in the Adirondack region increases from amphibolite facies in the Grenville Lowlands to hornblende granulite subfacies in the Southeastern Adirondacks, including this study area. Silver (1969) concluded, based on U-Pb dates from zircon concentrates, that the granulite facies metamorphism occurred during the period 1020±20 million years ago to 1100±15 m.y.. He concluded further that metamorphic activity was not continuous in time and space. McLelland and Whitney (1977) conclude that the metamorphic mineral assemblages now exposed at the surface equilibrated at about 25 Km. depth, indicating that crustal thicknesses must have been doubled at the time.

PREVIOUS WORK

General Garnet-Forming Reactions

Buddington (1939) proposed the reaction:

hypersthene + plagioclase $\longrightarrow$ augite + hornblende + garnet

as a general garnet-forming reaction in anorthosites and gabbroic anorthosites. He later modified this reaction to:

anorthite + hypersthene + olivine $\longrightarrow$ garnet + clinopyroxene

(Buddington, 1965). He mapped three garnet isograds, the first in biotite-quartz-plagioclase paragneisses, the second in metabasites, and the third in syenitic granulites, which he thought represented an increase in metamorphic grade to the southeast rather than bulk compositional effects.

DeWaard (1965) disagreed, claiming that the major control upon garnet formation was the bulk composition of the rock, based on ACF plots of garnetiferous versus non-garnetiferous rocks. He suggested that the reaction at Buddington's third isograd was:

orthopyroxene + anorthite $\longrightarrow$ clinopyroxene + garnet + quartz

This reaction would proceed to the left with increasing grade. Buddington (1966) in a reply, noted that quartz-consuming reactions were unlikely in mafic rocks. DeWaard (1967) contended that hydration reactions may produce five to ten percent of modal quartz in the conversion of olivine dolerite to amphibolite. However, he did not propose any reactions which would do so. Additionally,

Luther did not observe quartz in the transition zone from gabbro to garnet amphibolite at Gore Mountain.

Martignole and Schrijver (1971), studying garnet distribution in the Morin Anorthosite, attributed garnet formation to:

orthopyroxene + anorthite $\longrightarrow$ (Ca, Mg, Fe) garnet + quartz

or:

orthopyroxene + anorthite $\longrightarrow$ (Mg, Fe) garnet + quartz + clinopyroxene

They contend that the hornblende-garnet-clinopyroxene subfacies of the granulite facies is not regionally developed. They attribute this reaction to the heat supplied by the cooling Morin anorthosite which caused the assemblage hornblende-orthopyroxene-plagioclase to react to form hornblende-garnet-clinopyroxene.

Griffin and Heier (1969), in their study on garnet formation in some Norwegian anorthosites, suggested the reactions:

olivine + anorthite $\longrightarrow$ orthopyroxene + clinopyroxene + spinel

and:

orthopyroxene + clinopyroxene + spinel $\longrightarrow$ garnet

to give an overall reaction:

olivine + anorthite $\longrightarrow$ orthopyroxene + garnet

to form garnet in olivine-orthopyroxene-clinopyroxene+spinel coronas, in which garnet is usually found between the pyroxene zones. These reactions were interpreted to have occurred as a result of retrograde metamorphism of granulite facies assemblages.

Griffin (1971), in studying coronas of orthopyroxene-clinopyroxene-garnet, which sometimes contain relict olivine cores, and outer rims of a clinopyroxene-spinel symplectite in anorthosites, concluded that the garnet formed by the reaction:

initial orthopyroxene + initial clinopyroxene + spinel + anorthite $\longrightarrow$ orthopyroxene + clinopyroxene + garnet

He also noted that the corona-forming reactions of Griffin and Heier (1969) probably formed concurrently.

Whitney and McLelland (1973) explained occurrences of garnet replacing clinopyroxene+spinel symplectites in coronas of olivine-orthopyroxene-clinopyroxene+spinel-plagioclase, by the partial reactions:

$$\text{orthopyroxene} + Ca^{++} \longrightarrow \text{clinopyroxene} + (Mg\ Fe)^{++}$$

$$\text{clinopyroxene} + \text{spinel} + \text{plagioclase} + (Mg, Fe)^{++} \longrightarrow \text{garnet} + Ca^{++} + Na^{+}$$

$$\text{plagioclase} + (Mg, Fe)^{++} + Na^{+} \longrightarrow \text{spinel} + \text{more sodic plagioclase} + Ca^{++}.$$

In a later paper (McLelland and Whitney, 1977), they suggested that the development of garnets in the silica saturated anorthosites and syenitic granulites was due to the reaction:

$$2\ \text{anorthite} + (6-\alpha)\ \text{orthopyroxene} + \text{Fe-oxide} + (\alpha-2)\ \text{quartz} \longrightarrow \text{garnet} + \text{clinopyroxene}$$

where α is a function of the Fe and Mg distribution among the coexisting mafic phases. They later (McLelland and Whitney, 1980)

developed a generalized garnet-forming reaction for all meta-igneous rocks in the Adirondacks:

$$(4y + 1 + w)\ \text{anorthite} + 4k(y + 1 + 2w)\ \text{olivine}$$
$$+ 4(1 - k)(y + 1 + 2w)\ \text{Fe-oxide} + (8(y + 1)$$
$$+ 4k(y + 1 + 2w)\ \text{orthopyroxene}$$
$$\longrightarrow$$
$$2(y + 1)\ \text{garnet} + 2(y + 1 + 2w)\ \text{clinopyroxene} + 4w\ \text{spinel}$$

where y is a function of plagioclase composition, k considers the relative amounts of olivine and Fe-oxide participating in the reaction, and w is a measure of Si mobility. When w=2, Si is relatively immobile, and when w=0, Si mobility is at its maximum possible value. The actual garnet-forming reactions which occurred are considered to be cases of the above reaction.

Whitney and McLelland (1983) considered the occurrence of biotite-hornblende-garnet coronas between oxides and plagioclase in olivine metagabbro to be due to a two-stage reaction:

$$\text{plagioclase} + \text{Fe-Ti oxides} + \text{olivine} + H_2O \longrightarrow$$
$$\text{hornblende} + \text{spinel} + \text{orthopyroxene} \pm \text{biotite}$$
$$+ \text{more sodic plagioclase}$$

and:

$$\text{hornblende} + \text{orthopyroxene} \pm \text{spinel} + \text{plagioclase} \longrightarrow$$
$$\text{garnet} + \text{clinopyroxene} + \text{more sodic plagioclase}$$

They note that this reaction is linked to the reactions forming pyroxene and garnet coronas in the same rocks by exchange of Mg^{2+} and Fe^{2+}.

Gore Mountain Metagabbro

The garnet deposit at Gore Mountain, derived from an olivine metagabbro, is the largest garnet-bearing body in the region and has been studied many times in the past. The earlier theories on its origin are:

1) A metasedimentary xenolith in syenite (Miller, 1912).
2) Flow segregations in syenite (Balk, 1932).
3) Grenville series metasedimentary rocks which became "involved" with metagabbro (Kreiger, 1937).
4) Double contact metamorphism of the metagabbro, first by anorthosite, then by syenite (Miller, 1938).
5) Regional metamorphism (Buddington, 1939, 1952).
6) Contact metamorphism of the gabbro by syenite (Levin, 1950).
7) Regional metamorphism with concurrent deformation (Bartholeme, 1960).

The most recent study is that of Luther (1976), who followed the transformation from gabbro to garnet amphibolite in the field. He observed relict ophitic textures and igneous layering in metagabbro farthest from the garnet amphibolite. He also observed coronitic structures consisting of a core of olivine, surrounded sucessively by igneous clino-or orthopyroxene, equidimensional metamorphic orthopyroxene, clear plagioclase, and a garnet-pyroxene

symplectite, as well as coronas of igneous magnetite-biotite-yellow-brown hornblende. Finally, igneous plagioclase grains are clouded by numerous minute inclusions of spinel. Closer to the garnet body, coronas become larger, less well developed, and eventually disappear. Spinel-clouded plagioclase disappears. Garnet is disseminated throughout the rock, and its size gradually increases. The amount of hornblende increases. After passing through this transition zone into the garnet amphibolite proper, very large garnet porphryroblasts with a thin inner shell of plagioclase with minor biotite, and a thick outer shell of hornblende occur. The hornblende shells represent zones of plagioclase depletion (Bartholeme, 1960; Luther, 1976). Pressure shadows of plagioclase and orthopyroxene are also observed. The transformation of the gabbro to garnet amphibolite is isochemical, except for the addition of water. Luther concluded that the reaction producing the the garnet amphibolite was:

19 plagioclase + 8 clinopyroxene + 4 olivine + 6 H_2O + 1 magnetite

$\rightarrow$

6 hornblende + 9 plagioclase + 4 garnet + 1 orthopyroxene

Luther concluded that the inner shell of plagioclase was apparently formed by the reaction of hornblende with the garnet.

Ruby Mountain Anorthosite

The only detailed study of the Ruby Mountain anorthosite is that of Novillo (1981). She concluded that the garnetiferous anorthositic gneiss, which occurs as a lenticular mass surrounded by syenitic granulite, is related to the Thirteenth Lake anorthosite dome to the south. In this body, garnet porphryroblasts are surrounded by thick plagioclase rims. She deduced that two separate garnet-forming reactions had occurred; an interface reaction between brown hornblende and plagioclase:

brown hornblende + plagioclase $\longrightarrow$

garnet + quartz + plagioclase

and an interface reaction between mafic aggregates and plagioclase:

green hornblende + clinopyroxene + orthopyroxene

+ matrix plagioclase $\longrightarrow$

garnet + quartz

She concluded that PH_2O and fO_2 were variable within the body, based upon the variable pyroxene to hornblende ratio, and wet chemical analyses for Fe^{2+} and Fe^{3+} in brown and green hornblendes.

In addition, she concluded that two garnet consuming reactions had occurred, one of which produced thin plagioclase rims around the garnet inside garnet-hornblende corona structures:

brown hornblende + garnet + sphene $\longrightarrow$

plagioclase + ilmenite + garnet + quartz

In this reaction, there is very little difference between the composition of the reactant garnet and the product garnet. The second reaction occurs locally around some garnet porphryroblasts:

plagioclase + garnet + quartz $\longrightarrow$

orthopyroxene + Ca-plagioclase

RUBY MOUNTAIN METAGABBRO

Introduction

In 1981, the Barton Mines Corporation blasted an exploratory trench just below outcrops of the anorthositic gneiss (Figure 3), and exposed a mafic layer. Another similar unit was exposed during construction of a nearby water reservoir. This unit apparently was not recognized by Novillo. In her work (1981), which was based on diamond-drill cores, she gave a chemical analysis of a mafic gneiss which represented about ten percent of the body, but she did not mention the unit further.

Field Relationships

The mafic layer (hereafter referred to as the Ruby Mountain metagabbro) occurs structurally below the anorthosite. Sample locations are shown in Figure 4. It is apparently a continuous layer, although other exposures are rare. The grain size and mineral abundances vary between outcrops. It is weakly to moderately foliated, and the foliation is conformable with that in the overlying anorthosite. Conformable layers of garnet hornblendite up to 15 cm in thickness occur within the unit. Garnet size tends to increase as the anorthosite is approached. The actual contact with the anorthosite could not be observed; however, it must

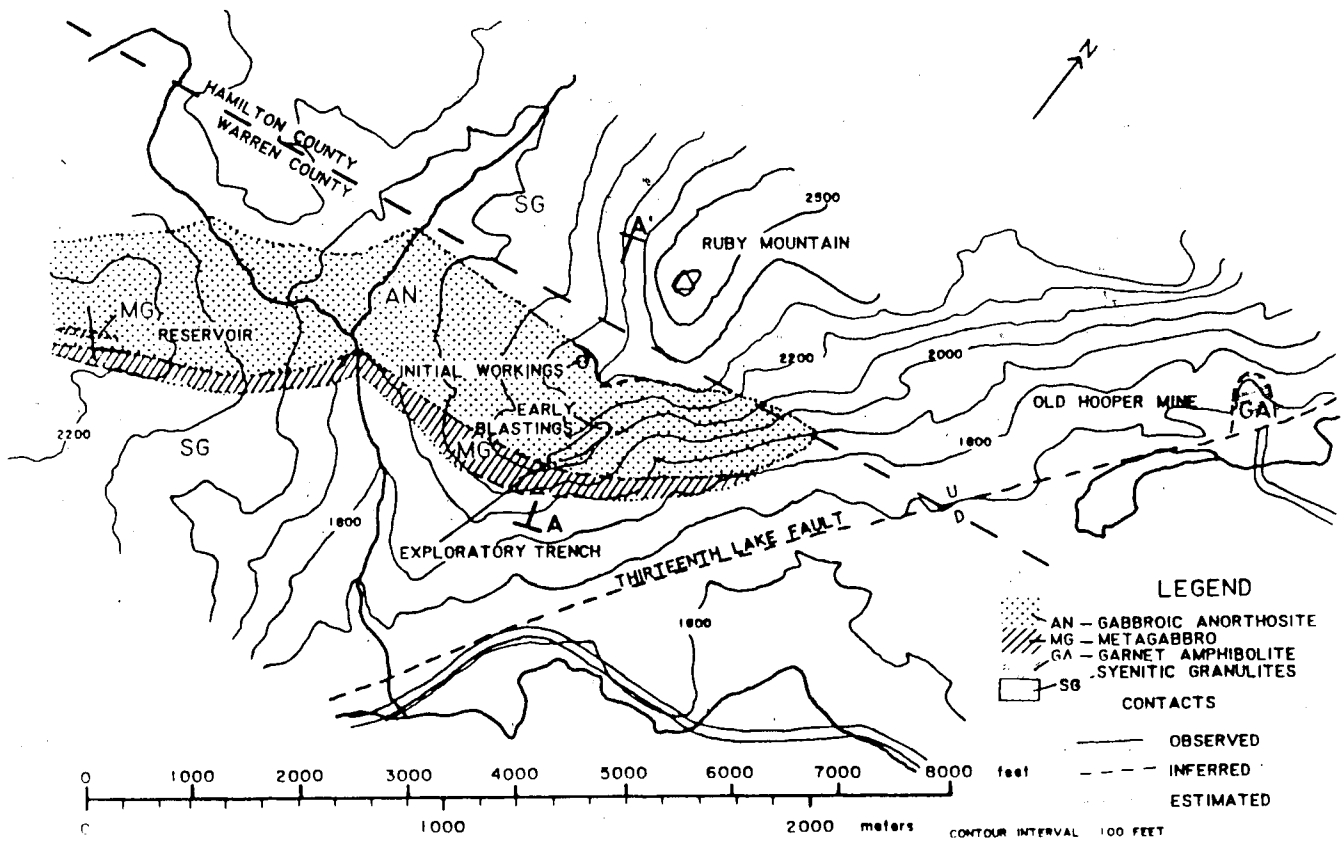

Figure 3 Geological map of the Ruby Mountain and Old Hooper mines.

INFERRED CROSS-SECTION OF THE RUBY MOUNTAIN ANORTHOSITE AND ASSOCIATED METAGABBRO

LINE OF SECTION SHOWN ON FIGURE 3

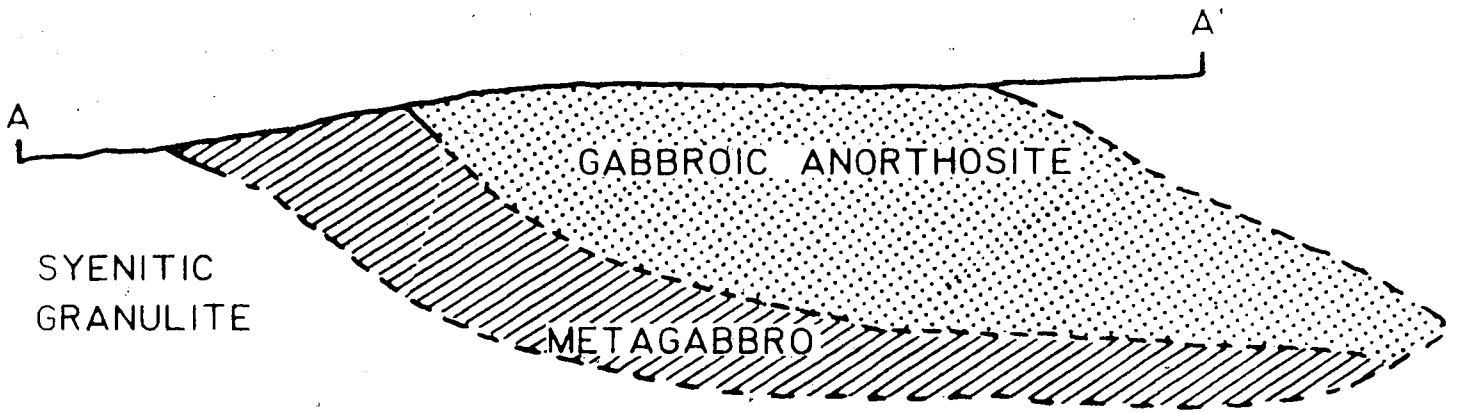

Figure 3 (continued)

NO VERTICAL EXAGGERATION

0 100 m

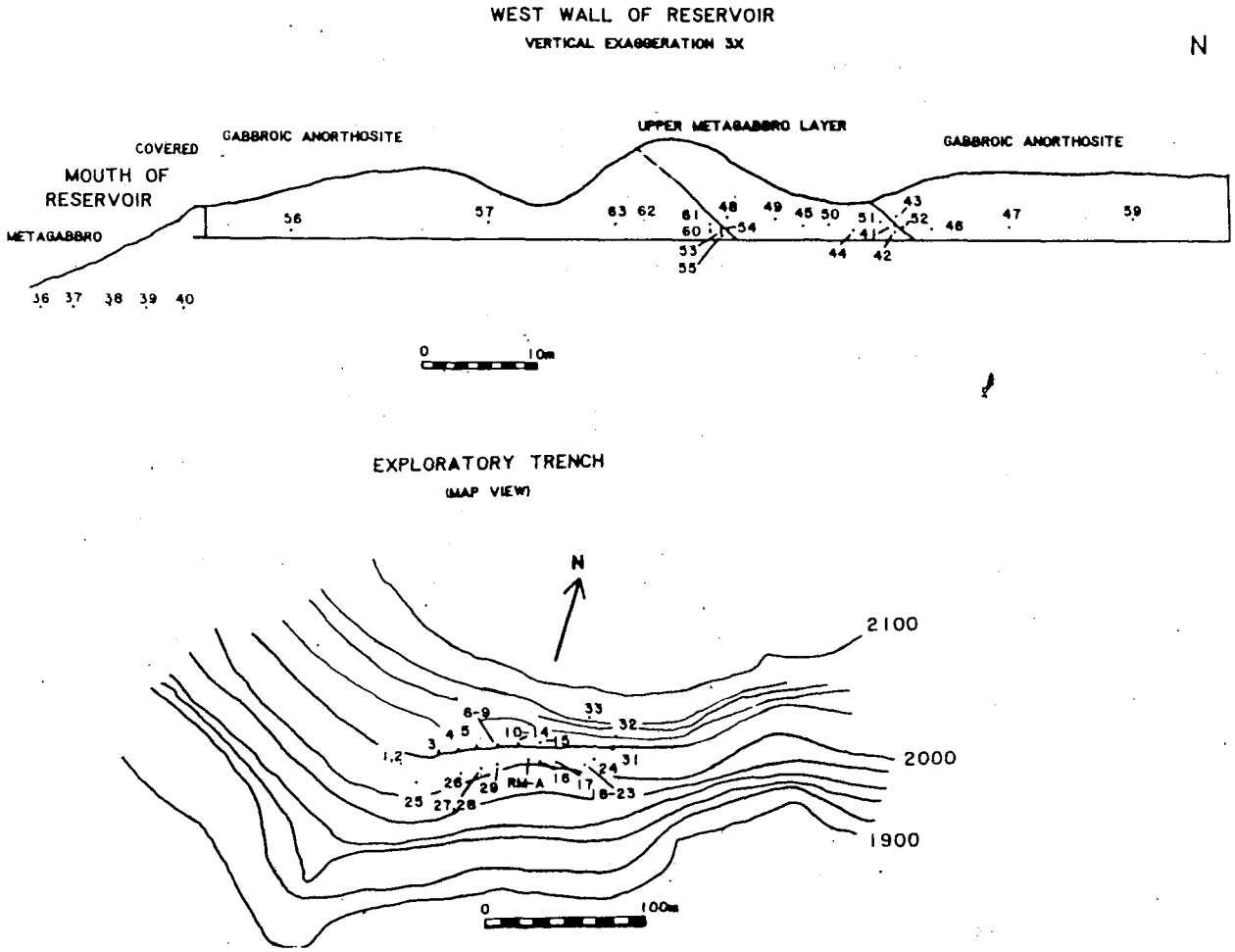

Figure 4. Sketch map showing sample location, Ruby Mountain metagabbro.

either be sharp or a narrow transition zone no more than one or two meters thick.

Several meters above the top of the metagabbro at the reservoir outcrop, a layer of metagabbro about two meters thick occurs conformably within the gabbroic anorthosite. It is not exposed in three dimensions, so a definite statement on its shape is not possible. It was not, however, observed in any other outcrops of the anorthosite. The contacts of this metagabbro with the surrounding anorthosite are sharp, and large garnets (up to 5 cm in diameter) occur along them.

Initial mining operations at Ruby Mountain have exposed the contact between the gabbroic anorthosite and the overlying syenitic granulite. No metagabbro occurs at this contact. The contact is not sharp. The syenitic granulites at the top of the outcrop grade downwards by an increase in mafic mineral content and thickness of mafic foliation bands into gabbroic anorthosite, which appears to be more mafic here than near the reservoir. Both units possess a strong, conformable foliation. Microtextures indicative of shearing are absent in thin sections of both rock types. If shearing along the contact did occur, as seems likely, based on the conformable foliation and the lack of a sharp contact in the field, it must have been at a time when the temperature was high enough to permit annealing after shearing.

Bulk Chemistry

XRF analyses of several representative samples from the Ruby Mountain metagabbro are given in Table 2, along with their CIPW norms. In comparing these analyses of the metagabbro with analyses from olivine metagabbros, such as the Gore Mountain metagabbro, the Ruby Mountain metagabbro is seen to have generally lower MgO and Al_2O_3, and higher SiO_2 and K_2O than do the olivine metagabbros. The MgO, total iron, K_2O, CaO, and TiO_2 contents of the Ruby Mountain metagabbro are, in general, similar to those of the gabbroic anorthosites and related norites. These observations indicate that the metagabbro may be related to the Ruby Mountain anorthosite, rather than being a separate intrusion of olivine gabbro. As can be seen in Table 2, the Ruby Mountain metagabbro is slightly olivine normative, which is not usually characteristic of gabbroic rocks related to anorthosites. However, the Ruby Mountain anorthosite itself has 14.27% normative olivine (Novillo, 1981).

Trends within the metagabbro are not well defined, but K_2O decreases, and CaO and MgO increase upwards. Total iron does not exhibit a unique trend. In the exploratory trench, the iron content is greatest farthest from the anorthosite, whereas at the reservoir mouth the opposite trend is seen.

There are differences in bulk composition between the anorthosite and the metagabbro as well. The metagabbro is lower in

Table 2

Bulk Chemical Analyses of Ruby Mountain and Speculator Metagabbro

	RM-1	RM-24a	RM-36	RM-40	RM-45	S-10	S-33
SiO_2	49.54	49.64	50.36	46.47	44.64	46.40	45.50
TiO_2	2.39	2.51	2.89	2.90	2.58	1.12	1.30
Al_2O_3	13.37	14.59	13.75	12.83	15.31	10.04	11.29
Fe_2O_3	18.35	11.32	13.40	18.90	15.39	13.27	13.15
MnO	0.21	0.10	0.15	0.22	0.22	0.20	0.21
MgO	3.53	3.82	3.74	3.99	4.60	13.81	14.87
CaO	6.82	10.59	7.80	9.29	10.47	11.57	11.86
Na_2O	2.68	3.23	3.48	3.01	2.95	1.81	1.51
K_2O	2.01	0.74	0.95	1.37	0.72	0.16	0.19
P_2O_5	0.33	0.30	0.29	0.40	0.33	0.12	0.11
LOI	---	0.31	0.55	0.42	---	---	---
Total	99.24	97.15	102.50	99.80	96.90	99.31	99.96

* Total iron expressed as Fe_2O_3.

RM-L (From Novillo, 1981)

SiO_2	47.1
TiO_2	1.2
Al_2O_3	20.4
Fe_2O_3	1.2
FeO	7.6
MnO	0.2
MgO	5.5
CaO	10.6
Na_2O	2.9
K_2O	0.5
P_2O_5	0.1
Total	97.3

Table 2 (continued)

CIPW Norms of Selected Samples

	RM-1	RM-40	S-10	S-33
ap	1.1%	1.4%	0.5%	0.5%
ilm	6.4%	8.0%	3.2%	3.6%
or	13.9%	9.4%	0.5%	0.5%
ab	27.7%	31.8%	6.5%	5.4%
an	14.4%	14.0%	16.9%	19.2%
mte	3.4%	3.8%	0.0%	6.5%
di	10.3%	10.4%	27.0%	27.8%
hy	22.1%	19.1%	28.8%	6.5%
ol	1.1%	1.1%	16.7%	30.0%

	RM-L
ap	.31%
il	2.28%
or	2.78%
ab	25.15%
an	42.53%
mt	1.86%
di	8.89%
hy	2.02%
ol	14.27%

(Table 2, Continued)
Sample locations

Ruby Mountain metagabbro

RM-1	Base of main metagabbro layer, exploratory trench.
RM-24a	Top of main metagabbro layer, exploratory trench.
RM-36	Base of main metagabbro layer, reservoir mouth.
RM-40	Top of main metagabbro layer, reservoir mouth.
RM-45	Center or upper metagabbro layer.

Speculator metagabbro

S-10, S-33	Normal metagabbro, from south of large-garnet zone.

Ca, Mg, Al, and higher in total iron and Ti than the anorthosite. The differences in Fe and Mg between the metagabbro and the anorthosite are also consistent with the hypothesis that the metagabbro may be layer related to the anorthosite, inasmuch as Davis (1969) noted that the Fe/Mg ratio increases with increasing mafic content in rocks of the anorthositic series.

Mineralogy, Petrography, and Mineral Chemistry

General Statement: The minerals in the metagabbro include plagioclase, clinopyroxene, orthopyroxene, hornblende, garnet, biotite, magnetite, and ilmenite. Minor amounts of apatite, clinozoisite, and quartz also occur. Apatite and clinozoisite are uniformly disseminated. Quartz occurs rarely as small inclusions in garnet porphyroblasts. The proportions of the major minerals show a wide range throughout the body. Table 3 gives some point counts obtained from representative samples in different parts of the body.

In thin section, the texture of the Ruby Mountain metagabbro is generally granoblastic, and the foliation is defined by concentrations of mafic minerals. Corona structures are absent, in contrast to the anorthosite. Relict igneous textures were not observed in the metagabbro, nor were they observed in the gabbroic anorthosite (Novillo, 1981).

Comparison of electron microprobe analyses of the ferromagnesian phases in the metagabbro shows that they are more iron-rich than the ferromagnesian phases in the anorthosite. In samples closer to the anorthosite however, the Mg/Fe ratio increases, due to changes in the bulk composition. The exact nature of the mineralogical relationships will be examined in the following sections.

Table 3

Modal Mineralogy of Ruby Mountain Metagabbro

	RM-1	RM-18	RM-24	RM-40	RM-45
garnet	tr	8.7	4.0	11.4	14.8
plagioclase	38.6	51.7	39.6	52.5	52.9
orthopyroxene	15.9	1.8	6.3	7.4	2.5
clinopyroxene	13.7	10.0	23.2	12.0	11.8
hornblende	7.8	24.0	24.1	13.5	12.0
biotite	20.5	tr	0.0	0.2	tr
opaques	2.1	3.4	2.7	2.7	5.6
acessories*	1.3	tr	tr	tr	tr
total	99.9	99.6	99.9	99.7	99.6

* clinozoisite, apatite, quartz

Opaques consist of ilmenite with minor magnetite.

Plagioclase: Plagioclase occurs in three major textural associations, none of which exhibits spinel clouding.

The first type consists of scattered antiperthitic plagioclase grains which are usually 1 to 2 mm in diameter, but may be as large as 5 mm (Figure 5). Where present, they compose only a few percent of the mode. Zoning is rare, and is weak when present. A few show signs of strain, such as bent twin lamellae or slight undulose extinction. They are generally surrounded by matrix plagioclase, rather than being associated with the ferromagnesian phases in the matrix. The potassium-feldspar component of the antiperthitic plagioclase occurs towards the interior of the grains. Where biotite occurs within the grain, K-feldspar patches are absent from the immediate area. In places, very small (less than .1 mm) idiomorphic grains of biotite or hornblende occur as inclusions.

The second type of plagioclase consists of equant xenoblastic grains up to about 1 mm in diameter which form a granoblastic matrix. These grains are neither zoned nor strained, and appear to represent an equilibrium texture (Figure 6). Their texture is very similar to that of the matrix plagioclase in the anorthosite.

The third type of plagioclase occurs as small round grains between garnet porphryroblasts and hornblende (Figure 7), or along grain boundaries of hornblende. They are not always present, and do not form a continuous rim between the garnet and hornblende. The grains are often reversely zoned. This textural association has been seen at both Gore Mountain (Luther, 1976) and at Ruby Mountain

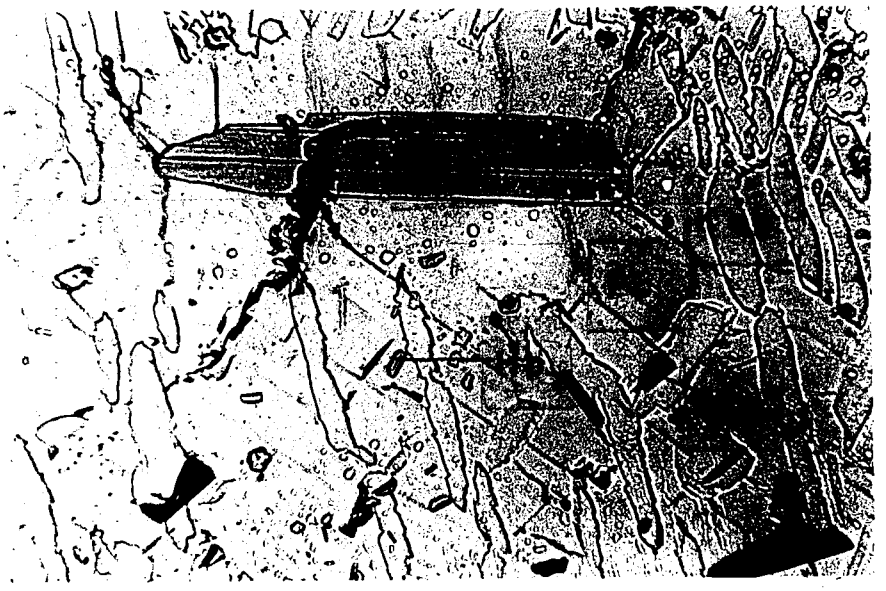

Figure 5. Photomicrograph of a biotite inclusion within antiperthitic plagioclase. Smaller inclusions of hornblende and biotite are also present. Note the lack of potassium-feldspar patches near the large biotite grain. Plane polarized light, 130X. Pc=plagioclase, Bio=biotite, Hb=hornblende, Ksp=potassiun feldspar.

Figure 6. Photomicrograph of plagioclase matrix showing relative lack of strain and apparent equilibrium texture. Crossed polarizers, 45X. Pc=plagioclase.

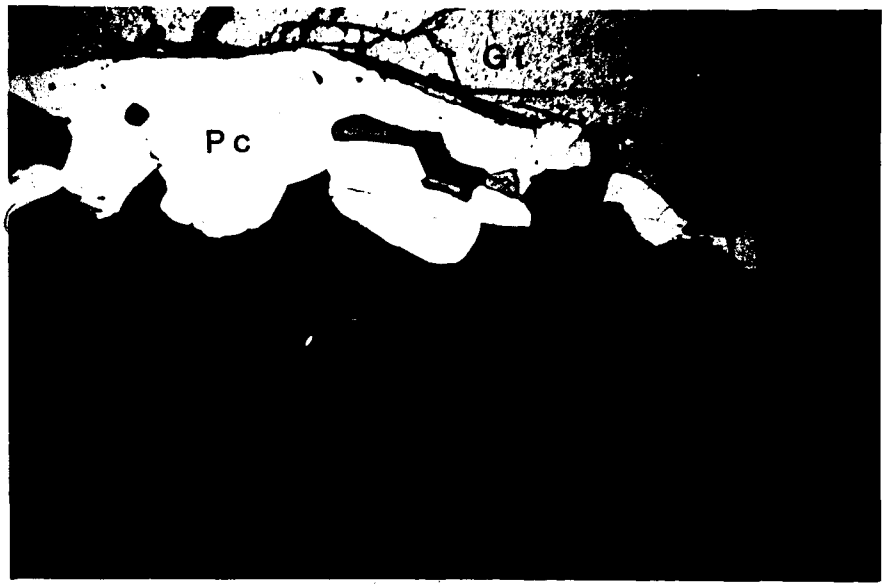

Figure 7. Photomicrograph of thin rim of plagioclase between large garnet porphyroblast and hornblende shell. Note that hornblende is embayed by plagiocase. Plane polarized light, 45X. Gt-garnet, Pc=plagioclase, Hb=hornblende.

(Novillo, 1981).

A fourth textural type of plagioclase that was observed consists of small irregular grains less than 1 mm in diameter which are intergrown symplectically with clinopyroxene, and which surrounds a large grain of potassium feldspar (Figure 8). This unusual texture was observed in only one thin section. It is not associated with any reaction products involving the breakdown of ferromagnesian phases.

Composition: The plagioclase in the metagabbro is, in general, more sodic than in the anorthosite. The composition reflects different textural types within the metagabbro. Representative analyses are listed in Table 4.

Readers will note that the quality of the analyses is very poor, as shown by the high totals. Examination of these analyses shows that the sodium analyses are consistently too high. This is evidently due to the standard used for sodium. A crystalline standard of suitable composition was not available, so a synthetic glass of composition An_{50} had to be used. The error may be due to the fact that the plagioclase of the metagabbro is more sodic than the standard. Using silica and alumina contents to calculate the amount of sodium that should be present does not greatly change the end-member molecular proportions. In addition, the error is consistent, so that general trends can be deduced.

Matrix plagioclase in the metagabbro has a composition of An_{31}.

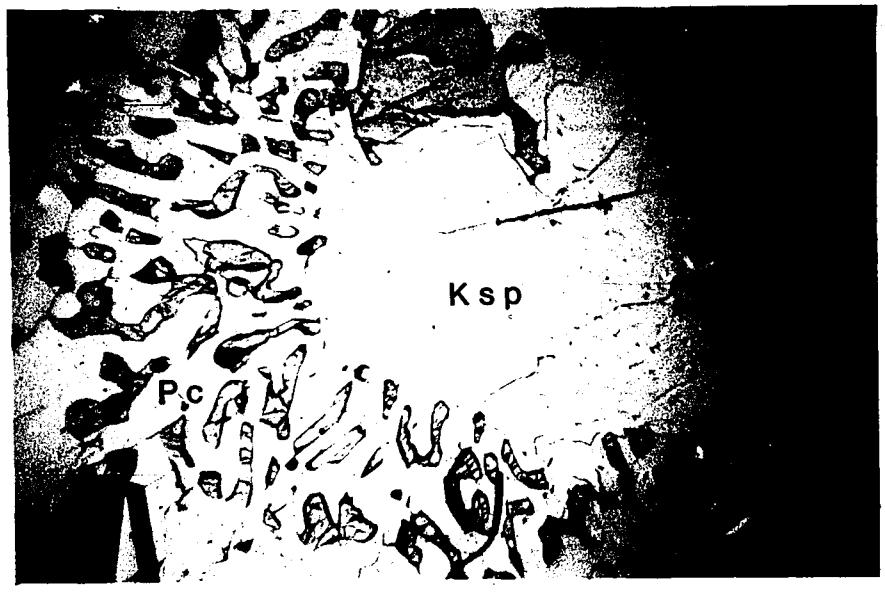

Figure 8. Photomicrograph of potassium feldspar surrounded by vermicular clinopyroxene and plagioclase. Plane polarized light, 45X. Ksp=potassium feldspar, Pc=plagioclase, Cpx=clinopyroxene.

Table 4

Electron Microprobe Analyses of Feldspars, Ruby Mountain Metagabbro

	RM51-1	RM51-2	RM51-3	RM29-1	RM1	RM29-2
SiO_2	58.33	57.33	59.06	59.91	63.34	65.57
Al_2O_3	28.22	28.95	26.82	26.52	26.58	18.56
CaO	9.30	8.94	7.83	7.40	6.47	0.10
Na_2O	7.03	8.47	9.30	9.24	5.86	0.90
K_2O	0.27	0.21	0.42	0.37	0.24	15.55
Total	103.15	103.89	103.43	103.44	102.49	100.68
	Number of Cations per 8 Oxygens					
Si	2.542	2.496	2.578	2.607	2.718	3.000
Al	1.450	1.485	1.380	1.360	1.344	1.000
Ca	.434	.416	.366	.344	.297	.005
Na	.594	.714	.787	.780	.487	.080
K	.015	.011	.023	.020	.013	.907
	Molecular Proportions					
An	41.6	36.5	31.1	30.1	37.3	0.5
Ab	56.9	62.5	66.9	68.1	61.0	8.1
Or	1.5	1.0	2.0	1.8	1.7	91.4

(Table 4, Continued)
Sample Description

RM 51-1 Center of rounded plagioclase grain adjacent to garnet porphryroblast, upper metagabbro layer.

RM 51-2 Rim of same grain as RM 51-1.

RM 51-3 Matrix plagioclase, same thin section.

RM 29-1 Plagioclase from plagioclase-diopsidic augite symplectite.

RM 29-2 K feldspar grain at center of symplectite.

RM 1 Antiperthitic plagioclase grain.

The antiperthitic plagioclase grains are more calcic, with a composition of An_{37}. The small plagioclase grains between garnet porphryroblasts and the hornblende rims are more calcic with cores of $An_{41.6}$, and rims of $An_{36.5}$. There does not appear to be any systematic compositional variation in the plagioclase with location in the metagabbro, in contrast to the ferromagnesian minerals.

Pyroxene: Both clinopyroxene and orthopyroxene occur in the metagabbro. The clinopyroxene is a gray-green, non-pleochroic diopsidic augite. The orthopyroxene is a moderately pleochroic (pink to gray-green) hypersthene. They exist in a number of textural associations, and define the foliation along with hornblende and garnet. Pyroxene is present in variable proportions, except near the contacts of the upper metagabbro layer.

Clinopyroxene: Clinopyroxene occurs in several textural types. The first consists of prismatic pyroxenes which are of intermediate grain size, and in places are rimmed by smaller, more equant grains of both clino-and orthopyroxene. They contain lamellae which occur on {100} of the clinopyroxene (Figure 9). They resemble lamellar igneous pyroxenes, however microprobe analyses reveal that the lamellae are of the same composition as the host. They are probably twins. The small grains are equant and xenoblastic. They are not present in every thin section.

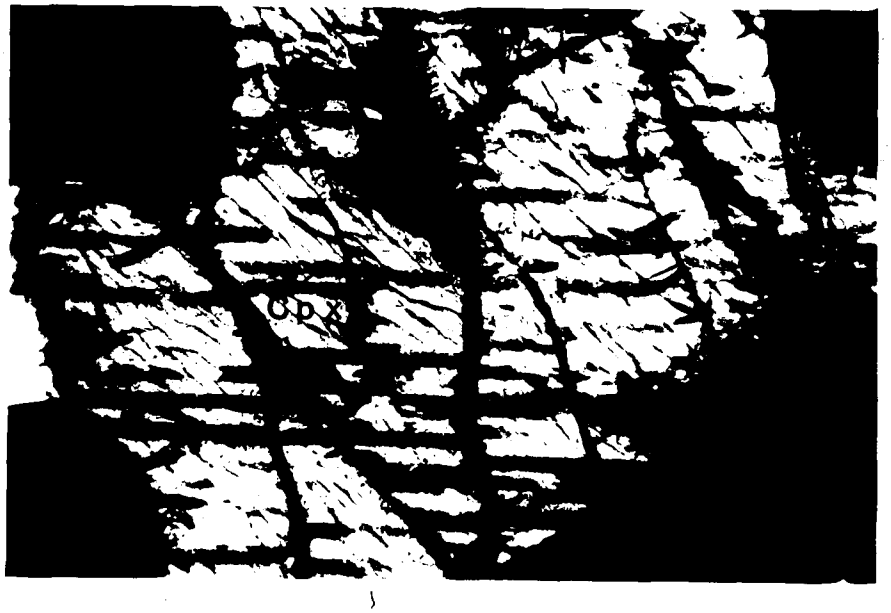

Figure 9. Photomicrograph of inequant diopsidic augite twinned on {100}. Twin lamellae are oriented horizontally in this photomicrograph. Crossed polarizers, 130X. Cpx=clinopyroxene.

The second type consists of relatively large clinopyroxenes which contain abundant hornblende lamellae (Figure 10). These grains occur only in thin sections containing abundant biotite and relatively little hornblende. They occur as inequant xenoblastic grains with irregular grain boundaries. This type of clinopyroxene also contains minute opaque inclusions in the interior, and is usually in contact with hornblende. The hornblende lamellae are crystallographically oriented, with the orientation apparently controlled by the host pyroxene, and they are optically continuous with adjacent discrete hornblende grains.

The smaller, more equant clinopyroxene grains tend to display a granoblastic texture, with straight grain boundaries. Their grain size ranges from .5 mm to 1 mm. They occur either as isolated grains in the matrix plagioclase, as granular rims around prismatic clinopyroxene along with orthopyroxene (Figure 11), or in ferromagnesian-rich layers associated with hornblende, garnet, or orthopyroxene (Figure 12). Some contain small, irregular inclusions of hornblende. This textural type is the most abundant.

Composition: Representative electron microprobe analyses are given in Table 5. The composition of the clinopyroxenes in the different textural associations is very similar. The average composition of all clinopyroxenes is Wo 42.4, En 35.8, Fs 21.7. This is lower in Wo and En components, and consequently higher in Fs, than are clinopyroxenes in the overlying gabbroic anorthosite (Figure 13).

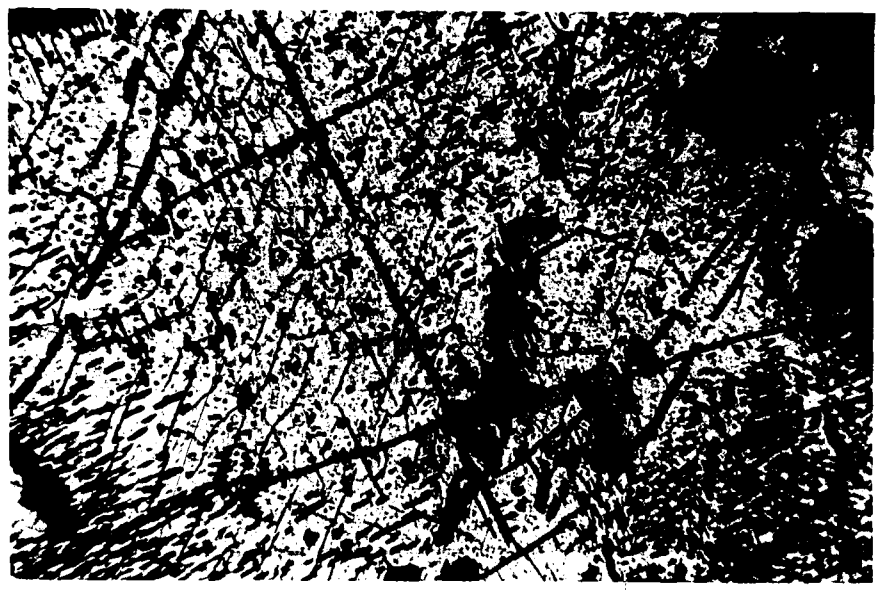

Figure 10. Photomicrograph of clinopyroxene containing hornblende inclusions and minute opaque inclusions. The hornblende inclusions are optically continuous with adjacent hornblende grains. Crossed polarizers, 130X. Hb=hornblende, Cpx=clinopyroxene.

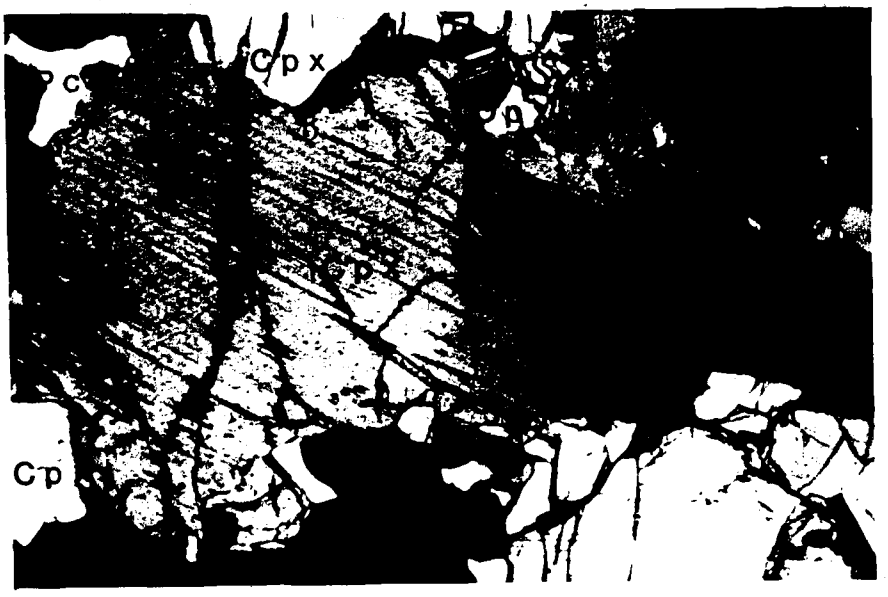

Figure 11. Photomicrograph of a large, inequant clinopyroxene surrounded by smaller, more equant clinopyroxene and minor orthopyroxene. Large grain shows twinning. Crossed polarizers, 45X. Pc=plagioclase, Cpx=clinopyroxene, Opx=orthopyroxene.

Figure 12. Photomicrograph of mafic foliation band from metagabbro at reservoir mouth. Note embayed clinopyroxene and anhedral garnet porphyroblast. Plane polarized light, 45X. Pc=plagioclase, Gt=garnet, Hb=hornblende, Opx=orthopyroxene, Cpx=clinopyroxene.

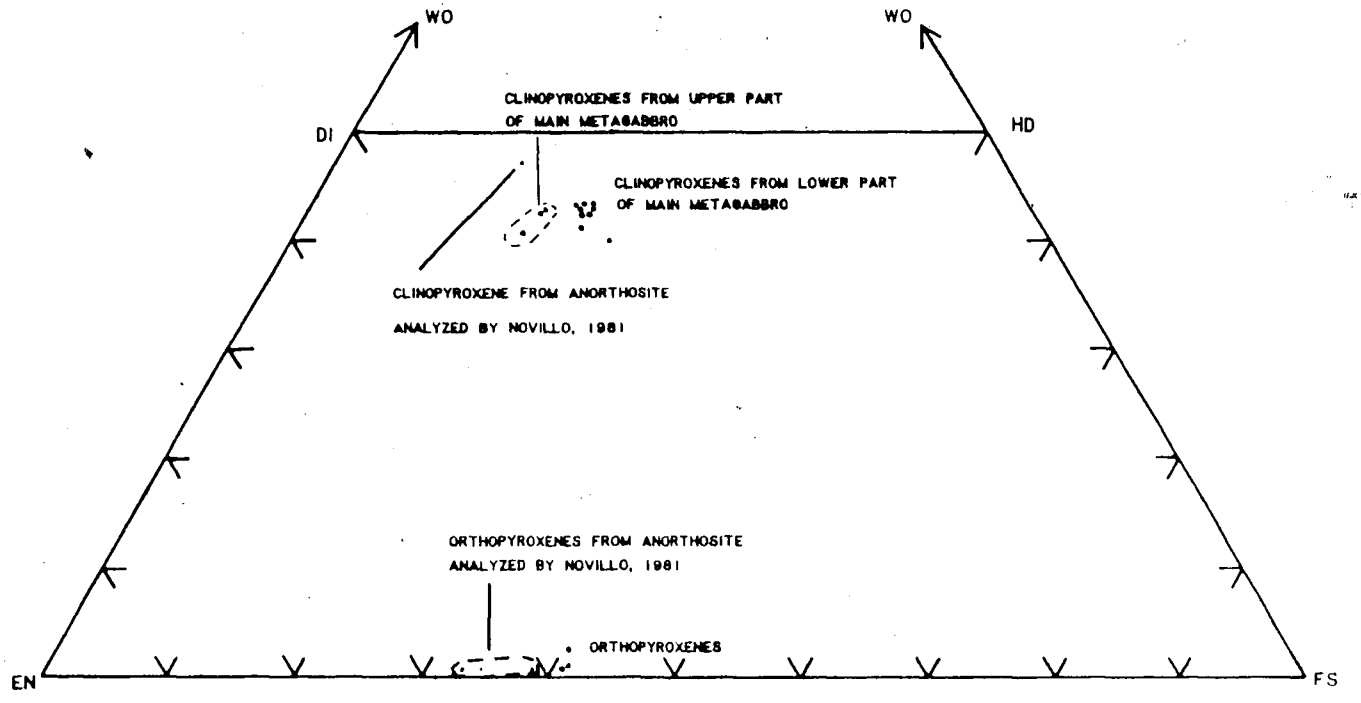

Figure 13. Ternary plot of microprobe analyses of pyroxenes from the Ruby Mountain metagabbro in terms of Wo, En, and Fs.

Table 5

Electron Microprobe Analyses of Pyroxenes, Ruby Mountain Metagabbro

	RM1-1	RM1-6	RM29-1	RM13-1
SiO_2	50.03	50.74	49.91	49.92
TiO_2	0.17	0.30	0.30	0.05
Al_2O_3	2.81	2.52	2.26	2.40
FeO	12.90	15.27	12.86	26.25
MnO	0.0	0.0	0.0	0.0
MgO	11.22	11.97	11.91	21.02
CaO	19.79	18.17	20.00	0.47
Na_2O	1.19	0.93	1.15	0.0
K_2O	0.0	0.0	0.0	0.0
Total	98.13	99.88	98.39	100.11

	RM13-3	RM24-1	RM7-1	RM7-2
SiO_2	50.70	50.79	50.16	49.44
TiO_2	0.01	0.31	0.27	0.31
Al_2O_3	2.42	2.72	3.19	3.43
FeO	25.69	10.94	12.47	12.50
MnO	0.0	0.0	0.0	0.0
MgO	20.40	12.96	11.63	11.47
CaO	0.43	19.65	19.28	19.65
Na_2O	0.0	0.92	1.43	1.39
K_2O	0.0	0.0	0.0	0.0
Total	99.65	98.29	98.43	98.20

(Table 5, Continued)
Number of Cations per 6 Oxygens

Si	1.934	1.934	1.927	1.896
Ti	.005	.008	.008	.001
Al	.128	.113	.102	.107
Fe	.417	.486	.415	.833
Mg	.646	.680	.686	1.190
Ca	.819	.742	.827	.019
Na	.089	.068	.086	0.0

Si	1.924	1.937	1.927	1.909
Ti	.000	.008	.007	.009
Al	.108	.122	.144	.156
Fe	.815	.349	.400	.403
Mg	1.154	.736	.665	.660
Ca	.017	.803	.793	.813
Na	0.0	.067	.106	.104

Normative Molecules

Wo	43.5	38.9	42.9	0.9
En	34.3	35.6	35.6	58.2
Fs	22.1	25.5	21.5	40.8

Wo	0.9	42.5	42.7	39.0
En	58.1	39.0	35.8	35.2
Fs	41.0	18.5	21.5	21.5

(Table 5, Continued)
Sample Descriptions

RM1-1 Clinopyroxene containing hornblende lamellae, base of main body of metagabbro.

RM1-6 Clinopyroxene grain adjacent to hornblende, same location, main body of metagabbro.

RM29-1 Clinopyroxene from plagioclase-clinopyroxene symplectite, main body of metagabbro.

RM13-1, and RM13-3 Orthopyroxenes from garnet hornblendite near large garnet porphyroblast, main body of metagabbro.

RM24-1 Clinopyroxene adjacent to hornblende, top of main body of metagabbro.

RM7-1 Twinned clinopyroxene main body of metagabbro.

RM7-2 Twin lamellae within same grain as RM7-1.

Within the metagabbro, there is a slight increase in Wo and En components as the anorthosite is approached. These trends reflect the compositional differences within the metagabbro. These doubtless originated through igneous differentiation of the original gabbro. The Al_2O_3 content appears to be dependent on textural association; it is highest in twinned pyroxenes, and lowest in pyroxenes containing hornblende.

Figure 13 also shows that the present composition of the pyroxenes is metamorphic rather than igneous, based on the high Wo content. It has been observed that augites which have equilibrated at metamorphic temperatures contain more of the Wo component than do augites from igneous rocks. Conversely, hypersthenes which have equilibrated at metamorphic temperatures contain less Wo than do hypersthenes from igneous rocks (Huebner, 1981). The absence of igneous pyroxenes in the Ruby Mountain anorthosite was also noted by Novillo (1981). The high Al_2O_3 content of the twinned pyroxene might be a relict igneous feature, inasmuch as Luther (1976) observed that undoubted igneous pyroxenes in olivine metagabbro were higher in Al_2O_3 than metamorphic pyroxenes at Gore Mountain. The content of Al_2O_3 in a pyroxene is a function of temperature as well as pressure (Bohlen and Essene, 1978; Gasparik and Lindsley, 1980). However, Bohlen and Essene found high Al_2O_3 concentrations in completely re-equilibrated metamorphic pyroxenes. In view of the lack of unequivocal igneous textures or chemical indicators, none of

the clinopyroxenes in the metagabbro may be considered to be relict igneous clinopyroxenes.

Orthopyroxene: Orthopyroxenes occur as fairly large xenoblastic grains either within mafic bands or the plagioclase matrix, as small equant grains associated with clinopyroxene in the aforementioned granoblastic pyroxene aggregates, as small grains along the rims of hornblende crystals in the mafic foliation bands, or associated with hornblende in rims around garnet porphryroblasts. In the latter association, the orthopyroxenes are large and inequant, and occur within a granoblastic hornblende aggregate in an apparent equilibrium texture, with straight grain boundaries and triple point junctions. Some of these grains exhibit thin veins filled with optically unresolvable birefringent material (Figure 14). An EDS analysis of one of these veins shows it to contain Mg, Fe, Si, and Al. It is probably a hydrous ferromagnesian silicate, possibly talc. In the hypersthene walls of the vein, there are numerous minute inclusions of green spinel. These decrease in amount with increasing distance from the vein. This texture represents the reaction of aluminous orthopyroxene with water to form talc (or some other hydrous ferromagnesian silicate low in Al) and spinel, and is thus a retrograde reaction.

The small grains associated with hornblende are inequant and irregular in shape, and are associated with small plagioclase grains of similar habit. They generally occur along the rims of hornblende

Figure 14. Photomicrograph of a vein of a microcrystalline mineral, probably talc, associated with minute inclusions of spinel, in aluminous orthopyroxene located within the hornblende shell around a large garnet porphyroblast. Crossed polarizers, 320X. Opx=orthopyroxene, Sp=spinel, Ta?=optically unresolvable ferromagnesian mineral, probably talc.

grains where in contact with matrix plagioclase, and probably represent a hornblende-consuming reaction. The same texture was observed in the anorthosite (Novillo, 1981), and will be discussed in more detail in later sections.

Composition: The orthopyroxenes also plot as metamorphic pyroxenes on the pyroxene quadrilateral based on their low Ca content (p. 54). They were developed either by recrystallization of igneous pyroxenes, or as products of metamorphic reactions. They are very low in calcium and relatively high in aluminum (Table 5). Their magnesium content is lower and their iron and aluminum contents are higher than that of orthopyroxenes in the anorthosite.

Hornblende: Hornblende is present throughout the metagabbro in variable amounts. Its abundance does not vary sympathetically with that of garnet. However, where relatively large garnet porphyroblasts occur, hornblende is more abundant. In thin sections from the contacts of the upper metagabbro it is the only mafic mineral present. It is pleochroic in olive green to light olive brown. Brown hornblende was not observed.

Hornblende occurs as (1) equant grains in layers of garnet hornblendite and in mafic foliation bands, (2) irregular rims which partly surround and embay large irregularly shaped pyroxene grains (Figure 15), and (3) irregular inclusions within granoblastic clinopyroxene. Neither ilmenite-hornblende nor magnetite-hornblende

Figure 15. Photomicrograph of clinopyroxene from a mafic foliation band, rimmed and embayed by hornblende, adjacent to xenoblastic garnet. Plane polarized light, 45X. Gt=garnet, Pc=plagioclase, Hb=hornblende, Cpx=clinopyroxene.

coronas were found. The hornblende may, however, contain magnetite or ilmenite inclusions, as well as rounded or embayed inclusions of biotite, clinopyroxene, or plagioclase.

In the first textural type, the hornblende generally forms xenoblastic grains about 1 to 3 mm in diameter in a granoblastic aggregate of either hornblende or pyroxene. In the garnet hornblendite layers, it is coarser grained, generally equant in shape, and shows an apparent equilibrium texture. Where it is adjacent to the small plagioclase grains along the rim of garnet porphryroblasts, it is embayed by the plagioclase. In the mafic foliation bands, it may be either equant or elongate in shape, and generally exhibits straight grain boundaries. In places, small individual grains of orthopyroxene occur at the edge of hornblende grains where they are in contact with plagioclase (p. 54). Hornblende generally does not occur as isolated grains within the plagioclase matrix.

Composition: Table 6 gives several representative hornblende analyses. Hornblende, in common with the other minerals mentioned, has higher iron and lower magnesium contents in the metagabbro than in the anorthosite. An additional significant difference is the lack of brown hornblende in the metagabbro. Novillo (1981) noted the variability of fO_2 in the anorthosite, as based on the occurrence of both brown hornblende, which is relatively high in Ti

Table 6

Electron Microprobe Analyses of Hornblendes, Ruby Mountain Metagabbro

	RM1-a	RM1-b	RM1-6	RM13-9	RM13-10	RM13-11	RM13-12	RM13-14	RM13-15
SiO_2	41.30	41.05	40.85	41.17	41.21	41.09	41.03	40.93	40.72
TiO_2	2.62	2.38	3.02	2.30	2.12	2.24	2.38	2.22	2.33
Al_2O_3	12.74	12.35	12.62	14.19	13.86	14.20	13.75	13.92	13.50
FeO	20.09	19.66	19.47	15.56	15.74	15.49	15.46	16.11	16.14
MnO	0.0	0.0	0.0	0.0	0.0	0.0	0.0	0.0	0.0
MgO	7.85	8.29	8.99	10.06	10.35	10.10	10.04	10.24	10.02
CaO	10.91	11.17	10.85	11.48	11.41	11.06	11.31	11.18	11.61
Na_2O	1.66	1.81	1.70	1.80	2.02	1.95	1.92	1.89	1.94
K_2O	1.61	1.32	1.69	1.52	1.42	1.29	1.40	1.33	1.36
Total	98.78	98.03	99.21	98.07	98.14	97.42	97.29	97.81	97.62

Number of Cations per 23 Oxygens
(Normalized to 13 total cations, exclusive of Ca, Na, and K)

Si		6.186	6.191	6.056	6.106	6.106	6.103	6.136	6.065	6.097
Ti		.295	.270	.336	.257	.236	.250	.268	.246	.262
Al		2.248	2.194	2.204	2.230	2.240	2.485	2.423	2.430	2.382
Fe	$3+$	.448	.442	.682	.652	.381	.434	.289	.546	.314
Fe	$2+$	2.067	2.037	1.733	1.707	1.568	1.489	1.643	1.449	1.706
Mg		1.752	1.864	1.986	1.986	2.285	2.237	2.239	2.261	2.237
Ca		1.770	1.824	1.752	1.837	1.828	1.778	1.825	1.797	1.877
Na		.486	.536	.497	.473	.584	.443	.559	.549	.566
K		.310	.255	.324	.323	.270	.247	.268	.254	.262

Fe^{2+} and Fe^{3+} estimated by the procedure of Robinson et al (1981), outlined on p 10.

(Table 6, Continued)
Sample Description

RM-1a Olive-green hornblende adjacent to clinopyroxene which contains hornblende inclusions, lower part of main body of metagabbro.

RM-1b Olive-green hornblende inclusions within clinopyroxene grain associated with hornblende of previous analysis.

RM-1-6 Olive-green hornblende grain adjacent to equant clinopyroxene; lower part of main body of metagabbro.

RM-13-9, 10, 11, 12 Olive-green hornblendes from interior of hornblende shell around large garnet porphyroblast in garnet hornblendite; main body of metagabbro.

RM-13-14, 15 Olive-green hornblende grains from outer part of same hornblende shell described in RM13-9, 10, 11, 12.

and Fe^{3+}, and green hornblende which is relatively high in Fe^{2+}. In the metagabbro, fO_2 was apparently lower than in the anorthosite, inasmuch as brown hornblende was not observed. Although the lack of brown color in hornblende may also be due to relatively low TiO_2 content, the TiO_2 content in the hornblende of the metagabbro is higher than that of the green hornblende of the anorthosite. There is a noticeable difference in chemical composition between hornblendes in different textural associations. Hornblendes which are closely associated with clinopyroxenes, either as inclusions within a clinopyroxene host or as individual crystals adjacent to or partially rimming clinopyroxene, contain more total iron, and have a lower Fe^{3+}/Fe^{2+} ratio, as estimated by the procedure of Robinson et al. (1981) outlined on p. 10, than hornblendes from garnet hornblendite layers. In addition, titanium is higher, and aluminum and magnesium are lower in hornblende associated with clinopyroxene than in hornblende in garnet hornblendite. The composition of the hornblendes in the garnet hornblendite layers is similar to the composition of green hornblendes in the anorthosite. These trends may be explained as follows. The hornblendes closely associated with clinopyroxene as inclusions or grains embaying the clinopyroxene probably represent the initial formation of hornblende from metamorphic clinopyroxene. This initial stage has probably been preserved due to relatively low PH_2O locally. Under conditions of prograde metamorphism, in other parts of the metagabbro, such as in the garnet hornblendite, hornblende began to be consumed in later

metamorphic reactions, which formed either garnet or orthopyroxene plus clinopyroxene plus plagioclase. These products preferentially consumed Fe^{2+} leaving the remaining hornblende both enriched in magnesium, and with a higher Fe^{3+}/Fe^{2+} ratio. Thus, these hornblendes represent a "final" hornblende chemistry under conditions of prograde metamorphism. This is in agreement with amphibole phase relations (Gilbert et al., 1982) which show that magnesium-rich end members are stable at higher temperatures than Fe^{2+} -rich end members.

Garnet: Garnet occurs in varying proportions throughout the metagabbro. In general, it is slightly more abundant and forms larger porphryroblasts either near the gabbroic anorthosite or within the garnet hornblendite layers. In the upper metagabbro layer, garnet porphryroblasts up to 5 cm in diameter occur at the contact with the gabbroic anorthosite, but in the interior of the body they are much smaller. The garnet is post-deformational, as shown by the foliation does not wrap around the porphyroblasts. Also, some porphyroblasts are highly irregular in shape, and would therefore be unlikely to survive a strong deformational event.

Three main textural types occur. The first type consists of small xenoblastic crystals (Figure 16). They may be equant or irregular in shape. This type is either surrounded by matrix plagioclase, or occurs as inclusions within large antiperthitic

Figure 16. Photomicrograph of xenoblastic garnet and biotite within plagioclase matrix. Plane polarized light, 45X. Gt=garnet, Pc=plagioclase, Hb=hornblende, Bio=biotite.

plagioclase grains in thin sections with relatively few mafic minerals.

The second textural type consists of xenoblastic individuals or clusters of grains, and occurs in mafic foliation bands (Figure 15). The same type of texture was observed in the anorthosite (Novillo, 1981). Grain boundaries are irregular and embayed, and in places the garnet is separated from the ferromagnesian phases by a rim of small, zoned plagioclase grains. The garnet may contain large, rounded and embayed inclusions of hornblende, plagioclase, twinned or untwinned clinopyroxene and ilmenite, and occasionally very small, round quartz grains.

The third textural type consists of garnet porphryroblasts up to 5 cm in diameter, surrounded by a distinct hornblende shell (Figure 7). These occur in garnet hornblendite layers and other parts of the body that are rich in hornblende. The garnet grains are equant but xenoblastic. Between the garnet and the hornblende shell occur small zoned plagioclase grains. The garnet porphryroblasts may contain inclusions of orthopyroxene, zoned plagioclase, or hornblende. Large garnet porphryroblasts with thick plagioclase rims were not observed in the metagabbro.

Composition: The garnets in the metagabbro show the same trends; i.e. lower MgO and higher FeO, as compared with garnet in the Ruby Mountain anorthosite. It is interesting to note that RM-51, a garnet porphryroblast from the upper metagabbro layer, is closer

chemically to the garnets in the anorthosite than are the garnets from lower in the metagabbro. Table 7 gives some representative compositions of the garnet in the metagabbro. Figure 17 shows representative zoning trends in two garnets, one .2 cm in diameter, and the other of 1.5 cm in diameter. Small garnets show a slight increase in magnesium and a corresponding decrease in iron and manganese from the core to the rim. Large porphryroblasts, however, are virtually chemically homogeneous.

It is significant that these zoning trends are identical to those observed in the garnets in the Ruby Mountain anorthosite by Novillo (1981). She interpreted these trends by means of the fractionation-depletion model of Hollister (1966). In this model, the garnet rim is considered to be in equilibrium with the reservoir during garnet growth. As the garnet grows, the elements that are preferentially incorporated into the lattice are depleted in the reservoir. The expression:

$$M_G = M_0 (1-W^G/W^O)^{\lambda-1}$$

gives the weight fraction of an element at the rim of a garnet, where M_0 is the weight fraction of that element in the rock as a whole, W^G is the weight of the crystallized garnet, W^O is the weight of the original system, and λ is the fractionation factor between garnet and the reservoir minerals, which is assumed to be a constant. This holds only for low concentrations of the element.

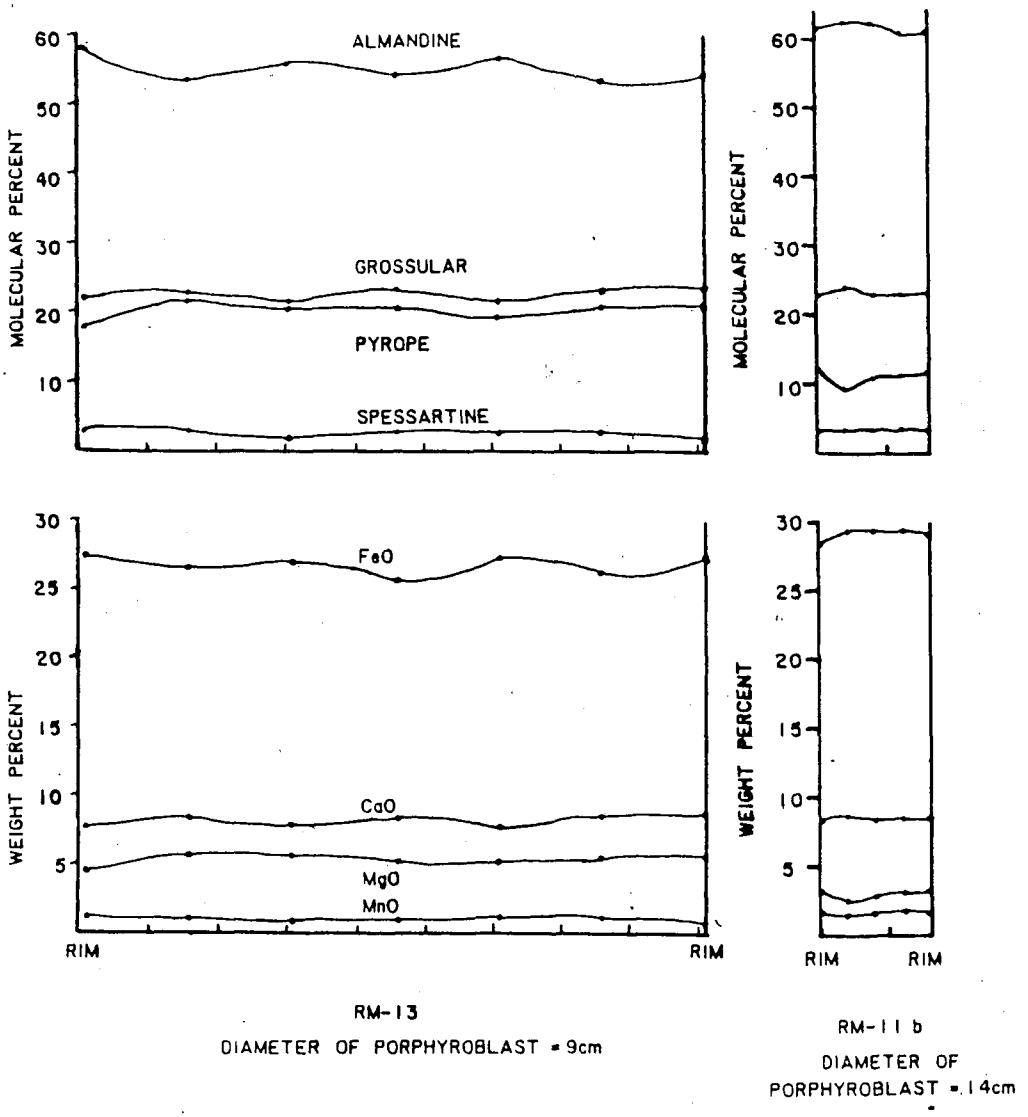

Figure 17. Representative zoning trends in two garnet porphyroblasts, Ruby Mountain metagabbro.

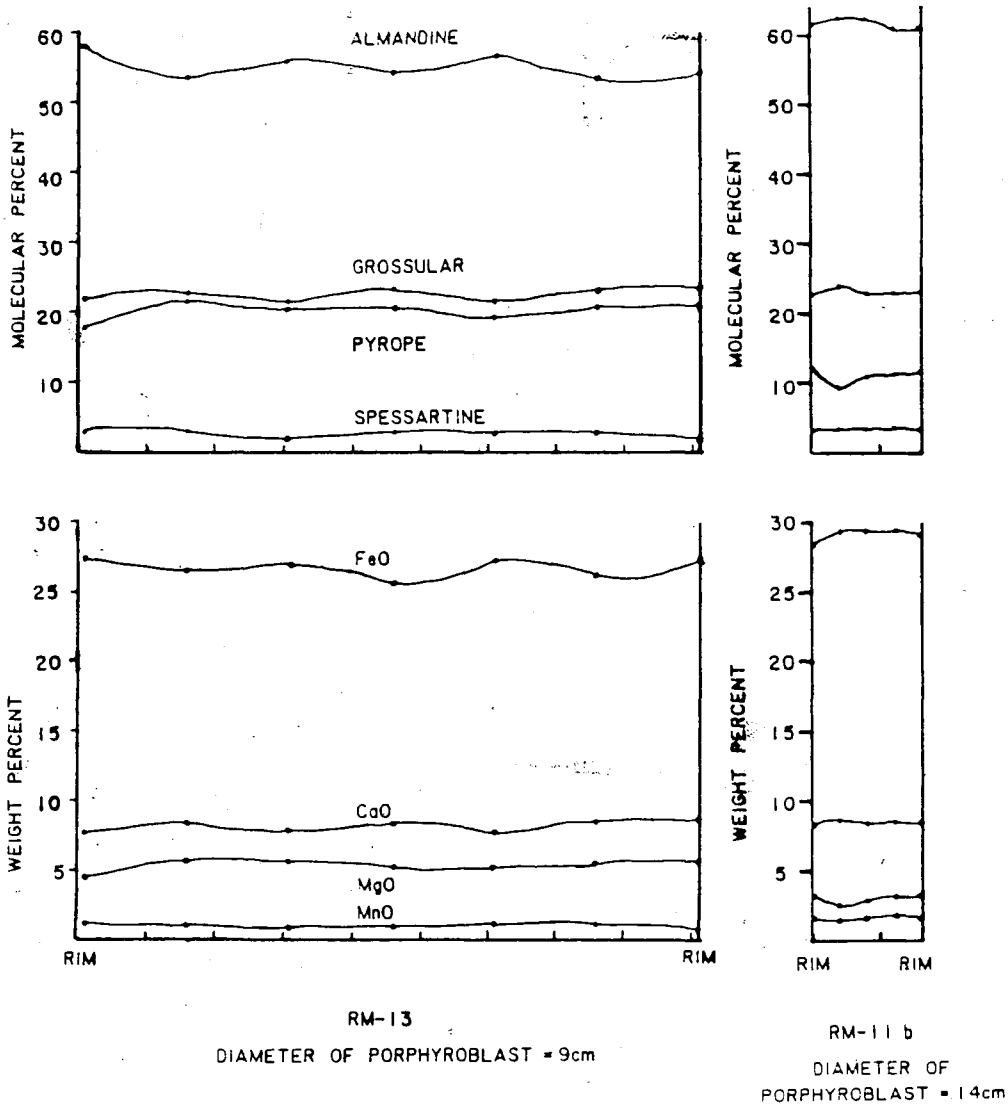

Figure 17. Representative zoning trends in two garnet porphyroblasts, Ruby Mountain metagabbro.

Table 7

Electron Microprobe Analyses From a Traverse Taken Across a Garnet Porphyroblast, Ruby Mountain Metagabbro

RM29b
Diameter of porphyroblast=.2cm, sample interval=.4mm

	Rim					Rim
SiO_2	37.03	36.87	37.03	36.77	35.94	36.85
Al_2O_3	21.02	20.90	20.85	21.32	20.87	21.14
FeO	29.19	29.36	29.21	28.70	28.72	30.01
MnO	1.41	1.30	1.42	1.47	1.56	1.60
MgO	3.84	4.09	4.13	3.95	3.58	3.39
CaO	7.97	8.45	8.02	8.05	8.18	8.36
Total	100.46	100.97	100.66	100.26	98.86	101.35

Number of Cations per 12 Oxygens

Si	2.941	2.920	2.936	2.922	2.909	2.917
Al	1.967	1.950	1.949	1.996	1.991	1.973
Fe	1.938	1.944	1.936	1.907	1.944	1.987
Mn	.094	.087	.045	.098	.107	.107
Mg	.454	.483	.488	.467	.432	.400
Ca	.678	.716	.681	.685	.709	.709

(Table 7, Continued)
Electron Microprobe Analyses From a Traverse Taken across a Garnet Porphyroblast, Ruby Mountain Metagabbro

RM13
Diameter of porphyroblast=.9cm, sample interval=1.5mm

	Rim						Rim
SiO_2	37.96	37.88	38.02	38.31	37.78	38.28	38.55
Al_2O_3	22.11	21.76	21.96	21.88	22.34	21.90	21.96
FeO	27.31	26.42	26.96	25.57	27.12	26.21	26.31
MnO	1.22	1.06	0.94	1.00	1.11	1.08	0.71
MgO	4.67	5.69	5.47	5.30	5.09	5.50	5.56
CaO	7.82	8.39	7.91	8.38	7.82	8.47	8.61
Total	101.11	101.20	101.25	100.44	101.26	101.45	101.70

Number of Cations per 12 Oxygens

Si	2.953	2.938	2.946	2.977	2.931	2.956	2.965
Al	2.027	1.989	2.005	2.003	2.042	1.992	1.989
Fe	1.776	1.713	1.747	1.661	1.759	1.692	1.691
Mn	.080	.069	.061	.065	.073	.070	.046
Mg	.541	.657	.631	.614	.589	.633	.637
Ca	.652	.697	.656	.697	.649	.701	.709

She considered the chemical homogeneity of the large garnet porphryroblasts in the anorthosite to be due to the earlier nucleation of these crystals, so that they were subjected to high temperature for a longer period than the smaller younger garnets. Thus, the larger garnets would have had more time in which to homogenize through intracrystalline diffusion.

Biotite: Biotite occurs in two textures and is present in very variable concentrations. Some samples do not contain any biotite whereas others, generally farther from the anorthosite, contain as much as 20 percent. It is strongly pleochroic in deep red-brown to very pale brown. The first texture occurs only in garnet hornblendite, and forms hypidioblastic grains scattered through the hornblende. It generally forms a few percent of the hornblende rims around garnet porphyroblasts.

The other textural occurrence of biotite occurs in thin sections with low hornblende content. Here biotite is generally lath shaped, and may be very abundant. Where it is in contact with large, inequant clinopyroxenes, the pyroxene is embayed by biotite. In some thin sections biotite occurs as small, irregular inclusions in pyroxene, hornblende, and locally garnet.

Metamorphic Reactions

There is evidence for several different metamorphic events in the metagabbro. In general, they are similar to those that occurred in the anorthosite.

Igneous ortho-and clinopyroxene and plagioclase was recrystallized during deformation (Novillo, 1981). These minerals now have a metamorphic composition. During this event, which obliterated the igneous texture, clinopyroxene was enriched in calcium, and orthopyroxene was depleted in calcium. The extra calcium in the metamorphic clinopyroxene was probably supplied by the orthopyroxene.

A variable influx of water resulted in the formation of hornblende or biotite from clinopyroxene and plagioclase. The initial stage in this reaction was the formation of hornblende inclusions within the clinopyroxene. These inclusions are preserved only in thin sections which contain abundant biotite. This was probably due to the competition between the growing biotite and hornblende for water and ferromagnesian reactants, resulting in an arrested hornblende reaction where the rock was potassic enough to form biotite. Where the metagabbro did not contain enough potassium to form biotite, the hornblende-forming reaction was able to proceed instead. The water content was low enough in most of the metagabbro to prevent all of the pyroxene from being consumed. As the hornblende-forming reaction proceeded, the hornblende became

richer in magnesium, and the biotite became locally unstable, and reacted to form more hornblende, as evidenced by irregular and embayed inclusions of biotite within hornblende in some thin sections.

The garnet-forming reaction apparently occured sometime after the hornblende-forming reaction had been able to proceed, inasmuch as large embayed hornblendes occur within garnet, and twinned clinopyroxenes embayed by hornblende occur as inclusions within garnet. Based upon the similar textural and chemical zoning patterns of garnet in the metagabbro and the anorthosite, the occurrences of the rounded and embayed inclusions within the garnet porphryroblasts, and the association of the larger garnet porphyroblasts with mafic layers, it is concluded that the reaction was:

orthopyroxene + hornblende + clinopyroxene
+ more calcic plagioclase $\longrightarrow$
garnet + quartz

This is the same as the reaction proposed by Novillo to account for garnet in those parts of the anorthosite which contain green hornblende.

The small orthopyroxene and plagioclase grains which locally occur adjacent to the hornblende, and the irregular inclusions of hornblende in clinopyroxene are interpreted to result from the reaction of hornblende with increasing temperature to form orthopyroxene, clinopyroxene, and plagioclase. The timing of this

reaction relative to the garnet-forming reaction cannot be specified. A similar reaction was noted in the anorthosite by Novillo (1981), although this did not produce clinopyroxene. A similar reaction involving quartz is generally used to define the transition from the hornblende-granulite subfacies to the pyroxene-granulite subfacies (Winkler, 1979).

The final reaction involves the consumption of garnet. Its timing relative to the hornblende-consuming reaction cannot be deduced from the petrographic evidence available. It occurs at the interface between hornblende and garnet, and produces the small zoned plagioclase grains which embay both phases, and perhaps the associated biotite as well, i.e.:

hornblende + garnet $\longrightarrow$ plagioclase + biotite

This same reaction was proposed by Luther (1976) to produce the thin inner corona of plagioclase and biotite between garnet porphyroblasts and their hornblende shells at Gore Mountain. He noted that it does not balance chemically, in that it produces too much Fe and Mg. In the garnet hornblendite, the biotite is not adjacent to the garnet, but is scattered through the hornblende rim, suggesting an open-system reaction, or that it may be linked with some other reaction.

Origin of the Ruby Mountain Metagabbro

Protolith: The Ruby Mountain metagabbro appears to represent a cumulate layer formed during the crystallization of the gabbroic anorthosite, based on the differences in bulk chemistry between the metagabbro and anorthosite. The upper metagabbro layer may be due to a later episode of accumulation of mafic minerals. Such repetition of cumulate layers is common in large basic igneous bodies. This origin follows the model suggested by Ashwal (1982) to account for the origin of conformable bodies of metagabbro within anorthosites. Based on the normative mineralogy, the cumulate phases were probably mainly orthopyroxene and plagioclase, with lesser amounts of clinopyroxene and minor olivine. A possible simplified structural interpretation is shown in Figure 18.

Metamorphic history: The metamorphism of the metagabbro and the anorthosite was identical in all aspects but one, namely the lower overall water content of the metagabbro as evidenced by locally high ratios of pyroxene to hornblende. This also resulted in a lower fO_2, as noted on p 58. Novillo (1981) estimated the peak temperature of metamorphism of the anorthosite as 723°C to 772°C, assuming a pressure of 8 Kbars (Whitney and McLelland, 1973). These same conditions must have held for the metagabbro as well. As in the anorthosite, water penetrated the body along foliation planes and contacts. Where fH_2O was relatively high, the metagabbro was

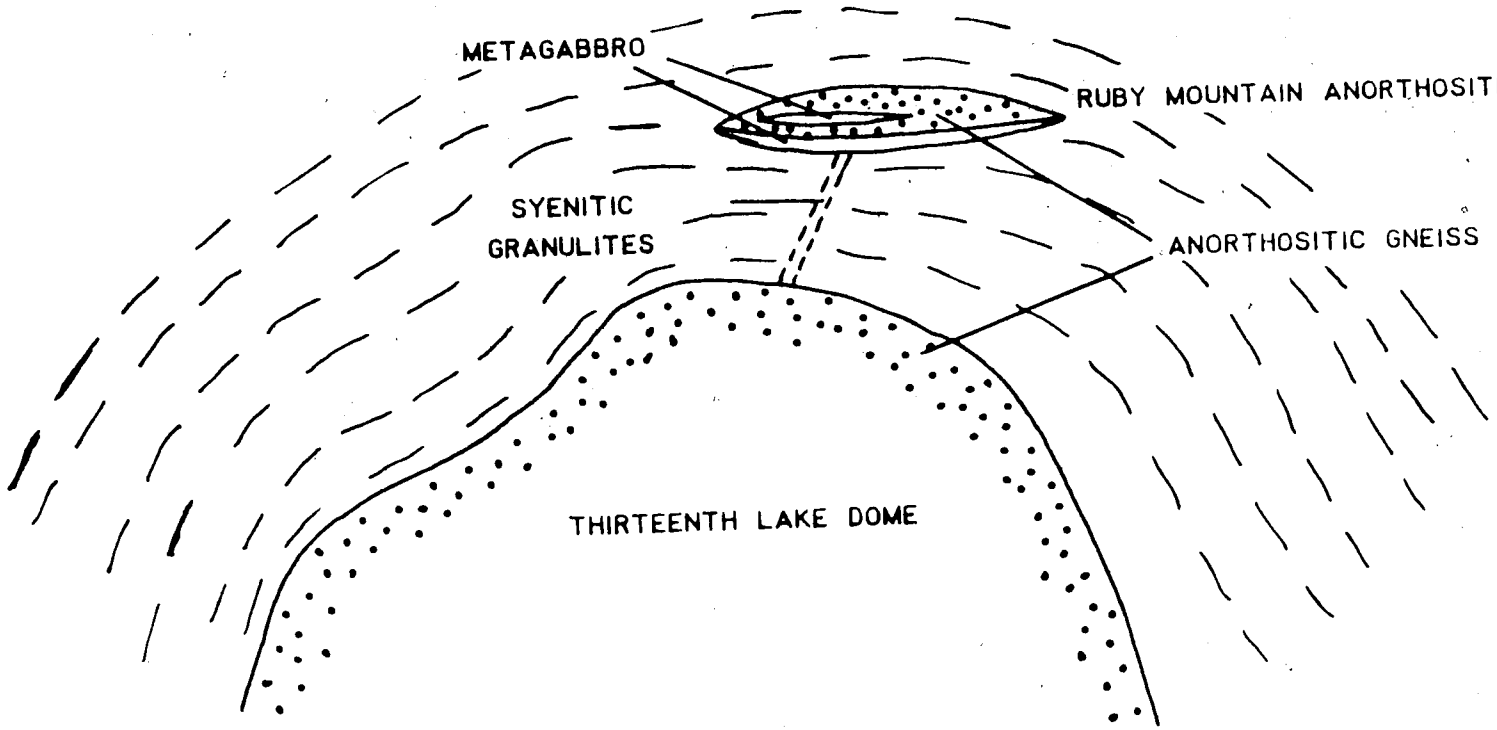

Figure 18. Schematic diagram of possible interpretation of the Ruby Mountain anorthosite and associated metagabbro with the Thirteenth Lake dome.

converted to a garnet hornblendite, or, where plagioclase was more abundant, a garnet amphibolite, with garnets growing to a relatively large size. Where fH_2O was relatively low, and consequently, hornblende was less abundant relative to pyroxene, garnet nucleation was favored over growth, and more individuals were formed.

THE SPECULATOR METAGABBRO

Introduction

The Speculator metagabbro is located about 1 Km. north of the village of Speculator, New York. Within it is a zone containing garnet porphryroblasts up to 8 cm in diameter. The rest of the metagabbro contains garnet, but as disseminated crystals rather than large porphryroblasts. This occurrence of garnet does not resemble other occurrences of large garnets in the Adirondacks such as Ruby Mountain and Gore Mountain. This study deals with the origin of this localized occurrence of large garnets in the Speculator metagabbro, the factors controlling the formation of the garnet, and the relationship of this metagabbro to other garnetiferous meta-igneous bodies.

Field Relations

The metagabbro is shown on the New York State Geological Map (Isachsen and Fisher, 1970) as both metagabbro and amphibolite derived from metagabbro. It is elliptical in outcrop pattern, roughly 10 Km. in length and 3 Km. at its maximum width (Figure 19). The country rock is composed of metasedimentary rocks and hornblende-biotite granitic gneisses which are locally pyroxene-bearing, rather than syenitic granulites as at other garnet-bearing

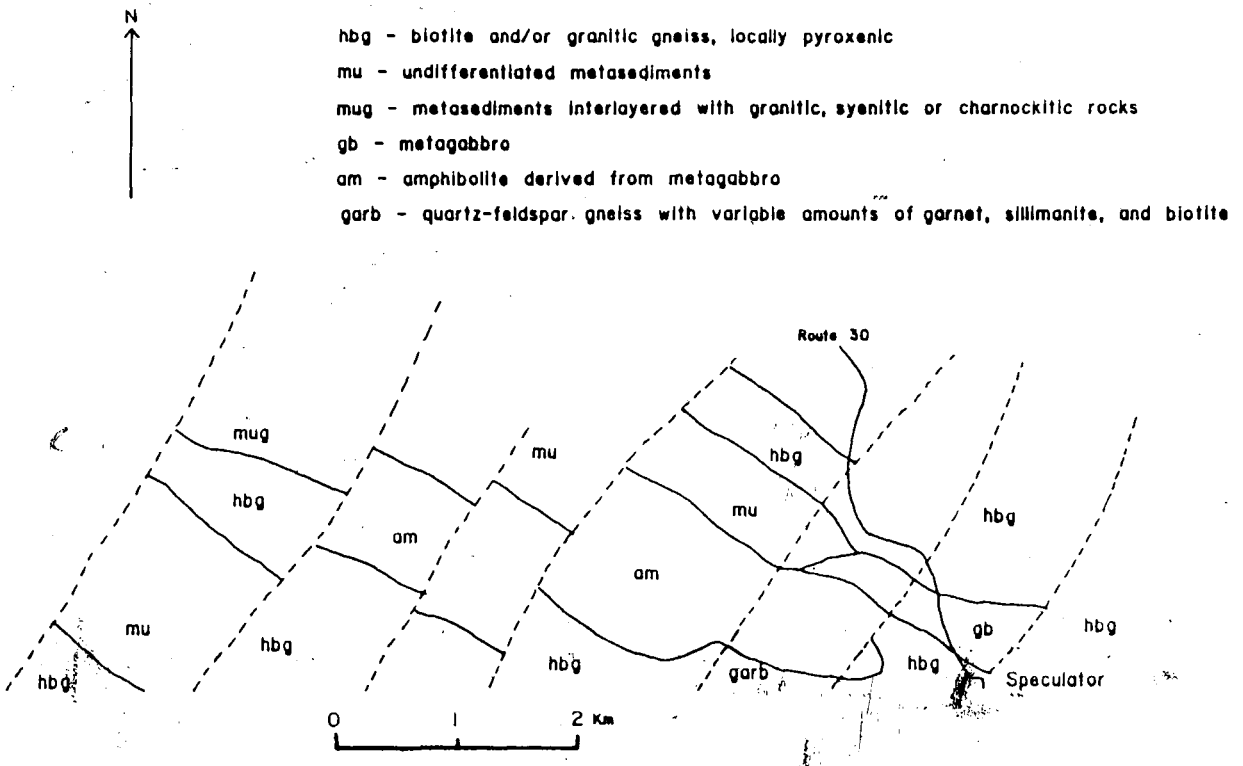

Figure 19. Geological map of the Speculator metagabbro (From the Geological Map of New York State, Isachsen and Fisher, 1970).

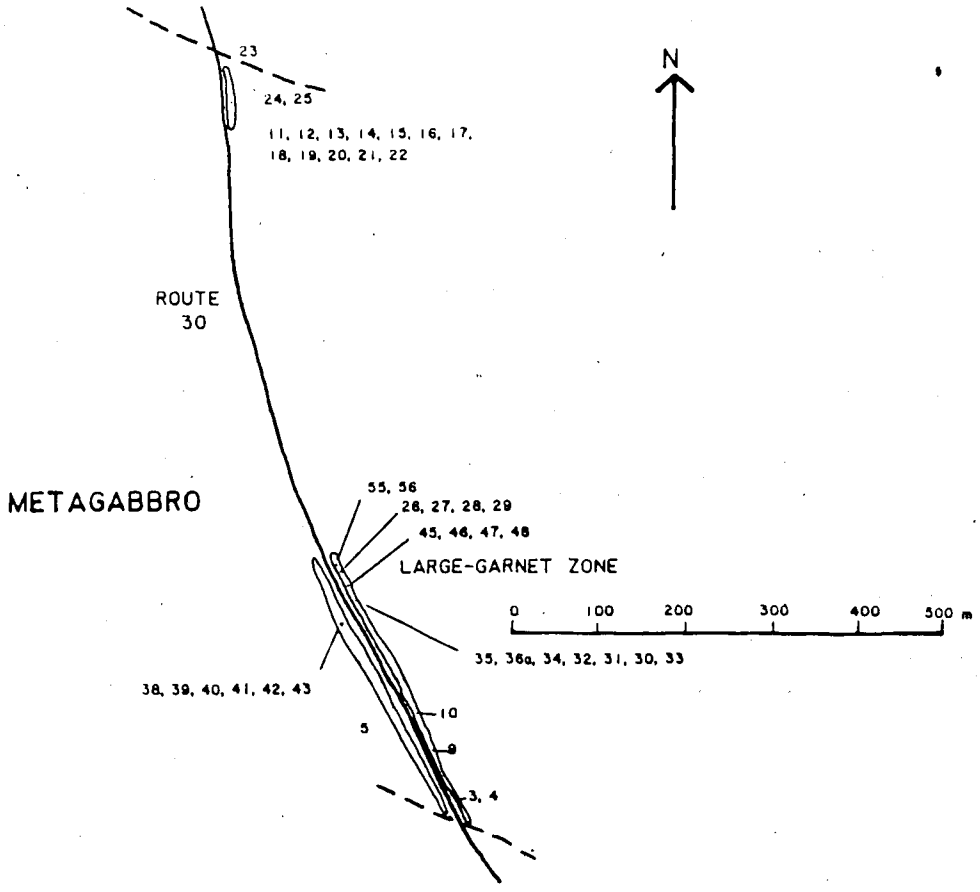

Figure 20. Sketch map of sample locations, Speculator metagabbro.

metagabbros. The exposure is extremely poor, except along State Highway 30. It is from the roadcuts on route 30, which are fairly continuous across the width of the metagabbro, that samples were taken (Figure 20).

The metagabbro is a medium-grained mafic rock. It is weakly foliated to massive. In the center of the metagabbro, there are several subhorizontal mafic layers, about 9 cm thick. They are not parallel to the large-garnet zone, and probably are relict igneous layering. These are thicker and more continuous than the metamorphic foliation. Several irregular pegmatitic segregations also occur in the interior of the metagabbro. They range from several meters to less than 1 meter in size, and are much coarser grained than the rest of the metagabbro, with crystals up to several cm in size.

The large garnets occur in a zone that dips shallowly to the north. Garnet sizes do not gradually increase towards the zone, which is fairly sharply bounded. It is coarser grained than the metagabbro. The garnets are generally spherical, highly fractured by parallel parting cracks, and do not show idiomorphic crystal faces. They occur scattered throughout a garnet-free matrix. Adjacent to the garnet, grains of hornblende locally up to one cm in size may occur. Rims of hornblende or plagioclase do not occur around these garnets. Furthermore, fewer individual garnets are present in this zone than elsewhere. The volume percentage of garnet is approximately the same in the metagabbro and in the large

garnet zone. The petrography will be described further in a later section.

The contacts of the metagabbro body are not exposed. However, the northernmost exposure of the metagabbro contains a large, irregular body of granitic gneiss within the metagabbro. The body is not exposed in three dimensions, so one cannot determine by the field relations alone whether it is a xenolith or a younger intrusion which cuts the metagabbro. Hovever, there are very diffuse pockets of less mafic metagabbro near the granitic gneiss, which may represent xenoliths of the granitic gneiss partly assimilated by the metagabbro. Additionally, examination of thin sections reveals evidences of strain within the gneiss, such as bent plagioclase twins and undulose extinction in quartz. Features indicative of strain are absent from the metagabbro. These features suggest that the body is a xenolith of strained gneiss within the metagabbro. The relative age of the metagabbro is thus younger than the granitic gneiss. However, the age relationship of this granitic gneiss to the syenitic granulite at Ruby Mountain and Gore Mountain is not known.

Bulk Chemistry

Chemical analyses of the Speculator metagabbro are given in Table 2, along with the corresponding norms. It is evident that this body is an olivine normative metagabbro. It is more mafic than the Gore Mountian metagabbro, with higher Fe, Mg, Ca, and Ti, and lower Na and Al. The body is not chemically homogeneous as can be seen from the variable mineralogy. There was an addition of potassium near the xenolith of granitic gneiss, as evidenced by abundant biotite. This may be an original igneous feature. In the interior of the gabbro, chemical variations are due to igneous differentiation, which resulted in the formation of mafic cumulate layers. During metamorphism, PH_2O must have been highly variable, perhaps on a scale of centimeters, based upon the local occurrence of pyroxene rather than hornblende in some thin sections. In addition, hornblendes seem to exhibit different Fe^{3+}/Fe^{2+} ratios, as estimated by the procedure of Robinson et al. (1982). If these interpretations are correct, they imply that fO_2, and, PH_2O were variable within the body during metamorphism.

Mineralogy, Petrography, and Mineral Chemistry

General Statement: The minerals in the metagabbro are plagioclase, garnet, clinopyroxene, orthopyroxene, magnetite, ilmenite, biotite and hornblende. Minor amounts of potassium feldspar, apatite, and clinozoisite also occur. Table 8 lists some representative modes from different locations within the body.

The texture in thin section is generally granoblastic. Some thin sections exhibit a foliation, defined by lenslike aggregates of mafic minerals. Neither relict igneous textures nor corona structures occur in the body. The mafic layers contain the same minerals and textures as the metagabbro. The proportion of plagioclase is less in these layers, and the ratio of pyroxene to hornblende is variable.

Plagioclase: Plagioclase occurs as equant grains, irregularly shaped antiperthitic grains, or zoned, highly embayed and partially sericitized grains. The antiperthitic grains only occur near the margins of the gabbro. The highly embayed grains sometimes occur in the neighborhood of garnet porphryroblasts in the large-garnet zone, and in a thin section from a region near the southern contact where some fairly large garnet porphryroblasts occur. The equant grains are distributed throughout the body. Spinel clouding was not observed.

Table 8

Modal Mineralogy of Speculator Metagabbro

	S-14	S-23	S-28	S-29	S-38	S-55
garnet	0.0	0.0	0.0	22.6	5.2	0.0
plagioclase	55.2	60.3	52.6	25.8	44.3	49.4
orthopyroxene	1.4	6.7	0.0	1.8	2.6	0.0
clinopyroxene	22.4	18.0	45.3	40.6	19.5	20.6
hornblende	15.9	6.4	2.1	4.4	26.7	29.8
biotite	5.1	tr	0.0	0.0	0.0	0.0
opaques	tr	7.4	tr	4.6	1.3	0.0
accessories*	tr	tr	tr	tr	tr	tr
total	100.0	98.8	100.0	99.8	99.6	99.8

* clinozoisite, apatite, calcite

Opaques consist of ilmenite and magnetite.

(Table 8, Continued)
Sample descriptions

S-14 Metagabbro from contact with granitic gneiss xenolith, northernmost outcrop of metagabbro.

S-23 Normal metagabbro, several meters from xenolith, northernmost outcrop of metagabbro.

S-28 Large-garnet zone, matrix between garnet porphyroblasts

S-29 Large-garnet zone, relatively fine-grained region containing small irregularly shaped garnet grains.

S-38 Normal metagabbro, just above mafic layer.

S-55 Large-garnet zone, several cm from garnet porphyroblast.

The equant plagioclase grains (Figure 21) are xenoblastic and range from about .5 mm in diameter at the margins of the gabbro to 3 mm in diameter in the large-garnet zone. There is no systematic grain-size variation within the body, with the exception of the large-garnet zone and the pegmatitic segregations. The individual grains possess straight or slightly curved grain boundaries. Zoning is fairly common. Some grains exhibit albite or pericline twinning, but many are untwinned. Grain boundaries between plagioclase and pyroxene or hornblende are sometimes irregular and embayed (Figure 22).

Antiperthitic grains are generally inequant and xenoblastic, with irregular grain boundaries. They are about 1 mm in diameter. Their occurrence is restricted to the vicinity of the the xenolith and the margins of the gabbro, where they may be fairly abundant. They often exhibit zoning.

The highly embayed plagioclase grains (Figure 23) are generally equant in shape. Their size is the same as the matrix plagioclase. Their distribution even within the large garnet zone is quite erratic. In general, they occur near garnet porphryroblasts, but they are not always present near them. They may be surrounded by symplectites of hornblende and sericitized plagioclase. This textural type often shows zoning, espescially when surrounded by a symplectite. The zoning is usually weak, except in a narrow rim along the grain boundary. In general, this texture appears to be of retrograde origin.

Figure 21. Photomicrograph of equant, granoblastic plagioclase matrix of Speculator metagabbro. Crossed polarizers, 45X. Pc=plagioclase, Cpx=clinopyroxene, Ct=secondary calcite.

Figure 22. Photomicrograph of embayed contacts between plagioclase and clinopyroxene. Plane polarized light, 45X. Pc=plagioclase, Cpx=clinopyroxene.

Figure 23. Photomicrograph of highly embayed plagioclase from large-garnet zone near a garnet porphyroblast. The grain is surrounded by optically unresolvable microcrystalline material, outside of which is an aggregate of hornblende and clinopyroxene. Crossed polarizers, 45X. Pc=plagioclase, Hb=hornblende.

Composition: Electron microprobe analyses of plagioclases are listed in Table 9. As with the Ruby Mountain plagioclases, the analyses are poor. The reasons for this are given in the section on the Ruby Mountain plagioclase.

Matrix plagioclase in the large-garnet zone has a composition of An_{61}, and contains only trace amounts of Or. Where zoning is present, it is a slight reverse zoning, evidently resulting from the incorporation of sodium in the nearby hornblende. In the normal metagabbro, the matrix plagioclase has a composition of An_{34}, and the Or content is higher. When adjacent to garnet, the composition of this textural type is about An_{36}.

The other prominent textural type, the large embayed plagioclases in the large-garnet zone, show pronounced reverse zoning from An_{57} in the core to An_{78} on the rim. This is probably due to the incorporation of Na in hornblende, which is very abundant in this thin section.

Pyroxene: Both orthopyroxene and clinopyroxene are present in varying proportions within the body. The clinopyroxene is a gray-green, non-pleochroic, diopsidic augite. Orthopyroxenes are moderately pleochroic, pink to gray-green hypersthenes. Where metamorphic foliation is present, it is defined in part by pyroxenes.

Table 9

Electron Microprobe Analyses of Plagioclases, Speculator Metagabbro

	S28-1	S28-2	S38-1	S38-2	S26-1	S26-3	S38-3
SiO_2	51.75	51.52	57.69	56.36	51.85	48.13	58.04
Al_2O_3	32.37	32.56	28.61	29.41	32.42	35.26	28.12
CaO	13.77	13.72	9.00	10.19	12.98	16.63	8.51
Na_2O	4.86	4.64	8.89	7.33	5.31	2.50	9.03
K_2O	0.0	0.01	0.08	0.04	0.03	0.03	0.10
Total	102.75	102.46	104.27	103.32	102.59	102.54	103.80

Number of Cations per 8 Oxygens

Si	2.297	2.292	2.504	2.467	2.303	2.152	2.527
Al	1.693	1.707	1.463	1.517	1.697	1.858	1.443
Ca	.655	.653	.418	.477	.618	.797	.397
Na	.418	.400	.747	.621	.457	.216	.762
K	0.0	0.0	.004	.002	.001	.001	.005

End Member Molecular Proportions

An	61.0	62.0	35.8	43.4	57.3	78.5	34.0
Ab	39.0	38.0	63.9	56.4	42.4	21.3	65.4
Or	0.0	tr	0.4	0.2	0.3	0.2	0.6

(Table 9, Continued)
Sample Descriptions

S 28-1 Center of a matrix plagioclase grain, not associated with garnet, large garnet zone.

S 28-2 Rim of same grain, adjacent to grains of clinopyroxene and hornblende.

S 38-1 Small plagioclase grain, adjacent to hornblende and pyroxene, metagabbro south of large garnet zone.

S 38-2 Small plagioclase grain adjacent to garnet, same thin section.

S 38-3 Plagioclase grain associated with orthopyroxene, same thin section.

S 26-1 Center of heavily embayed, zoned plagioclase grain, large garnet zone.

S 26-3 Rim of same grain.

Clinopyroxene: Two textural types of clinopyroxene exist in the body. These are (1) slightly inequant grains which may be twinned or contain hornblende lamellae, or (2) small equant grains which are generally free of inclusions. The relative proportion of the two types varies throughout the body.

Type (1) occurs throughout the metagabbro as inequant, xenoblastic grains, generally up to 3 mm in diameter. The grain boundaries are generally irregular. As at Ruby Mountain, they may contain twin lamellae. In places, hornblende grains are adjacent, either partly or completely surrounding the clinopyroxene, and the clinopyroxene is slightly embayed. This type also occurs as highly embayed inclusions in garnet porphyroblasts. Clinopyroxene containing thin lamellae of hornblende occur only in the large-garnet zone. These lamellae are optically continuous with adjacent grains (Figure 24). In some places, small anhedral inclusions of hornblende occur as well. As at Ruby Mountain, this represents the incipient reaction of clinopyroxene to form hornblende in a relatively dry part of the gabbro.

The second type consists of roughly equant xenoblastic grains, which usually possess straight grain boundaries and exhibit a granoblastic texture. They may occur as rims around inequant clinopyroxene along with orthopyroxene (Figure 25), or as grains scattered throughout the plagioclase matrix, or as lens-like aggregates which define the foliation (Figure 26). Some of the grains may contain anhedral inclusions of brown hornblende. These

Clinopyroxene: Two textural types of clinopyroxene exist in the body. These are (1) slightly inequant grains which may be twinned or contain hornblende lamellae, or (2) small equant grains which are generally free of inclusions. The relative proportion of the two types varies throughout the body.

Type (1) occurs throughout the metagabbro as inequant, xenoblastic grains, generally up to 3 mm in diameter. The grain boundaries are generally irregular. As at Ruby Mountain, they may contain twin lamellae. In places, hornblende grains are adjacent, either partly or completely surrounding the clinopyroxene, and the clinopyroxene is slightly embayed. This type also occurs as highly embayed inclusions in garnet porphyroblasts. Clinopyroxene containing thin lamellae of hornblende occur only in the large-garnet zone. These lamellae are optically continuous with adjacent grains (Figure 24). In some places, small anhedral inclusions of hornblende occur as well. As at Ruby Mountain, this represents the incipient reaction of clinopyroxene to form hornblende in a relatively dry part of the gabbro.

The second type consists of roughly equant xenoblastic grains, which usually possess straight grain boundaries and exhibit a granoblastic texture. They may occur as rims around inequant clinopyroxene along with orthopyroxene (Figure 25), or as grains scattered throughout the plagioclase matrix, or as lens-like aggregates which define the foliation (Figure 26). Some of the grains may contain anhedral inclusions of brown hornblende. These

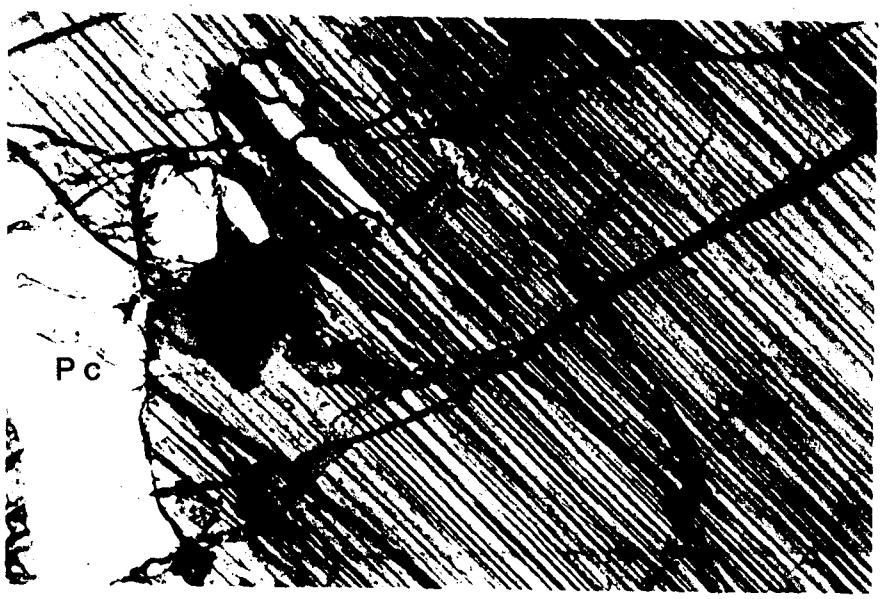

Figure 24. Photomicrograph of clinopyroxene from the large-garnet zone, showing hornblende lamellae and adjacent, optically continuous hornblende grains. Plane polarized light, 130X. Pc=plagioclase, Hb=hornblende, Cpx=clinopyroxene.

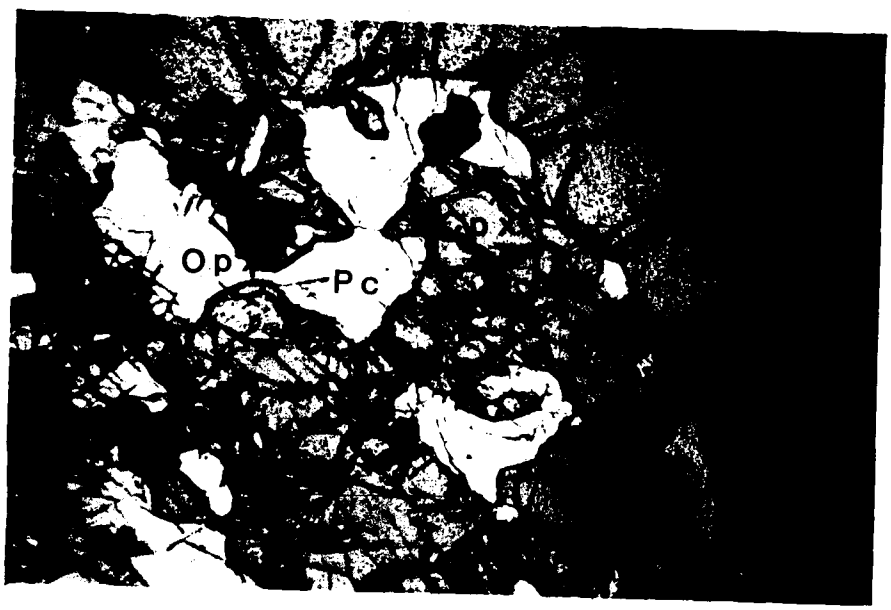

Figure 25. Photomicrograph of xenoblastic garnet associated with clinopyroxene, and exhibiting embayed and irregular grain boundaries. Plane polarized light, 45X. Gt=garnet, Pc=plagioclase, Opx=orthopyroxene, Cpx=clinopyroxene.

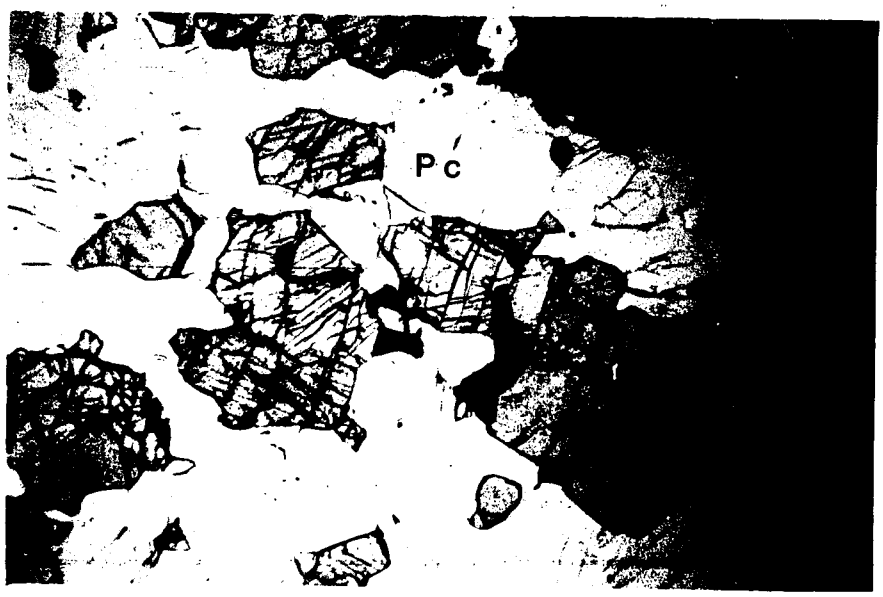

Figure 26. Photomicrograph of granoblastic aggregates of clinopyroxene which locally define the metamorphic foliation in the Speculator metagabbro. Plane polarized light, 45X. Pc=plagioclase, Cpx=clinopyroxene.

clinopyroxenes are obviously of metamorphic origin. An interesting point to note is that this type of clinopyroxene is absent in that portion of the large-garnet zone between the garnet porphyroblasts. It does occur near the porphyroblasts, along with hornblende and orthopyroxene.

Composition: There is a difference in composition between the clinopyroxenes in the large-garnet zone and those in the metagabbro. The average composition of inequant clinopyroxenes from the large-garnet zone is Wo 46.8, En 40.5, Fs 12.7. The average composition of clinopyroxene from the normal metagabbro is Wo 45.1, En 37.3, Fs 17.6. Both types plot as metamorphic pyroxenes, as can be seen from Figure 27 (based on their high Ca content). These differences probably reflect differences in bulk chemistry and time and mode of origin. An additional difference is that the inequant clinopyroxenes tend to show a higher content of Al_2O_3 than do the equant clinopyroxenes. This is not a sharp demarcation, however, and there is some overlap. Table 10 lists some representative analyses of pyroxenes.

Orthopyroxenes: Orthopyroxenes occur in variable amounts throughout the body. Three basic textural types occur.

The first textural type consists of equant, xenoblastic grains which are generally associated with clinopyroxenes of similar texture. They possess straight grain boundaries, and form a

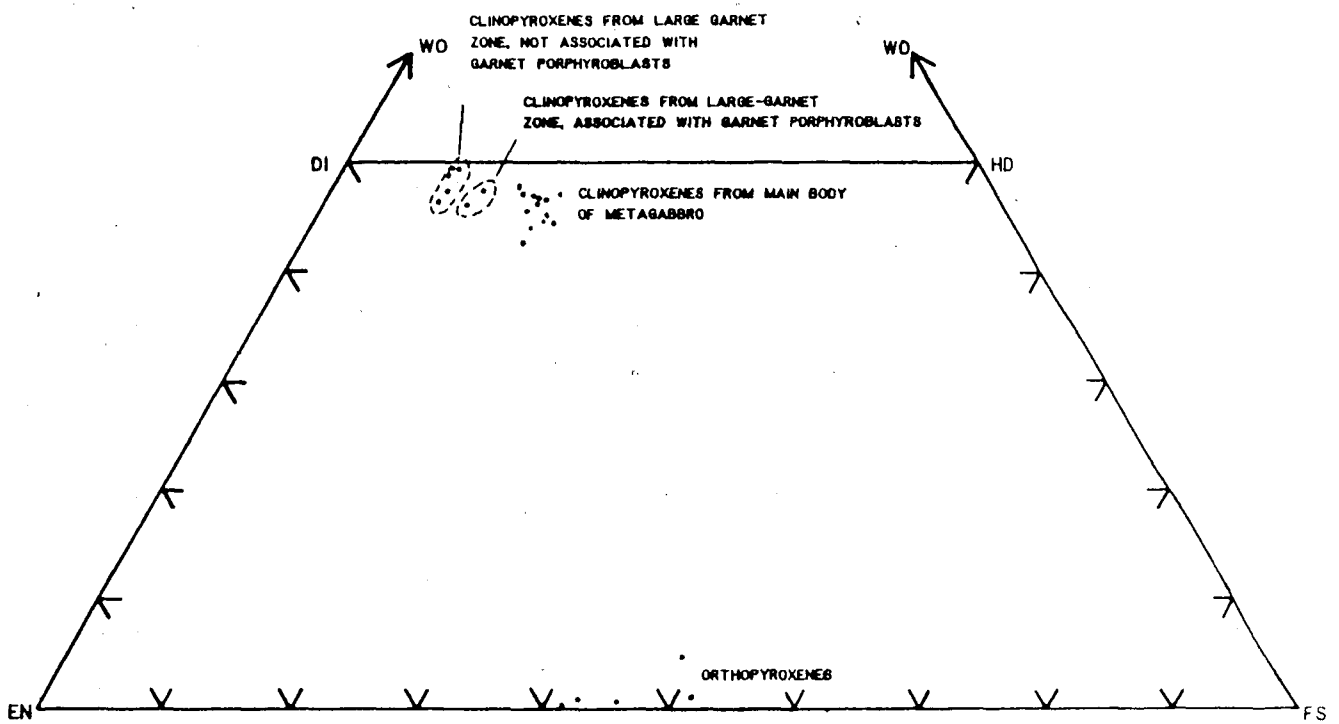

Figure 27. Ternary plot of microprobe analyses of pyroxenes from the Speculator metagabbro in terms of Wo, En, and Fs.

Table 10

Electron Microprobe Analyses of Pyroxenes and Hornblendes, Speculator Metagabbro

	S28-1	S38-1	S38-3	S38-8	S42-4	S42-5	S42-10	S42-11	S23-1
SiO_2	51.19	50.27	52.88	51.87	51.15	51.35	52.02	51.95	50.80
TiO_2	0.75	0.34	0.13	0.35	0.52	0.52	0.13	0.31	0.13
Al_2O_3	6.13	3.38	1.31	2.44	3.83	3.68	1.12	2.35	1.07
FeO	5.40	10.30	26.69	11.14	11.12	11.12	30.30	11.01	31.52
MnO	0.0	0.0	0.0	0.0	0.0	0.0	0.0	0.0	0.0
MgO	13.80	13.15	19.96	11.76	11.90	12.25	17.37	12.84	16.33
CaO	22.61	19.60	0.51	22.25	20.39	20.91	0.35	21.71	0.56
Na_2O	1.48	1.26	0.0	1.15	1.53	1.30	0.0	1.05	0.16
K_2O	0.0	0.0	0.0	0.0	0.0	0.0	0.0	0.0	0.0
Total	101.35	98.30	101.48	100.97	100.42	101.14	101.28	101.23	100.56

	S10-1	S10-3	S10-4	S28hb	S38hb	S56hb	S23hb
SiO_2	52.13	51.74	52.85	42.43	43.01	43.40	41.25
TiO_2	0.45	0.10	0.37	1.70	2.44	0.58	2.22
Al_2O_3	3.53	1.18	2.35	15.88	12.37	14.80	13.09
FeO	10.26	29.18	10.00	10.47	13.89	9.07	18.41
MnO	0.3	0.05	0.04	0.0	0.0	0.0	0.02
MgO	12.53	19.12	12.82	14.31	12.51	14.78	8.55
CaO	21.75	0.42	22.67	11.64	11.56	9.61	11.48
Na_2O	0.94	0.0	0.79	2.68	2.05	4.76	3.01
K_2O	0.0	0.0	0.0	0.04	0.43	0.10	1.39
Total	101.63	101.79	101.89	99.14	98.25	97.11	99.43

(Table 10, Continued)

Number of Cations (Normalized to 6 Oxygens for Pyroxenes, 23 Oxygens for Hornblendes; S28hb, S38hb, S56hb all have cations normalized to 13, exclusive of Ca, Na, K; S23hb analysis is as taken (i.e. all Fe is assumed to be present as Fe^{2+}))

	S28-1	S38-1	S38-3	S38-8	S42-4	S42-5	S42-10	S42-11	S23-1
Si	1.860	1.915	1.972	1.990	1.915	1.911	1.977	1.934	1.964
Ti	.020	.009	.003	.010	.014	.014	.003	.008	.003
Al	.262	.151	.057	.107	.169	.161	.050	.103	.048
Fe	.164	.328	.832	.348	.348	.346	.963	.342	1.019
Mg	.747	.747	1.109	.656	.664	.676	.984	.712	.941
Ca	.880	.800	.020	.891	.818	.833	.014	.865	.023
Na	.104	.093	0.0	.083	.110	.094	0.0	.075	.012

	S10-1	S10-3	S10-4	S28hb	S38hb	S56hb	S23hb
Si	1.922	1.950	1.945	5.962	6.230	6.207	6.190
Ti	.012	.002	.010	.179	.270	.062	.251
Al	.153	.052	.101	2.629	2.112	2.494	2.315
Fe^{3+}	----	----	----	.761	.580	.614	0.0
Fe^{2+}	.316	.920	.307	.468	1.100	.468	2.310
Mn	0.0	0.0	0.0	0.0	0.0	0.0	.003
Mg	.689	1.075	.703	2.997	2.700	3.150	1.931
Ca	.859	.016	.894	1.785	1.820	1.495	1.845
Na	.067	0.0	.056	.744	.583	1.340	.876
K	0.0	0.0	0.0	.008	.080	.019	.266

(Table 10, Continued)
End Member Molecular Proportions

	S28-1	S38-1	S38-3	S38-8	S42-4	S42-5	S42-10	S42-11	S23-1
Wo	41.1	38.6	1.0	44.5	40.3	40.5	0.7	42.0	1.2
En	41.6	39.8	56.5	33.1	35.7	36.3	50.1	37.1	47.5
Fs	3.6	12.5	42.4	17.6	14.3	13.9	49.1	13.9	51.4

	S10-1	S10-3	S10-4
Wo	41.9	0.8	44.3
En	36.6	53.4	36.7
Fs	14.4	45.7	13.7

Fe^{2+} and Fe^{3+} calculated by the procedure of Robinson et al. (1981), as outlined on p. 10.

(Table 10, Continued)
Sample Description

S 28-1 Clinopyroxene from large garnet zone, not associated with garnet.

S 38-1 Metamorphic clinopyroxene, from normal metagabbro south of large-garnet zone.

S 38-3 Small orthopyroxene grain adjacent to hornblende, same thin section as S 38-1.

S 38-8 Metamorphic clinopyroxene from lensoid granoblastic aggregate, same thin section as S 38-3.

S 42-4 Twinned clinopyroxene, south of large-garnet zone.

S 42-5 Analyses of a (twin) lamellae, same grain as S 42-4.

S 42-10 Orthopyroxene from granoblastic aggregate surrounding clinopyroxene grain of S 42-5.

S 42-11 Clinopyroxene from same granoblastic aggregate as S 42-10.

S 23-1 Orthopyroxene, near northern contact of metagabbro.

S 10-1 Twinned clinopyroxene, center of metagabbro.

S 10-3 Orthopyroxene from granoblastic aggregate surrounding clinopyroxene of S 10-1.

S 10-4 Clinopyroxene from S 10-3 granoblastic aggregate.

S 28hb Green hornblende lamellae from clinopyroxene in large-garnet zone.

S 38hb Brown hornblende from metagabbro south of large-garnet zone.

S 56hb Pale green hornblende in symplectite with plagioclase, adjacent to garnet porphryroblast, large-garnet zone.

S 23hb Green hornblende, near northern contact of metagabbro.

granoblastic texture. This type occurs either around inequant clinopyroxenes, or as granoblastic aggregates which define the metamorphic foliation in places. These probably result from either recrystallization of igneous clinopyroxenes or of older metamorphic minerals.

The second texture consists of small fingers of orthopyroxene rimming hornblende (Figure 28). It resembles the same textural type described at Ruby Mountain, and doubtless represents the same process, i.e. the breakdown of hornblende to form pyroxene.

The third textural type present consists of inequant, xenoblastic individuals scattered through a plagioclase matrix. These grains are rounded and embayed. This texture tends to occur in the margins of the metagabbro rather than in the interior, and occurs in conjunction with abundant rounded grains of magnetite and ilmenite scattered through the plagioclase matrix. This is definitely a metamorphic texture, and probably represents areas of the body which initially contained orthopyroxene and opaques, but were free of clinopyroxene.

Composition: The orthopyroxenes also plot as metamorphic pyroxenes on the pyroxene quadrilateral as based on Ca^{2+} content. An application of Kretz's (1963) Fe-Mg distribution coefficient (K_D) for an orthopyroxene and an adjacent clinopyroxene in an aggregate surrounding an inequant clinopyroxene yields a K_D value of .52, well

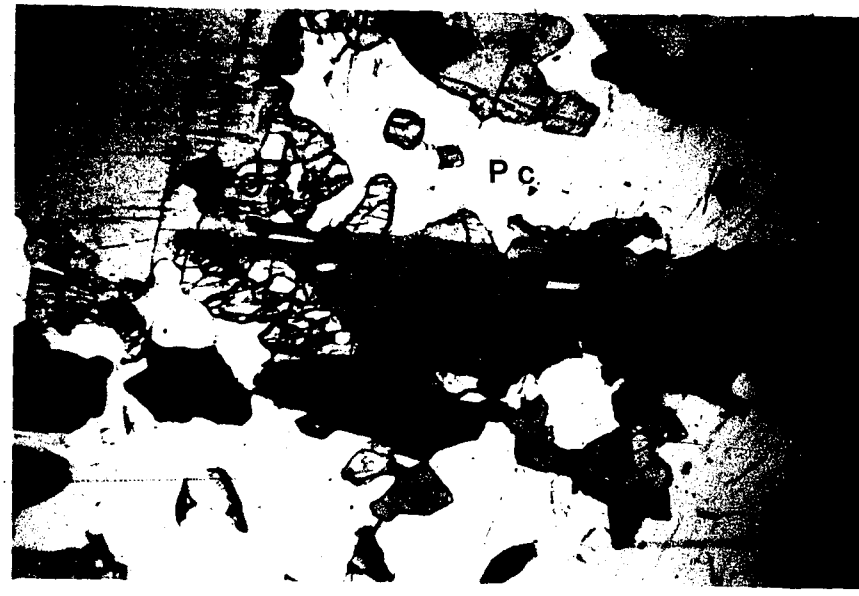

Figure 28. Photomicrograph of hornblende and clinopyroxene defining the metamorphic foliation. Hornblende grains are associated with adjacent small orthopyroxene grains. Plane polarized light, 45X. Pc=plagioclase, Hb=hornblende, Opx=orthopyroxene, Cpx=clinopyroxene.

within the metamorphic range of values. In addition, orthopyroxenes plot in the metamorphic fields of plots of $Fe^{2+}/(Fe^{2+} + Mg)$ versus $100\ Ca/Fe^{2+} + Mg + Ca)$(Rietmeijer, 1983), shown in Figure 29. One analysis of a of a lamellae within a clinopyroxene shows it to be a relatively calcic orthopyroxene; on Reitmeijer's plots, it plots as an igneous orthopyroxene. However, the K_D calculated for this pair is outside the range of values for both metamorphic and igneous pyroxenes (Kretz, 1963). It seems likely that this analysis is incorrect due to microprobe beam overlap with the host.

Hornblende: Several hornblende textures are present in the metagabbro. Most of the hornblende is a light brown to dark brown pleochroic variety. However, towards the margins of the body, the hornblende is pleochroic in dark green to medium green. Hornblende may occur as, (1) irregular grains rimming clinopyroxene, (2) equant clusters of grains defining the foliation, or, (3) in symplectic intergrowth with plagioclase between garnet porphryroblasts and either hornblende or clinopyroxene.

The first textural type is developed throughout the body. The hornblende partly rims and sometimes slightly embays inequant clinopyroxene. In places, hornblende forms rims between orthopyroxene and plagioclase, where it commonly contains abundant inclusions of ilmenite or magnetite (Figure 30). In the large-garnet zone, hornblende does not contain any Fe-Ti oxide

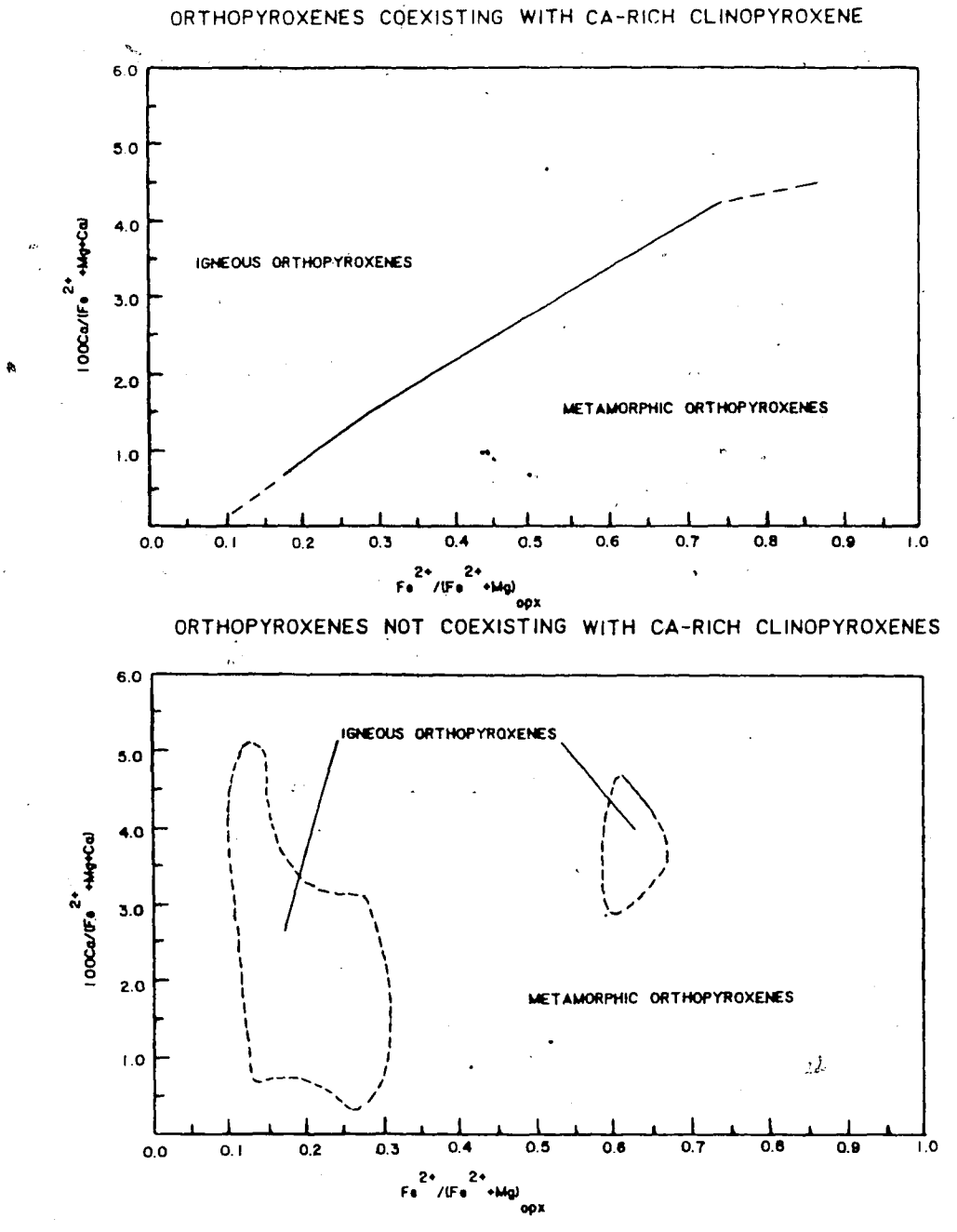

Figure 29. Plot of $Fe^{2+}/(Fe^{2+}+Mg)$ vs. $100Ca/(Fe^{2+}+Mg+Ca)$ for orthopyroxenes after Reitmeijer, 1983), Speculator metagabbro.

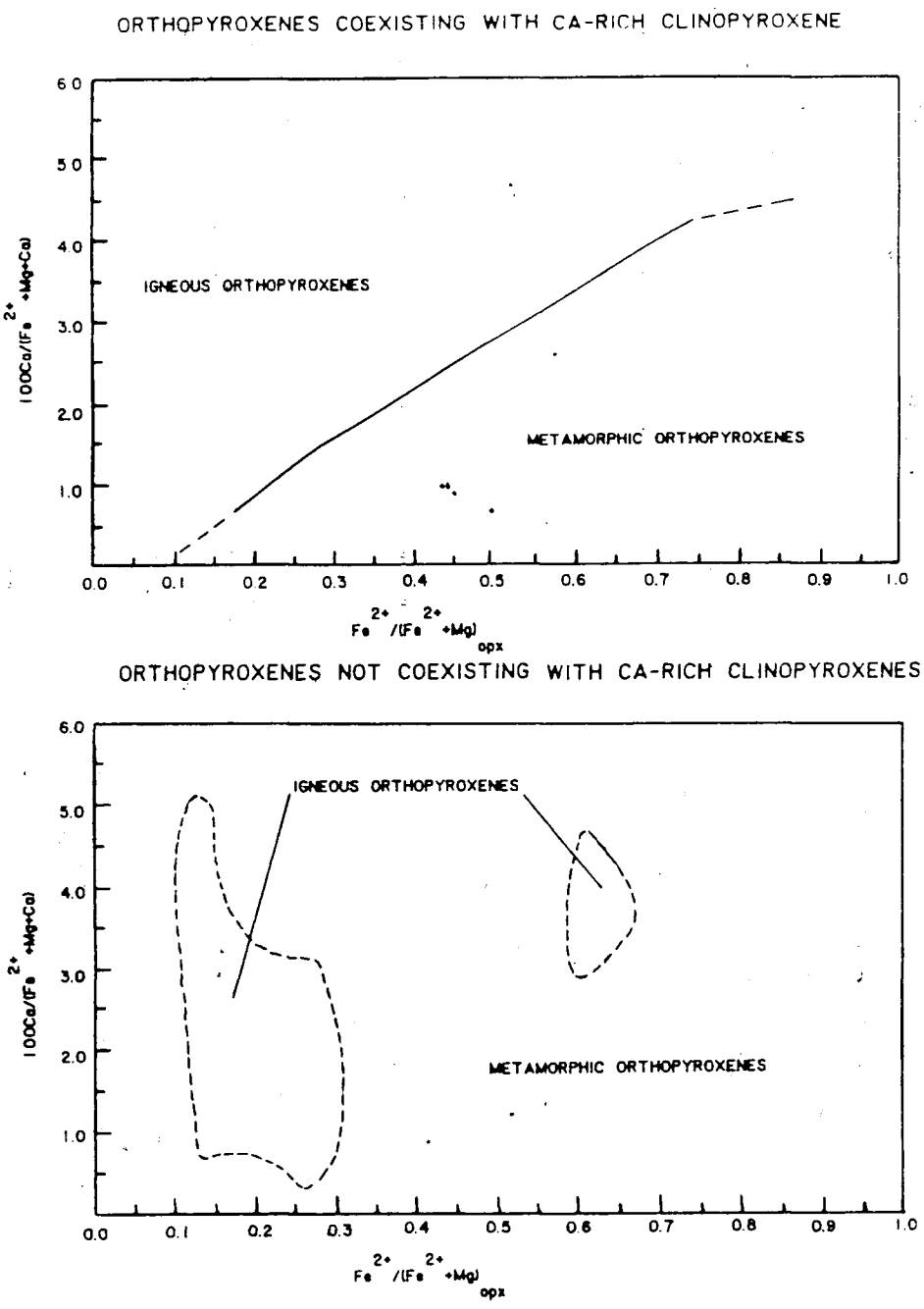

Figure 29. Plot of $Fe^{2+}/(Fe^{2+}+Mg)$ vs. $100Ca/(Fe^{2+}+Mg+Ca)$ for orthopyroxenes after Reitmeijer, 1983), Speculator metagabbro.

Figure 30. Photomicrograph showing hornblende grains with magnetite inclusions. Plane polarized light, 45X. Pc=plagioclase, Opx=orthopyroxene, Cpx=clinopyroxene, Hb=hornblende.

inclusions, and may occur as lamellae or as irregular inclusions within the clinopyroxene. As previously observed (p. 92), this represents the incipient reaction of clinopyroxene to form hornblende.

The second textural type is best developed in the central part of the metagabbro. The grains may be equant or inequant, but generally have straight grain boundaries and form a granoblastic aggregate. These grains may be associated with small protuberances or projections of orthopyroxene associated with small plagioclase grains. Small pyroxenes occurs interstitially within these aggregates. This type may occur in association with garnet porphryroblasts and clinopyroxenes in the large-garnet zone.

The third textural type occurs only as rims around the garnet porphryroblasts in the large-garnet zone (Figure 31). It consists of a symplectite of a very pale green hornblende and sericitized plagioclase. This intergrowth occurs between the garnet and the surrounding mafic phases. It is absent from other parts of the body, even when garnets are porphryroblastic.

Composition: The hornblende shows a wide range of composition. Representative analyses are given in Table 10. It is notable that all of the iron in hornblendes from the margins of the body is Fe^{2+}, as calculated by the procedure of Robinson et al. (1981) outlined on p. 10, possibly reflecting a lower fO_2. It is also noteworthy that the hornblende of the different textural types also show differences

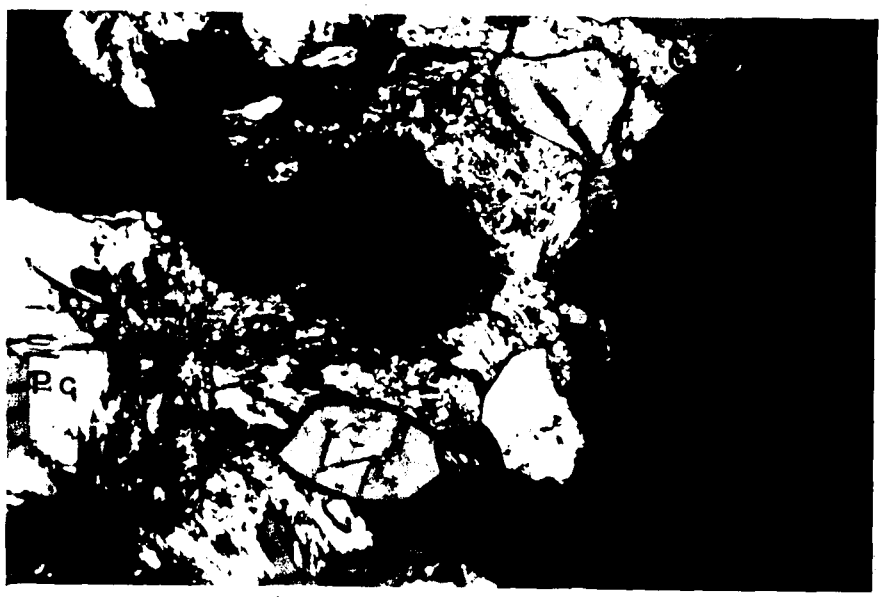

Figure 31. Photomicrograph of plagioclase-hornblende symplectite surrounding a garnet porphyroblast in the large-garnet zone. Hornblende is a sodic, pale-green variety. Plagioclase is sericitized. Crossed polarizers, 130×. Gt=garnet, Hb=hornblende, Pc=plagioclase.

in chemistry. This can be explained by considering the reactions involved. The hornblendes closely associated with clinopyroxenes in the large-garnet zone are high in Al_2O_3 and MgO, and low in total iron due to their derivation from diopsidic augites and plagioclases. As noted in the previous section, these hornblendes are a product of the incipient reaction of clinopyroxene, plagioclase, and water to form hornblende. Inasmuch as they do not show any textures which indicate that they have participated in later metamorphic reactions, except where garnet porphyroblasts are present, the high MgO content is probably not due to a preferential fractionation of iron into possible products of a hornblende-consuming reaction. The higher iron content of the equant hornblendes in other parts of the body may be due to participation of iron-rich phases such as ilmenite in hornblende formation. This is supported by the higher TiO_2 content of these hornblendes, and by the presence of many ilmenite inclusions. The composition of the hornblende in the hornblende-plagioclase symplectite, which apparently represents a garnet-consuming reaction, is also controlled by the composition of the reactants, which are, in this case, garnet and hornblende or clinopyroxene. The extremely low K_2O content in the product hornblende is due to the low K_2O content of the reactants.

Garnet: Garnet generally occurs throughout the metagabbro as xenoblastic grains or clusters of grains, or as cm-size

porphryroblasts. The other type of occurrence is as porphryroblasts in the large-garnet zone, in which the garnets range in size from less than 1 cm to 8 or 9 cm. Coronas are not observed around any textural type of garnet.

The first textural type is generally associated with ferromagnesian-rich layers or lenses, which are typically hornblende-rich. The garnets exhibit irregular grain boundaries which are sometimes slightly embayed by equant or twinned clinopyroxene, hornblende or plagioclase (Figure 32). They are inequant in shape, and commonly contain inclusions of clinopyroxene, hornblende, or plagioclase. Some garnets contain many round inclusions of ilmenite, about .5 mm in diameter. Some garnets are probably clusters of separate grains which have grown together. Garnet is less abundant at the margins of the metagabbro.

The other major textural type consists of the garnet porphryroblasts in the large-garnet zone. Their size ranges from about 1 cm to 8 cm. They are generally equant in shape, but xenoblastic. They may contain embayed inclusions of plagioclase, twinned clinopyroxene, or hornblende. These inclusions may occasionally reach a cm in size. The garnet occurs as individual crystals disseminated through the large-garnet zone. Some grains are inequant and slightly elongate. In some cases, the garnets appear to consist of several individuals which have grown together.

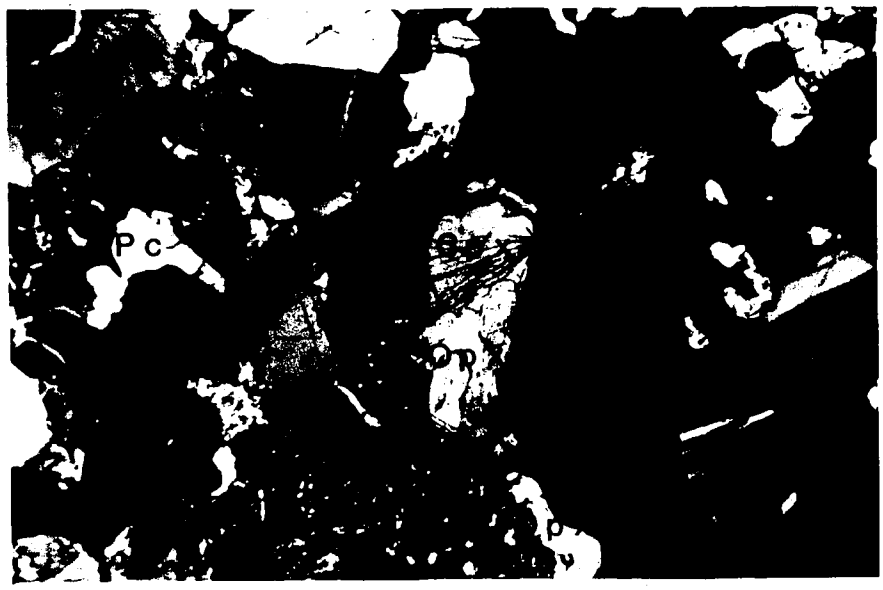

Figure 32. Photomicrograph of xenoblastic garnet, showing highly irregular shape with embayed grain boundaries. Crossed polarizers, 45X. Gt=garnet, Hb=hornblende, Pc=plagioclase, Opx=orthopyroxene, Cpx=clinopyroxene.

Composition: The garnets in the Speculator metagabbro are more almandine-rich than the garnets in the Gore Mountain metagabbro. Representative analyses are given in Table 11, and zoning trends are shown in Figure 33. It is obvious that the large porphryroblasts are unzoned, in contrast to the smaller garnets. This is identical to what has been observed in the Gore Mountain metagabbro, Ruby Mountain metagabbro, and Ruby Mountain gabbroic anorthosite. However, the smaller garnets show a slight decrease in Mg and a corresponding increase in Fe from core to rim. Their overall iron content is higher than that of the large porphryroblasts, making it difficult to produce the large garnet porphyroblasts through homogenization of garnets with the observed zoning trends.

The observed trends may be due to the formation of the large porphryroblasts at higher temperature, with later formation of the garnets in the rest of the body under retrograde conditions. Alternatively, these trends could be a reflection of higher iron content of the main body of the metagabbro relative to the large-garnet zone initially.

Biotite: Biotite is quite rare in the main body of the metagabbro, and exists only as sporadic interstitial flakes. However, it becomes quite abundant near the xenolith. It is closely associated with clinopyroxene, and grain boundaries with clinopyroxene are embayed and irregular. Other biotite flakes contain irregular clinopyroxene inclusions. There is no well-defined relationship

Table 11

Electron Microprobe Analyses From a Traverse Taken Across Garnet Porphyroblasts, Speculator Metagabbro

S42a
Diameter of porphyroblast=0.7cm

	Rim					Rim
SiO_2	37.37	37.75	37.41	37.79	37.26	37.23
Al_2O_3	21.71	22.00	22.13	21.74	22.31	22.13
FeO	27.35	26.07	25.53	25.28	27.32	28.72
MnO	0.93	0.76	0.73	0.72	0.73	0.98
MgO	4.78	5.20	5.19	5.15	5.02	3.93
CaO	7.93	7.89	8.20	8.45	7.68	8.47
Total	100.06	99.67	99.19	99.13	100.32	101.46

Number of Cations per 12 Oxygens

Si	2.942	2.960	2.944	2.974	2.919	2.913
Al	2.014	2.032	2.053	2.015	2.060	2.040
Fe	1.800	1.709	1.680	1.663	1.790	1.879
Mn	.061	.050	.048	.047	.048	.065
Mg	.561	.607	.608	.604	.586	.458
Ca	.669	.662	.691	.712	.645	.710

(Table 11, Continued)

S56

Diameter of porphyroblast=2.9cm

	Rim						
SiO_2	39.80	39.52	39.94	40.47	39.70	40.39	41.81
Al_2O_3	23.04	22.86	22.95	23.17	23.44	23.18	23.12
FeO	18.70	19.78	18.77	18.34	18.35	18.16	18.50
MnO	0.64	0.57	0.57	0.49	0.57	0.60	0.66
MgO	8.16	8.46	8.60	8.33	8.41	8.09	7.65
CaO	9.90	10.56	10.29	10.15	9.83	10.37	10.06
Total	100.24	101.75	101.12	100.96	100.28	100.80	101.81
SiO_2	39.83	39.11	39.25	39.42	38.91	38.87	38.84
Al_2O_3	22.80	22.62	22.95	22.97	22.72	22.39	22.14
FeO	18.42	19.43	18.93	20.69	20.87	20.30	20.92
MnO	0.65	0.84	0.70	1.00	0.96	1.03	0.85
MgO	8.09	8.16	8.13	7.03	7.08	7.07	7.51
CaO	10.13	9.87	10.07	10.72	10.77	10.36	8.93
Total	99.92	100.03	100.03	101.84	101.31	100.02	99.20
			Rim				
SiO_2	39.94	39.47	40.68				
Al_2O_3	22.84	22.48	23.46				
FeO	20.10	18.76	18.61				
MnO	0.74	0.63	0.48				
MgO	7.69	8.31	9.87				
CaO	9.80	9.64	9.87				
Total	101.12	99.28	101.77				

(Table 11, Continued)

Number of Cations per 12 Oxygens

	Rim						
Si	2.998	2.956	2.986	3.017	2.982	3.017	3.085
Al	2.045	2.015	2.022	2.035	2.075	2.040	2.009
Fe	1.178	1.237	1.173	1.143	1.152	1.134	1.140
Mn	.040	.036	.035	.031	.036	.038	.041
Mg	.916	.944	.958	.926	.941	.901	.841
Ca	.798	.846	.824	.811	.791	.830	.795
Si	3.009	2.972	2.973	2.964	2.948	2.974	2.991
Al	2.029	2.025	2.049	2.035	2.029	2.018	2.009
Fe	1.163	1.234	1.198	1.301	1.322	1.299	1.347
Mn	.041	.053	.045	.063	.061	.066	.055
Mg	.911	.924	.918	.788	.799	.806	.862
Ca	.819	.803	.817	.863	.874	.849	.737
			Rim				
Si	3.001	3.005	3.007				
Al	2.022	2.017	2.043				
Fe	1.263	1.194	1.150				
Mn	.047	.040	.030				
Mg	.862	.785	.782				
Ca	.789	.785	.782				

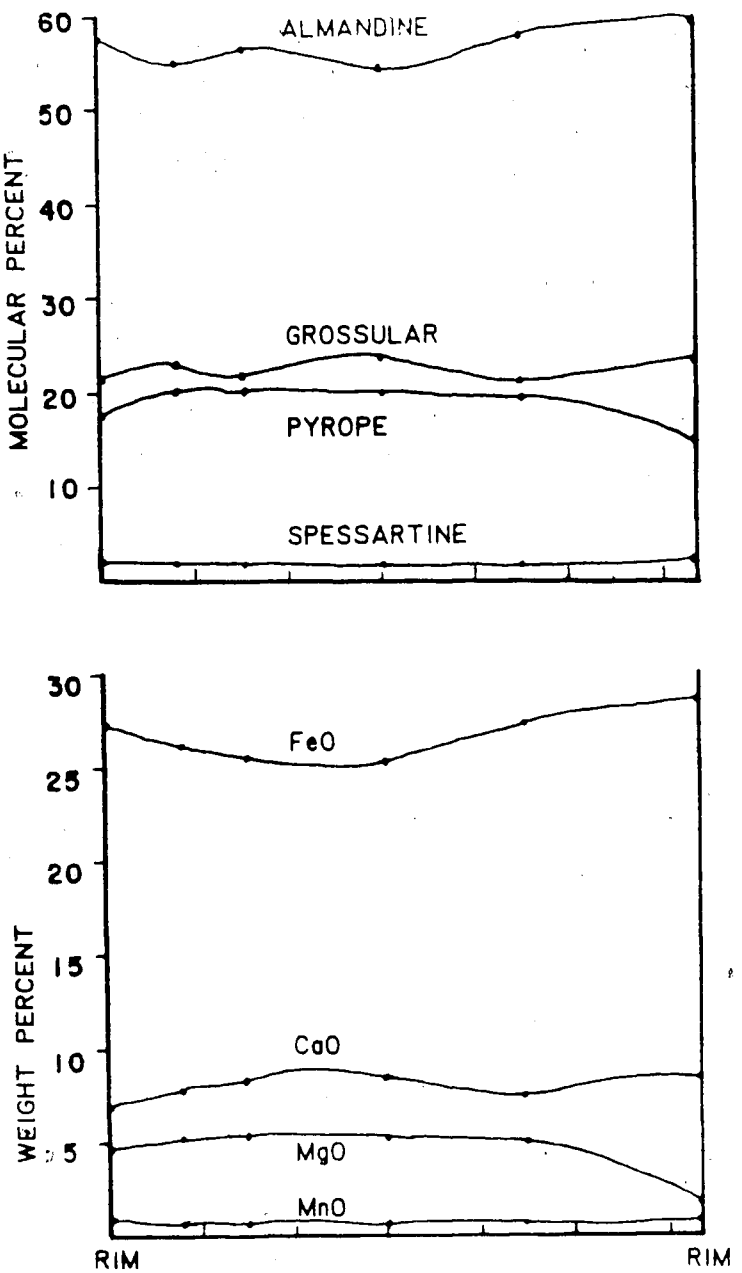

S-42

DIAMETER OF PORPHYROBLAST = 62cm

Figure 33. Representative zoning trends in two garnet porphyroblasts, Speculator metagabbro.

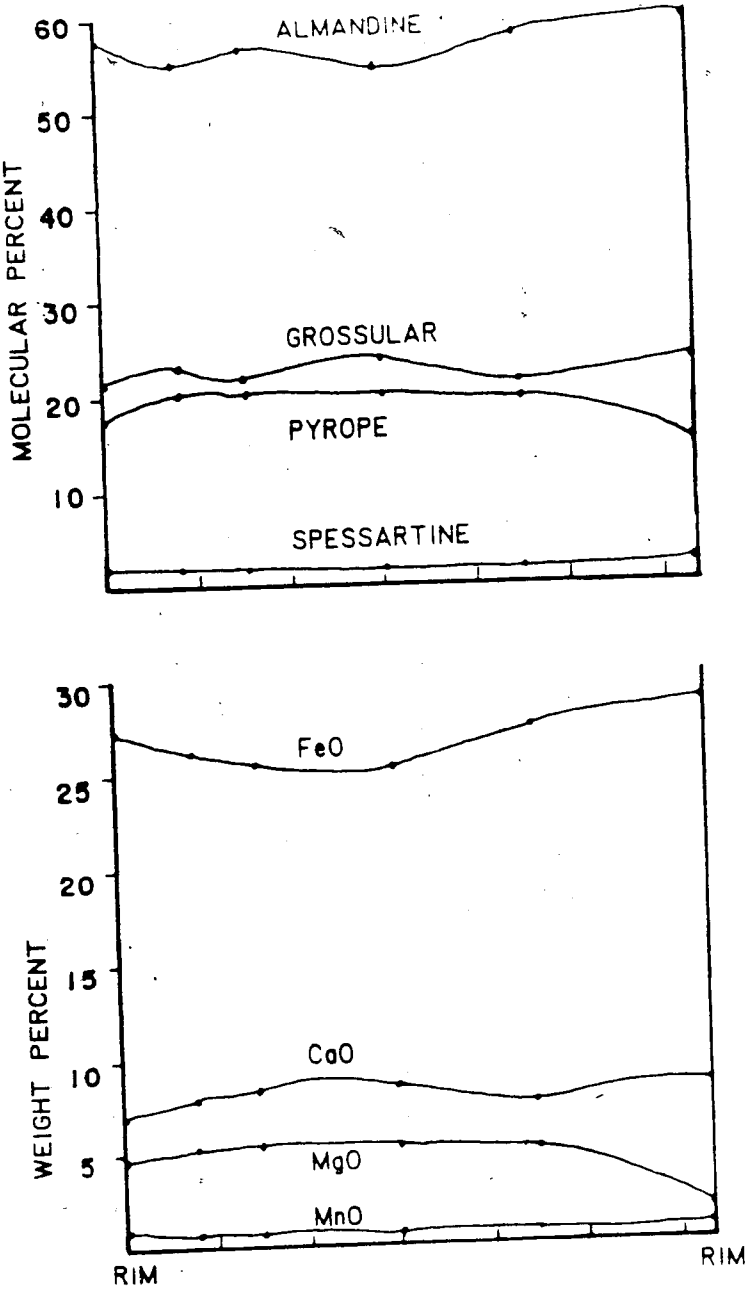

S-42

DIAMETER OF PORPHYROBLAST = 62cm

Figure 33. Representative zoning trends in two garnet porphyroblasts. Speculator metagabbro.

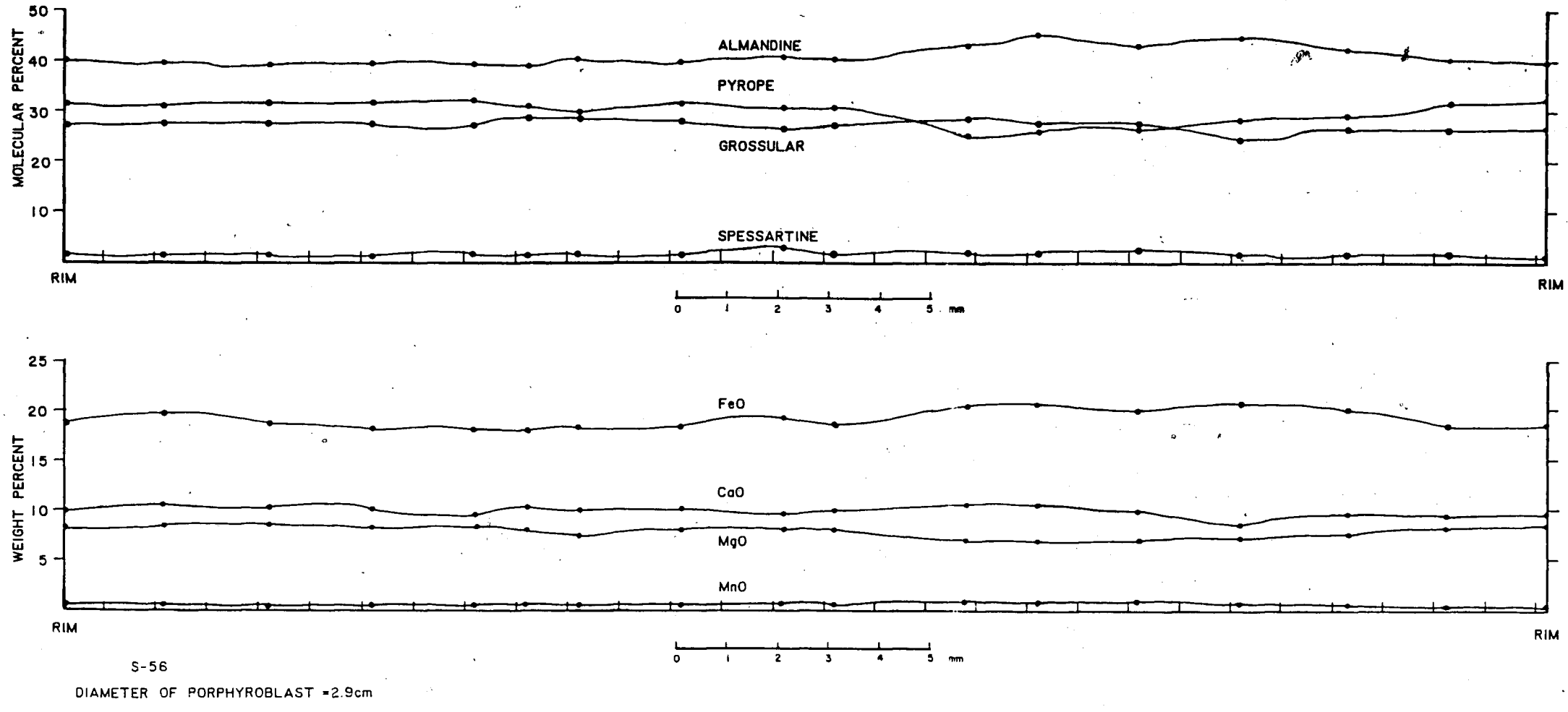

Figure 33 (continued)

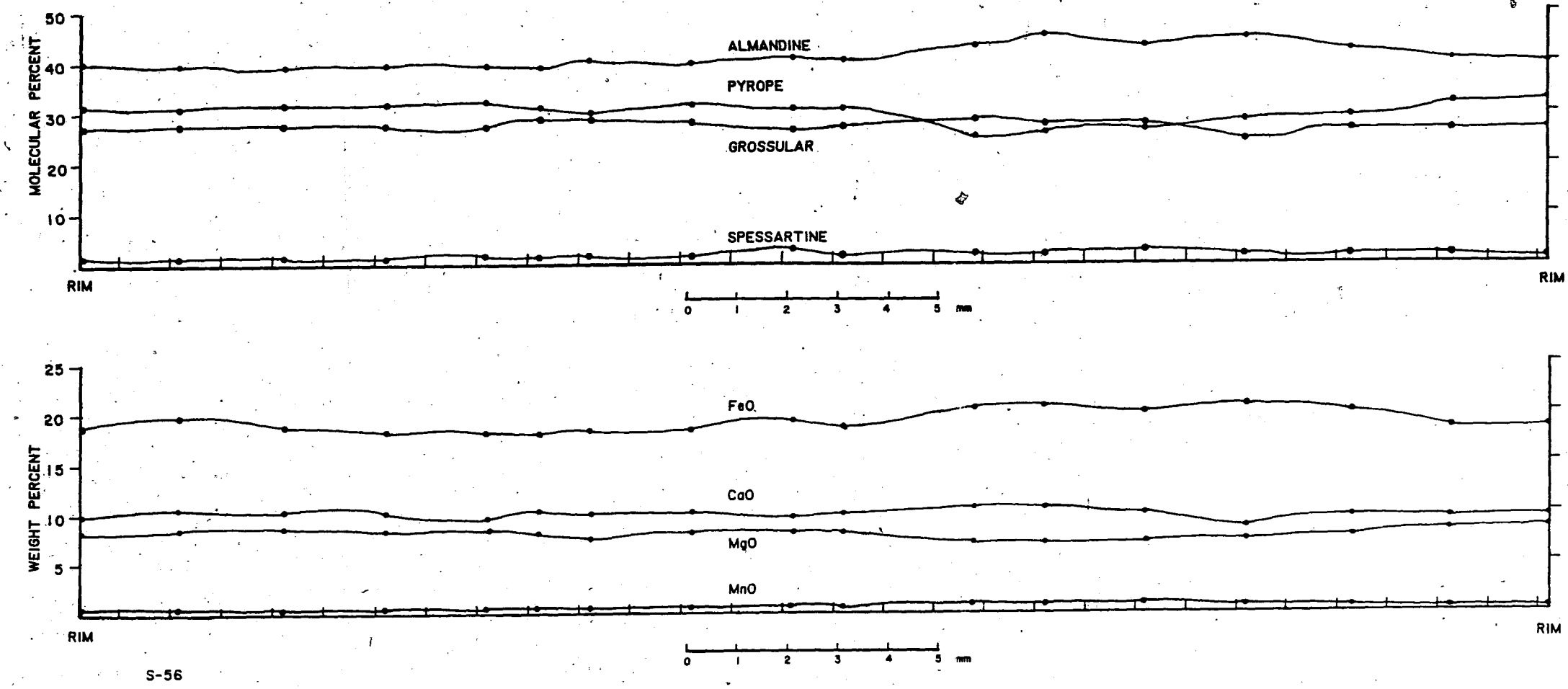

Figure 33 (continued)

with hornblende, although some biotite is partly rimmed by hornblende. The presence of biotite clearly results from the addition of K^+ and water to the gabbro from the xenolith.

The Large-Garnet Zone

Although the petrography of the large-garnet zone has been described in the previous sections, it will be summarized here to facilitate comparison with the normal metagabbro.

The minerals present consist of plagioclase, clinopyroxene, orthopyroxene, hornblende, and garnet. They are generally coarser grained than in the normal metagabbro. The texture is generally granoblastic. Opaque oxides were not observed.

Plagioclase exhibits a narrow normally zoned rim where adjacent to garnet. Where adjacent to hornblende and sometimes clinopyroxene, it is reversely zoned. It also occurs as small grains in a symplectite with hornblende adjacent to garnet, or with orthopyroxene adjacent to hornblende. As noted, these grains of plagioclase are richer in An than are the plagioclase grains in the normal metagabbro.

Clinopyroxene occurs both as twinned grains which are generally 1 to 3 mm in diameter and are equant or slightly inequant in shape, and as smaller, untwinned grains which are generally equant. The twinned grains (1) may occur as embayed inclusions within garnet, (2) be rimmed discontinuously with hornblende or (3) contain

lamellae of hornblende. Where in contact with larger hornblende grains, clinopyroxene contacts are generally irregular. The untwinned grains of clinopyroxene are generally less abundant; are free of inclusions; and are closely associated with garnet.

Hornblendes in the large-garnet zone are restricted to the vicinity of garnet porphyroblasts. Thin sections farther from garnet contain only a few percent of hornblende, as thin rims around or lamellae within clinopyroxene. Hornblendes do not occur as a monomineralic rim around garnet, and may sometimes form small, round or embayed inclusions within garnet. In places, hornblende is partially surrounded by the previously mentioned orthopyroxene-plagioclase symplectite, which represents the only occurrence of orthopyroxene in the large-garnet zone.

Garnet occurs as equant to slightly elongate porphyroblasts scattered throughout a garnet-free matrix. Hornblende-plagioclase symplectites occur between garnet and either clinopyroxene or hornblende. In places, small plagioclase grains occur as inclusions in the garnet porphyroblasts.

Chemically, clinopyroxene, hornblende, and garnet are all richer in Mg than are the same minerals in the normal metagabbro. Inasmuch as there are no Fe-Ti oxides present, in contrast to the normal metagabbro, this may represent a more Mg-rich bulk chemistry, due to differences in the bulk chemistry of the igneous protolith.

Metamorphic Reactions

The same metamorphic events that occured at Ruby Mountain occured at Speculator as well. Again, there is no petrographic evidence for any definite sequence of reactions.

Igneous plagioclase and clinopyroxene were recrystallized, and the clinopyroxene reequilibrated to a metamorphic composition. This is best preserved where the body was dry, as in the parts of the large-garnet zone where garnet porphryroblasts are absent. Original igneous pyroxenes also began to recrystallize to form the granoblastic aggregates of ortho-and clinopyroxene which surround irregular clinopyroxene grains. Again, all of these pyroxenes have reequilibrated to metamorphic compositions. These may represent completely recrystallized igneous clinopyroxenes which originally possessed exsolution lamellae of orthopyroxene. These lamellae have been completely reaggregated, and now form part of the equigranular rims. In addition, the high normative olivine content of the metagabbro suggests that olivine was originally present. This mineral may have been consumed in magmatic reactions, or possibly by early metamorphic reactions, for which no evidence remains.

Hornblende was formed in areas of higher PH_2O. In the large-garnet zone, the hornblende evidently formed by an interface reaction between clinopyroxene and plagioclase, as evidenced by zoning in the plagioclase adjacent to the hornblende, and by partial rims of hornblende around or lamellae within clinopyroxene. In the

rest of the body, magnetite and ilmenite were also reactants, resulting in a more iron-rich hornblende than in the large-garnet zone, where Mg-rich clinopyroxene was the main mafic reactant.

In order to deduce the garnet-forming reaction, the following observations must be considered. Garnet is not present where hornblende is absent. However, the amount of hornblende does not vary directly with the amount of garnet. The abundance of ortho-and clinopyroxenes also does not appear to vary in any systematic manner with the abundance of garnet. Embayed inclusions of clinopyroxene, hornblende, and plagioclase occur within garnet, and contacts of garnet with orthopyroxene are slightly embayed. Plagioclase is more sodic near garnet. Based on these observations, the reaction is deduced to be:

orthopyroxene + clinopyroxene + plagioclase + hornblende $\longrightarrow$ garnet + sodic plagioclase

Orthopyroxene is not present in the large-garnet zone, except as small grains adjacent to hornblende. However, in the rest of the metagabbro it appears to be a reactant. This implies that it was present in the large-garnet zone initially, and perhaps controlled the nucleation of the garnet porphryroblasts, or it may simply participate in the reaction in variable amounts, depending upon how much is present locally. Otherwise, this reaction apparently did not differ significantly in different locations within the metagabbro. Differences in composition of the garnet in the large-garnet zone and the garnet in the rest of the metagabbro are

apparently due to the different compositions of the reactant hornblende and pyroxene, and thus to differences in bulk chemistry.

A hornblende-consuming reaction, as evidenced by irregular inclusions of hornblende in granoblastic clinopyroxenes and the small grains of orthopyroxene and plagioclase around hornblende, resulted in the formation of orthopyroxene, clinopyroxene, and plagioclase from hornblende. This reaction may have occurred before the garnet-forming reaction. Where this reaction has gone to completion, the result is lens-like granoblastic aggregates of ortho-and clinopyroxene.

The final reaction which occurred is a garnet-consuming reaction:

garnet + hornblende or clinopyroxene $\longrightarrow$ hornblende + plagioclase

There is a considerable difference in chemical composition between the product and reactant hornblende, as described on p. 109. This reaction occured only in the large-garnet zone, and is probably a retrograde reaction, inasmuch as hornblende is present as the ferromagnesian product, rather then pyroxene.

Origin of the Speculator Metagabbro

Protolith: The complete metamorphic overprint which destroyed the original igneous texture, and the poor exposure, which prevents the extensive sampling needed in order to define trends in the bulk chemistry or the shape of the body, make it impossible to describe the protolith in the same detail as the Gore Mountain metagabbro. However, some conclusions are possible.

The Speculator metagabbro was an olivine-normative gabbro, similar to the Gore Mountain gabbro. It was probably intruded after at least one regional deformation, based on the occurrence of the lineated xenolith of granitic gneiss. It cooled slowly enough to permit igneous differentiation, and to develop igneous layering. The pegmatitic bodies of hornblende, K-feldspar, and quartz in the interior of the gabbro may be later intrusives. Near the borders of the intrusion, the gabbro gained potassium from the granitic gneiss which constitutes the country rock.

Metamorphic History: The initial stage in the metamorphism was the anhydrous recrystallization of the rock to a granoblastic texture. It is possible that coronitic garnets or garnets replacing plagioclase where in contact with clinopyroxene, as described by Luther (1976) at Gore Mountain, formed at this stage, but there is no evidence for this here. Any original olivine was probably consumed in this stage.. Water was able to enter the body, perhaps

along foliation planes. The amount of water was apparently variable, even on the scale of a thin section as shown by the variable hornblende content. The large-garnet zone was the driest part of the metagabbro, with only small local pockets which were relatively rich in water. During this stage, hornblende and garnet were formed. The hornblende later reacted to form pyroxenes, perhaps due to higher temperature. Locally, this reaction consumed all of the hornblende.

Whitney and McLelland (1973), showed that the origin of coronitic olivine gabbros was by isobaric cooling from the liquidus temperature. Although the Speculator metagabbro is not coronitic, this is probably due to the more complete metamorphic recrystallization which occurred. It appears that the Speculator metagabbro may have originated in the manner proposed by Whitney and McLelland (1973). This would explain the retrograde zoning trends observed in garnets, as noted on p. 112, as well as the homogeneity of the larger garnets, which are more Mg-rich, and thus would have nucleated earlier, when the metagabbro was at a higher temperature.

As noted above, much of the metagabbro was mapped as amphibolite on the New York State Geological Map (Fisher and Isachsen, 1970). Exposures of the amphibolite are very poor, so only a few samples were collected. Those that were obtained contain more hornblende than the metagabbro. The PH_2O must have been higher in the amphibolite than in the metagabbro. Garnets up to a centimeter in size are present; larger porphryroblasts were not

observed. These rocks show signs of retrograde alteration as mentioned above (p. 85), similar to those in thin sections of rocks containing large garnet porphryroblasts fron the large-garnet zone.

Origin of the Large-Garnet Zone: One of the primary goals of this study was to determine the origin of the large-garnet zone, and the controls on its development. Unlike the Gore Mountain body, the largest garnets apparently occur in the part of the body which appears to have been subjected to the lowest PH_2O. There are no obvious features which would suggest any controls upon garnet formation. Thus, it is concluded that the Speculator metagabbro does not represent a stage in the development of a garnet-rich body of the Gore Mountain type.

In considering the origin of the large-garnet zone, it is evident that garnet nucleated only where hornblende was abundant, and that an additional phase may have been necessary for garnet nucleation within the large-garnet zone, inasmuch as there are thin sections from this zone which contain abundant hornblende but no garnet.

Another control upon the occurrence of large garnets is the chemistry of the hornblende. In the large-garnet zone, as noted above (p. 107), hornblende is more magnesian than elsewhere in the body, due to its formation from Mg-rich clinopyroxenes. It has been noted by Gilbert et al. (1982) that iron-rich hornblende commonly reacts to form garnet (p. 251). More magnesian hornblendes,

however, do not tend to form garnet when they break down. Thus, the magnesium-rich hornblendes of the large-garnet zone would show less of a tendancy to react with plagioclase and pyroxene to form garnet than would the iron-rich hornblendes in the rest of the body. When they did so it would be at a higher temperature, due to the greater thermal stability of the magnesium-rich hornblende.

Thus, in the large garnet zone, the greater stability of Mg-rich hornblende relative to garnet inhibited the nucleation of garnet. Few garnets nucleated, due to the locally relatively high PH_2O and the relatively unfavorable composition of the reactant hornblende, but those that did could grow to a large size, as there was no competition for essential reactants with other nuclei. In contrast, garnet nucleated readily in the rest of the body, due to the larger supply of Fe-rich hornblende. Individuals could not grow to a large size due to the competition for reactants.

OLD HOOPER MINE

Field Relations

The Old Hooper Mine is an open pit mine in a small, isolated body of garnet amphibolite which occurs within syenitic granulite. The body shows some resemblance to the Gore Mountain garnet amphibolite. It possesses a weak metamorphic foliation which is not uniformly present. In places, it contains mafic layers, 2 to 8 cm thick, which suggest igneous layering. Garnet porphryroblasts are usually less than 5 cm in diameter, and exhibit fairly well-developed hornblende coronas. Some garnet porphryroblasts are slightly elongated parallel to the foliation. A few exhibit pressure shadows of plagioclase. Also, inside the hornblende corona, a thin plagioclase rim is present. The distribution of the garnet is variable. The amount and size of the garnets apparently decreases away from the Thirteenth Lake fault, which cuts off the eastern end of the body. In the western wall of the pit, several irregular bodies several meters in size which resemble syenitic granulite occur within the garnet amphibolite. Inasmuch as they are not exposed in three dimensions, it cannot be determined if they are xenoliths, or projections of the country rock into the garnet amphibolite, or even intrusive apophyses of an igneous protolith of the syenitic granulite.

Mineralogy and Petrography

The Old Hooper garnet amphibolite consists dominantly of plagioclase, garnet, and hornblende which is pleochroic in shades of green and olive. Minor amounts of opaques, augite, and optically unresolvable alteration products also occur. The texture is granoblastic, with the metamorphic foliation being defined by the preferred orientation of hornblende prisms, rather than by lenticular bodies of mafic minerals as in the Speculator and Ruby Mountain metagabbros. The garnets occur as xenoblastic porphryroblasts, and often contain round inclusions of hornblende.

This body has evidently undergone complete metamorphic recrystallization as has the Gore Mountain garnet amphibolite. No reaction relationships or corona structures are present. PH_2O was certainly high, and probably higher than at Speculator or Ruby Mountain as evidenced by the virtual absence of clinopyroxene. This was probably the controlling factor in allowing individual garnet crystals to grow to a large size. If the Thirteenth Lake fault was the channel utilized by the water during metamorphism, as is likely, this would explain the observed size distribution of the garnets within the body.

Garnet Chemistry

A traverse across a garnet porphryroblast was made with the electron microprobe in order to compare its zoning trends and chemistry with those of garnets in the Speculator and Ruby Mountain metagabbros. These results are summarized in Figure 34 and Table 12. The average composition is similar to that of garnet from the Ruby Mountain anorthosite and Gore Mountain metagabbro, although it is richer in calcium. The Old Hooper garnet is much richer in grossular and poorer in pyrope components than is the garnet from Gore Mountain. The interior of the porphryroblasts is chemically homogeneous, although the rims show slight increases in iron and manganese.

Type of Deposit

As noted, this body resembles the Gore Mountain metagabbro. Chemically, however, the garnet is not similar to the garnet in any of the other bodies studied. Almost certainly this is due to differences in bulk chemistry of the protolith. Based on the field relationships, mineralogy, and proximity to the Gore Mountain and Ruby Mountain metagabbros, this body probably developed under the same physical conditions as the Gore Mountain gabbro, but, unlike the Gore Mountain gabbro, was completely transformed to garnet amphibolite due to its smaller size.

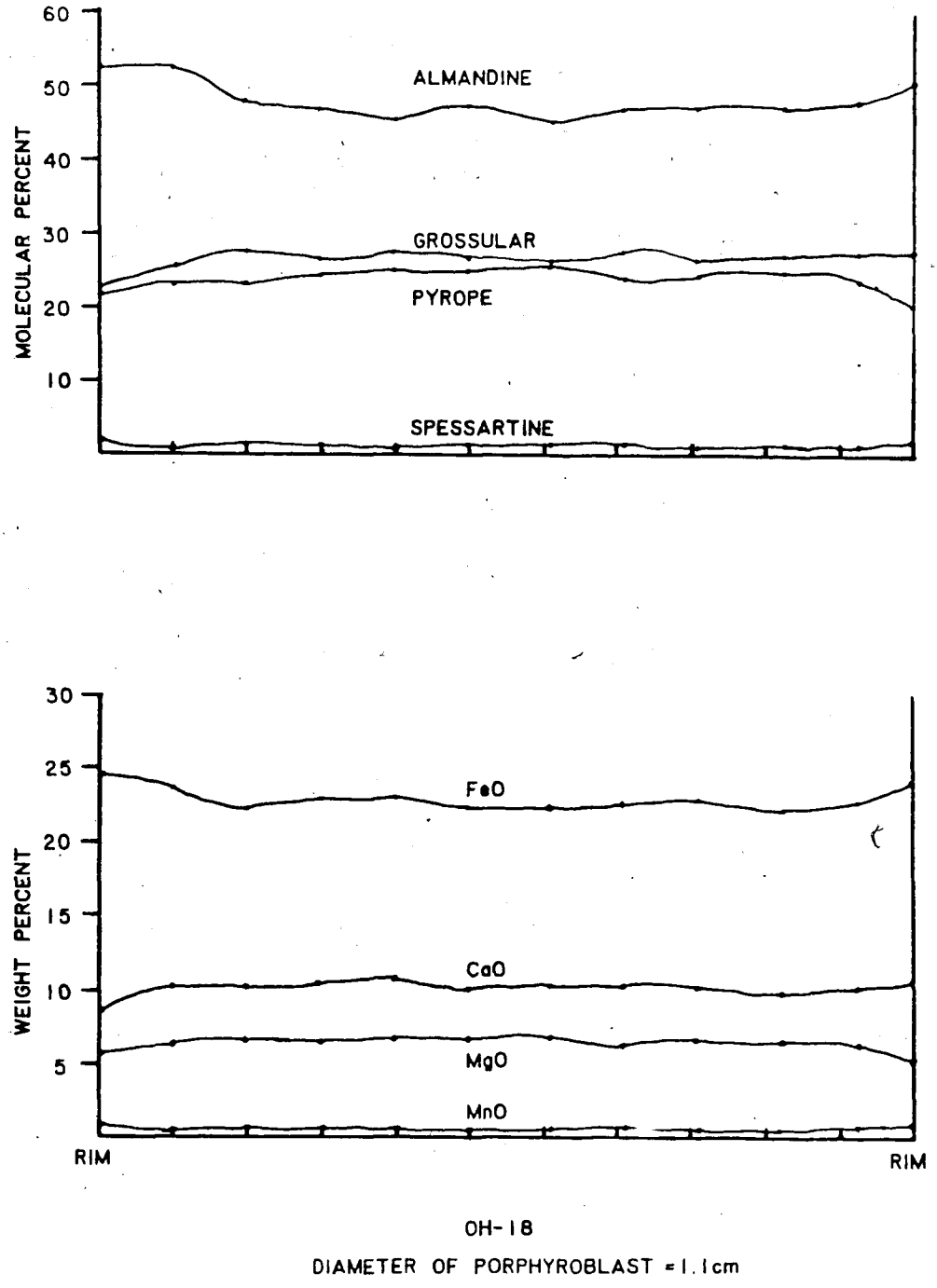

Figure 34. Zoning trend in garnet porphyroblast, Old Hooper garnet amphibolite.

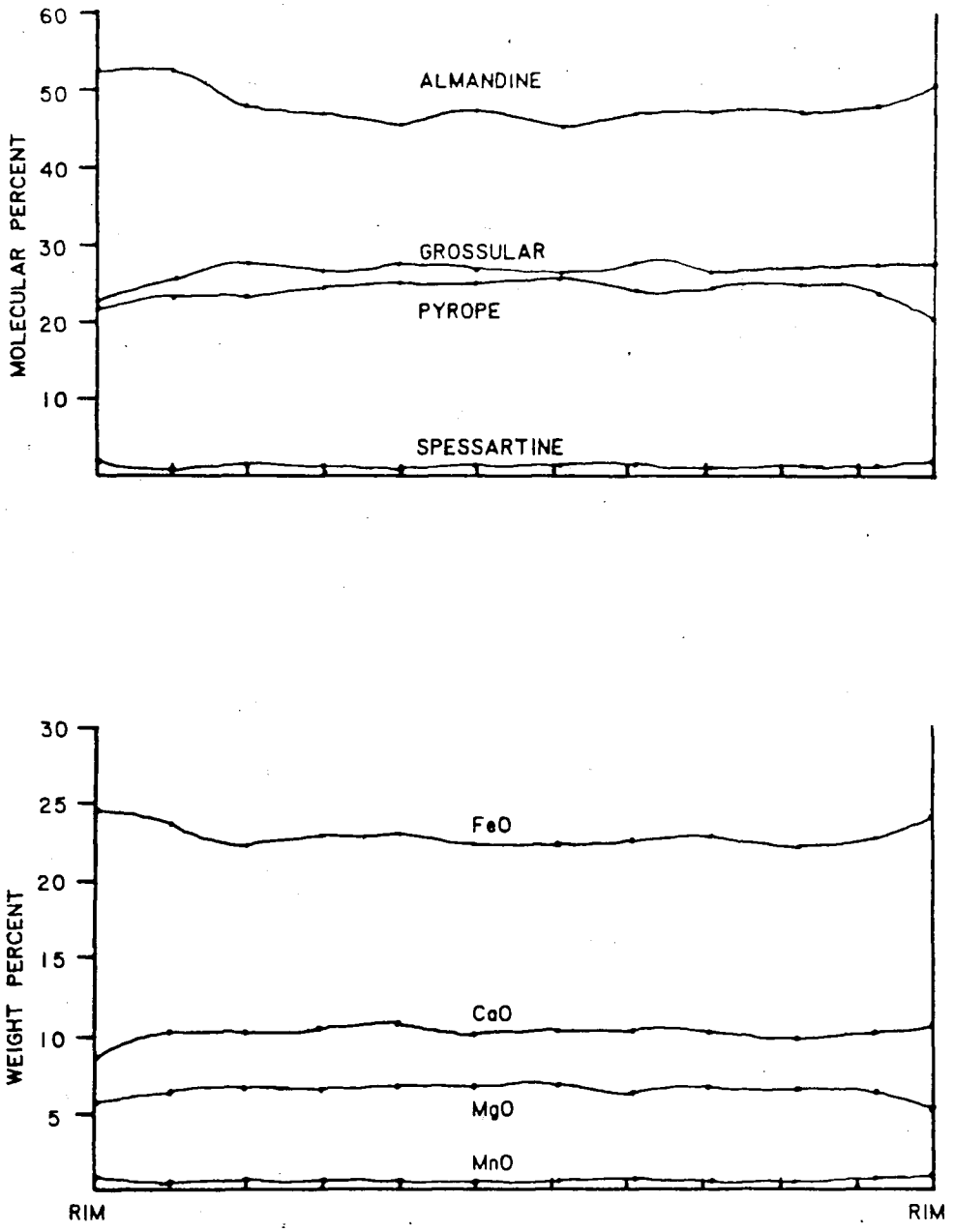

Figure 34. Zoning trend in garnet porphyroblast, Old Hooper garnet amphibolite.

Table 12

Electron Microprobe Analyses From a Traverse Taken Across a Garnet Porphyroblast, Old Hooper Mine

OH18
Diameter of porphyroblast=1.1cm

	Rim						
SiO_2	38.50	38.51	39.35	39.05	39.15	39.22	38.91
Al_2O_3	22.84	22.72	22.95	23.08	22.26	23.35	22.62
FeO	24.63	23.65	22.60	22.98	22.94	22.49	22.42
MnO	0.87	0.51	0.58	0.58	0.53	0.52	0.54
MgO	5.75	6.28	6.21	6.63	6.74	6.64	6.90
CaO	8.67	10.27	10.11	10.45	10.75	10.02	10.26
Total	101.28	101.95	101.80	102.77	102.37	102.23	101.66
					Rim		
SiO_2	39.10	39.11	39.21	39.30	38.68		
Al_2O_3	23.02	23.07	22.31	22.90	22.67		
FeO	22.55	22.97	22.15	22.88	24.16		
MnO	0.70	0.54	0.49	0.59	0.88		
MgO	6.45	6.64	6.56	6.37	5.36		
CaO	10.42	10.18	9.87	10.14	10.27		
Total	102.23	102.50	100.60	102.18	102.03		

Number of Cations per 12 Oxygens

	Rim						
Si	2.950	2.928	2.974	2.934	2.957	2.949	2.949
Al	2.062	2.036	2.044	2.043	1.981	2.068	2.020
Fe	1.578	1.504	1.428	1.444	1.449	1.413	1.421
Mn	.056	.033	.037	.037	.034	.033	.034
Mg	.656	.711	.699	.743	.759	.744	.780
Ca	.713	.837	.819	.840	.870	.806	.833
					Rim		
Si	2.948	2.943	2.993	2.964	2.948		
Al	2.046	2.045	2.007	2.036	2.037		
Fe	1.421	1.445	1.414	1.443	1.540		
Mn	.044	.034	.031	.037	.056		
Mg	.724	.744	.746	.716	.609		
Ca	.841	.820	.807	.819	.839		

(Table 12, Continued)
Electron Microprobe Analyses From a Traverse Taken Across a Garnet Porphyroblast, North River Garnet Company Mine

NR8
Diameter of porphyroblast=.9cm

	Rim				Rim
SiO_2	38.63	39.09	38.84	38.03	38.98
Al_2O_3	22.62	23.25	23.03	22.71	22.49
FeO	24.51	25.29	26.56	27.38	24.96
MnO	0.75	0.84	1.18	1.15	0.74
MgO	6.04	6.11	5.70	5.51	6.42
CaO	9.06	8.11	6.99	7.17	7.62
Total	101.63	102.68	102.31	101.95	101.21

Number of Cations per 12 Oxygens

	Rim				Rim
Si	2.950	2.951	2.957	2.925	2.980
Al	2.036	2.068	2.066	2.059	2.026
Fe	1.565	1.596	1.691	1.761	1.595
Mn	.048	.053	.076	.074	.048
Mg	.688	.688	.646	.632	.732
Ca	.741	.655	.570	.590	.624

NORTH RIVER GARNET COMPANY MINE

Field Relations

The North River Garnet Company Mine (sometimes referred to as the Garnet Hill Mine or New Hooper Mine) is located within a small body of gabbroic anorthositic gneiss which appears to be very similar mineralogically to the Ruby Mountain gabbroic anorthosite. It possesses both a foliation and a lineation and appears to have been intensely sheared. The grain size is finer than that of the Ruby Mountain anorthosite. The foliation is defined by small mafic streaks rather than thick mafic lenses. Metagabbro layers are not present. Garnet porphryroblasts reach a maximum of 7 cm in diameter. Neither plagioclase nor hornblende coronas around garnet porphyroblasts are present.

Mineralogy and Petrography

Mineralogically, the anorthositic gneiss consists of biotite, hypersthene, diopsidic augite, hornblende, plagioclase, and garnet. Trace amounts of transparent green spinel are also present. The texture is entirely metamorphic, with the plagioclase forming granoblastic aggregates. The plagioclase grains are often twinned, and generally exhibit strain and zoning.

Hornblende is pleochroic in dark to light brown. It is usually surrounded by a corona of vermicular orthopyroxene+plagioclase+ clinopyroxene symplectite. This may be replaced locally by garnet adjacent to the matrix plagioclase (Figures 35, 36). In some cases the hornblende core is almost entirely consumed. Clinopyroxene and orthopyroxene also exist as equant grains or clusters of grains. Garnet also occurs as large porphryroblasts. The largest of these are equant, but smaller ones show arms protruding into the matrix plagioclase. The garnet is probably post-deformational, inasmuch as the preservation of corona structures is not likely during deformation. In addition, the garnet porphyroblasts transect the foliation. Biotite generally occurs in decussate clusters.

The textures in this rock suggest that the following reactions took place. First, hornblende broke down by the reaction:

plagioclase + hornblende $\longrightarrow$ orthopyroxene + clinopyroxene + plagioclase + minor spinel

Then, garnet formed by:

orthopyroxene + clinopyroxene + plagioclase + spinel $\longrightarrow$ garnet

The occurrence of these coronas indicates that the gneiss here was drier than at Ruby Mountain, inasmuch as the preservation of coronas implies a low enough diffusional transport rate to prevent a complete reaction. The garnet porphryroblasts probably record a complete reaction, either by nucleating earlier and thus having more time available for the reaction to go to completion, or by growth in a wetter region within the body. The latter hypothesis is not as

Figure 35. Photomicrograph showing coronitic structures between hornblende and plagioclase in anorthositic gneiss, North River Garnet Company Mine. This consists of a symplectite of vermicular orthopyroxene and plagioclase with minor clinooyroxene and trace amounts of green spinel. Crossed polarizers, 130X. Pc=plagioclase, Gt=garnet, Hb=hornblende, S=symplectite of orthopyroxene + plagioclase + minor clinopyroxene + traces of spinel.

Figure 36. Photomicrograph showing symplectite in more detail. The outer shell of garnet is not present in this photomicrograph. Crossed polarizers, 130X. Pc=plagioclase, Hb=hornblende, S= symplectite of plagioclase + orthopyroxene + minor clinopyroxene + traces of spinel, Opx= orthopyroxene.

likely, inasmuch as neither hornblende nor biotite are abundant near the porphryroblasts.

Garnet Composition

A garnet porphryroblast was analyzed with the electron microprobe to determine its composition and zoning trends. The results are given in Table 12 and Figure 37. The composition of the garnet is similar to that of garnet from the Ruby Mountain anorthosite, except that the North River garnet is slightly richer in Ca^{2+} and Fe^{2+}. This is doubtless due to differences in bulk composition between the two protoliths.

The weak zoning trends in these garnets are identical to those of the garnets from Ruby Mountain. This suggests that they were probably formed by the fractionation-depletion model of Hollister (1966), as proposed for the garnets of the Ruby Mountain body.

Type of Deposit

This body may be classified with the Ruby Mountain anorthosite, based on the rock type. However, there are marked dissimalarities in mineralogy, texture, and garnet-forming reactions. It appears that the North River garnetiferous anorthosite represents the dry equivalent of the Ruby Mountain anorthosite. A comparison of these

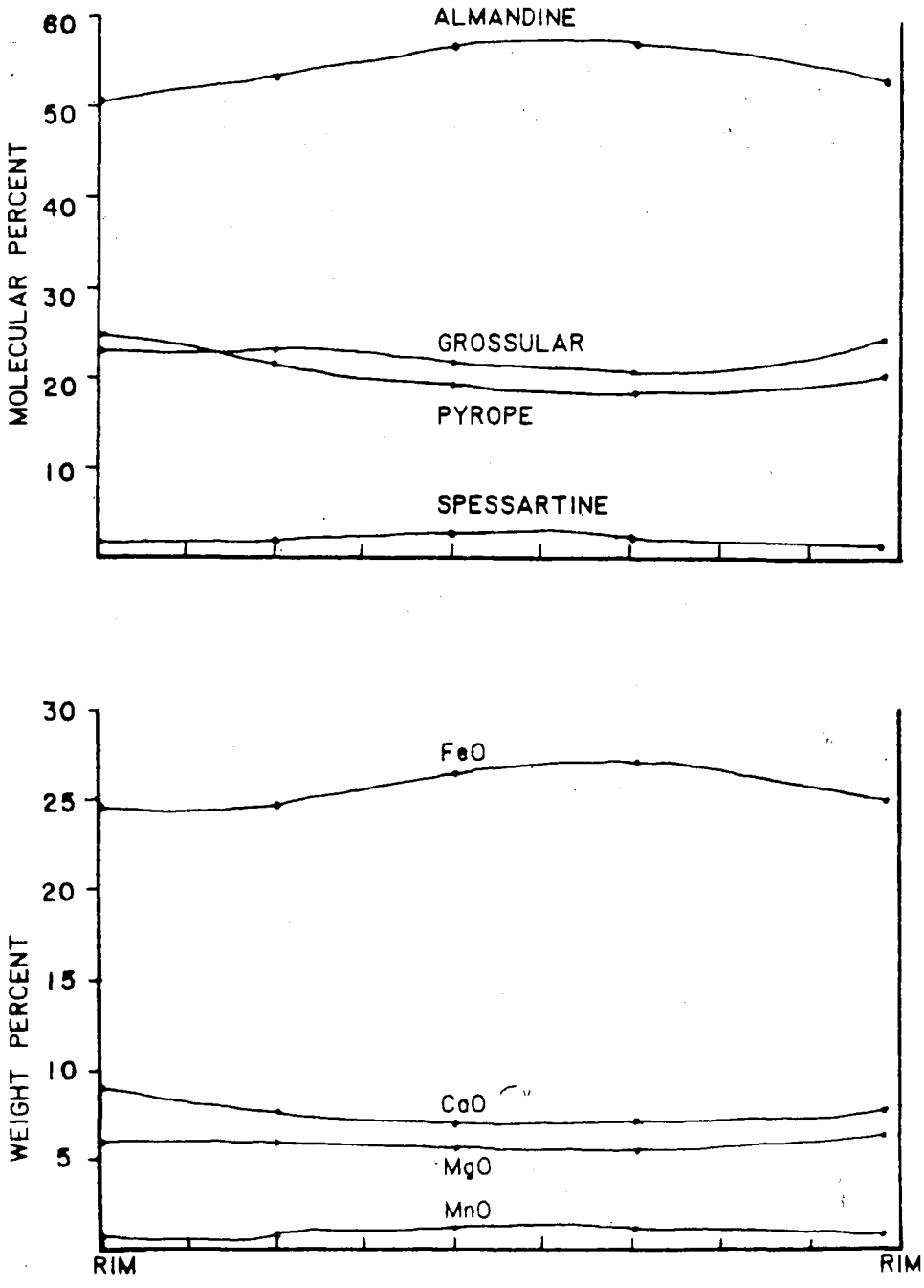

Figure 37. Zoning trend in garnet porphyroblast from North River Garnet Company anorthositic gneiss.

two bodies indicates that the presence or absence of water has a profound influence on the garnet-forming reaction, beyond simply increasing the size due to increased material transport.

COMPARISON OF GARNET CHEMISTRY FROM VARIOUS BODIES

General Statement

A major objective of this study was to compare garnet-forming reactions and the composition of the resultant garnets in different bodies. In addition, a comparison of these reactions with previously proposed garnet-forming reactions in the literature was made.

Garnet-Forming Reactions

Most of the garnet-forming reactions which have been proposed in the literature produce coronitic garnet. They often involve olivine, orthopyroxene, plagioclase, and sometimes spinel or Fe-Ti oxides as reactants, and quartz or clinopyroxene as products along with the garnet. They do not usually involve hydrous phases, and generally occur in anhydrous meta-igneous rocks, which may contain relict igneous textures.

In contrast, the garnet-forming reactions in the Ruby Mountain and Speculator metagabbros occur in completely recrystallized rocks which were subjected to a variable influx of water. They both involve hornblende and clinopyroxene as reactants. The products are small xenoblastic garnets, or larger porphyroblasts. These may originally have been coronitic, but no evidence of this remains.

Thus, it appears that the controlling factors in determining which garnet-forming reaction occurs and the textures produced are; PH_2O, the occurrence of hornblende, and the extent of deformation and recrystallization in the rock.

Compositions of Garnet

Figure 38 shows average garnet compositions normalized to Al + Py + Gr = 100%. The data comes from the present study and those of Luther (1976) and Novillo (1981). Table 13 shows all garnet analyses used in Figure 38. It is noteworthy that the garnets from the Ruby Mountain metagabbro do not plot in the same region as the garnets from the overlying anorthosite. Likewise, garnets from the Speculator and Old Hooper bodies do not plot in the same area as the garnets from the Gore Mountain metagabbro.

In the first case, this is doubtless due to the differences in bulk composition of the protoliths. The garnets from the Ruby Mountain metagabbro show a higher almandine content than do the garnets from the anorthosite. This correlates with the higher iron content of the metagabbro. However, this same trend is seen between the garnets from Speculator and the Gore Mountain metagabbro. In addition, the Ca content of the garnets from the Speculator metagabbro is greater than the Ca content of garnets from Gore Mountain. This may result from the greater Ca content of the Speculator metagabbro.

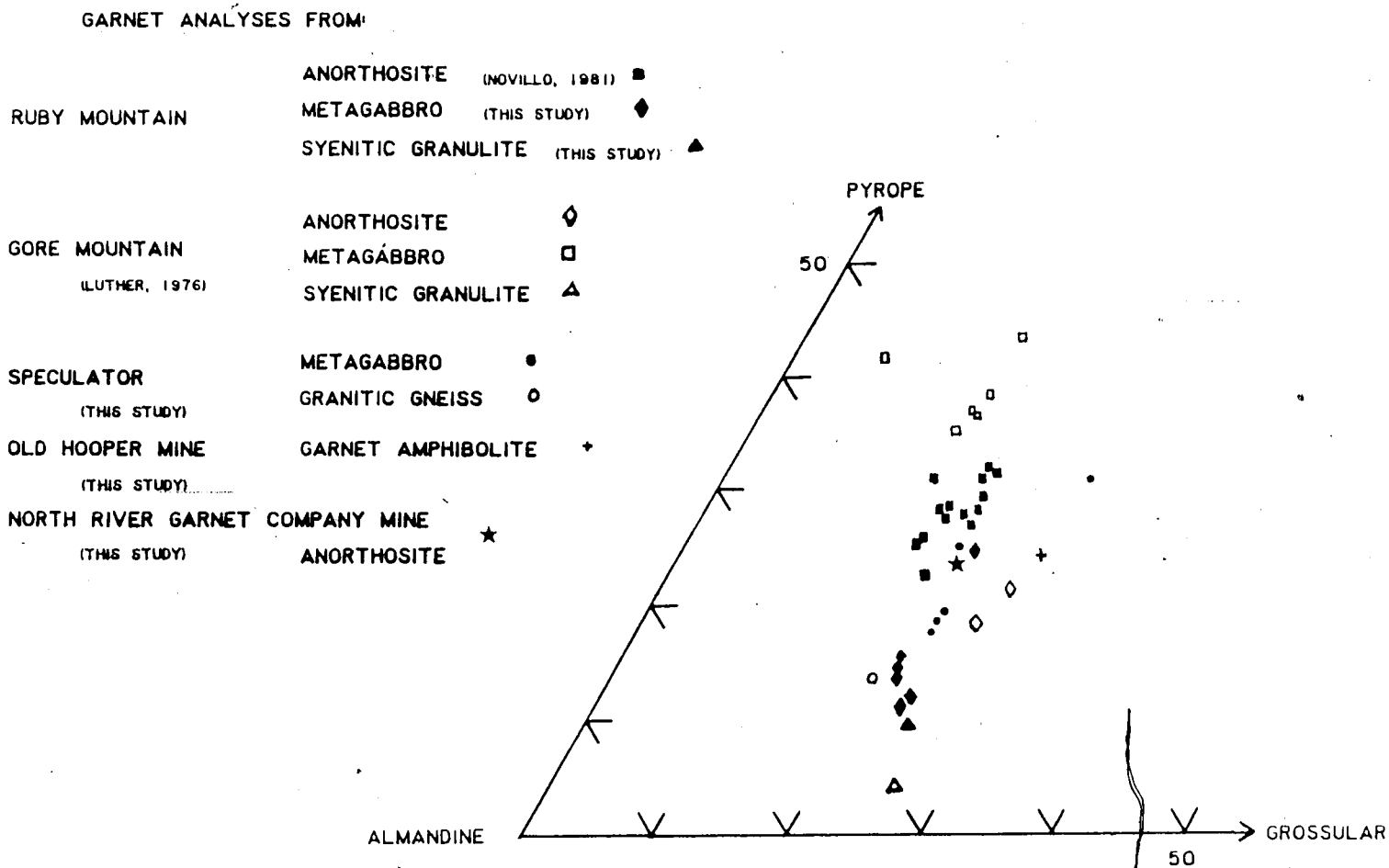

Figure 38. Ternary plot of microprobe analyses of garnet in terms of Py, Alm, and Gr, from the Ruby Mountain metagabbro, Ruby Mountain anorthosite, Gore Mountain metagabbro, Speculator metagabbro, Old Hooper garnet amphibolite, North River mine anorthositic gneiss, syenitic granulite, and granitic gneiss.

Table 13

Compilation of Average Garnet Compositions From Meta-Igneous Rocks of the Thirteenth Lake-Speculator Region

Ruby Mountain Metagabbro

Sample	Py	Al	Gr	Sp	And
RM-1	12.9	60.3	19.8	4.1	2.8
RM-29a	13.6	60.7	20.0	3.2	2.4
RM-29b	14.8	59.9	19.8	3.2	2.2
RM-51	23.3	51.9	21.2	2.7	0.9
RM-11	11.2	61.7	22.3	3.7	1.0
RM-11a	10.1	59.9	21.3	6.7	2.0

Speculator Metagabbro

Sample	Py	Al	Gr	Sp	And
S-10	23.8	53.7	20.4	1.6	0.5
S-42a	18.8	57.0	22.0	1.8	0.5
S-42b	17.0	58.8	21.8	2.0	0.4
S-56	30.1	40.9	27.4	1.6	0.0
n-38	17.8	58.4	21.9	1.9	0.0

Ruby Mountain Anorthosite

Sample	Py	Al	Gr	Sp	And
R7B7A-3	27.4	50.2	20.2	2.3	0.0
R7B7A-5	26.1	51.5	20.2	2.6	
R1#2-1	24.9	55.7	16.9	2.6	0.0
R10B8-3	30.9	47.9	19.9	1.4	0.0
R10B8-4	27.4	52.9	17.5	2.3	0.0
R7B7-X	21.8	56.8	19.2	2.3	0.0
R10B8	31.2	47.8	19.0	1.2	0.0
R3B4	30.3	49.1	18.9	1.7	0.0
R14B3	27.8	52.5	17.8	2.0	0.0
R2B5	29.3	50.4	20.4	1.5	0.0
R7B7	27.2	52.0	19.3	1.4	0.0
R14B4	30.3	52.4	15.6	1.9	0.0
R1#1	26.7	53.3	18.1	2.2	0.0
R1#2	25.0	55.6	17.0	2.5	0.0

Gore Mountain Metagabbro

Sample	Py	Al	Gr	Sp	And
3BN-1	38.2	45.4	16.3	1.0	0.0
3B7-5a	36.8	46.8	15.8	0.6	0.0
3B3-3e	36.4	46.7	15.9	1.0	0.0
3B7-5d	34.7	49.0	15.2	1.0	0.0
Levin	43	40	16	1	0
B1-11	41.3	51.0	6.7	1.0	0.0

(Table 13, Continued)

Other Rock Types

Anorthosites, Gore Mountain

Sample	Py	Al	Gr	Sp	And
B9-3	21.3	51.9	25.8	0.9	0.0
3B7-28A	18.1	55.7	24.8	1.3	0.0

Py	Al	Gr	Sp	And	
4	66	25	5	0	Average syenitic granulite (from Luther, 1976).
9.0	61.4	22.6	3.2	3.8	RM-1a, syenitic granulite from Ruby Mountain.
22.7	54.1	21.0	2.0	0.2	NR-8, North River anorthosite.
23.8	47.7	26.7	1.3	0.5	OH-58, Old Hooper Mine, garnet amphibolite.
12.2	60.7	17.9	3.4	5.8	S-11, granitic gneiss xenolith from Speculator metagabbro.

CONDITIONS OF METAMORPHISM

As noted above, the physical conditions of formation of some of the bodies have been estimated. At Ruby Mountain, Novillo (1981) estimated that the garnet-rich anorthositic gneiss was subjected to a peak metamorphic temperature of 723°C-772°C at a pressure of 8 Kbars. These must have been the conditions of metamorphism at the Old Hooper and North River bodies as well inasmuch as they are located very close to Ruby Mountain, and the temperature and pressure probably did not vary appreciably over such a short distance. Whitney and McLelland (1973) concluded that the formation of corona structures in olivine gabbros results from isobaric cooling from liquidus temperature at about 7 Kbars. The equation developed by Råheim and Green (1974), which uses the Fe-Mg distribution between coexisting garnet and clinopyroxene to indicate temperature of formation, yields 668°C at 7 Kb and 675°C at 8 Kb for the Speculator metagabbro. The equation developed by Ellis and Green (1979) to take into account the Ca content of the garnet, due to the non-ideal behavior of the garnet solution, yields 737°C at 7 Kb and 740°C at 8 Kb. In both of these calculations, the clinopyroxene was corrected for Fe^{3+} by the procedure of Whitney and McLelland (1973). Although the garnet and clinopyroxene are not products of the same reaction, it is assumed here that they grew under the same metamorphic conditions. This approach was sucessfully used by Novillo (1981) in the Ruby Mountain anorthosite.

In addition, these temperatures are consistient with those calculated by other workers. A petrogenetic grid cannot be constructed for these bodies because the relevant reactions have not been experimentally studied.

SUMMARY AND CONCLUSIONS

The origin of the Ruby Mountain metagabbro and the metamorphic conditions to which it was subjected may be summarized as follows:

1) The metagabbro originated as an igneous layer genetically related to the gabbroic anorthosite.
2) Recrystallization and deformation obliterated the original igneous texture, and resulted in re-equilibration of igneous minerals.
3) Influx of water along contacts and foliation planes resulted in local formation of hornblende.
4) The partial pressure of water appears to have been less in the metagabbro than in the gabbroic anorthosite; the PH_2O also appears to have been variable on a scale of centimeters.
5) Garnet formed as porphryroblasts or clusters of inequant grains by a reaction involving plagioclase, orthopyroxene, clinopyroxene, and hornblende.
6) Hornblende locally broke down to form pyroxene perhaps under the influence of increasing temperature; this may have occured before the garnet-forming reaction.
7) Garnet porphryroblasts locally reacted with

hornblende in an open-system reaction to form biotite and plagioclase.

The origin of the Speculator metagabbro and its metamorphic history may be summarized as follows:

1) Intrusion of olivine gabbro into deformed and metamorphosed granitic gneiss.
2) Crystallization of the gabbro, with the formation igneous layering followed by slow subsolidus isobaric cooling.
3) Recrystallization and reequilibration at about 740° C and a total pressure between 7 and 8 Kb.
4) Influx of water resulting in the formation of hornblende. The center of the body apparently remained dry except for small pockets. Hornblende which formed in the relatively dry interior was richer in Mg, due to the high Mg content of the reactants.
5) Formation of garnet where localized hornblende was present. In the large-garnet zone, nucleation was suppressed due to the relatively unfavorable (Mg-rich) hornblende composition with respect to garnet formation.

   Garnets which did nucleate were able to grow to a

large size due to the lack of competition for reactants.

6) Local reaction of hornblende to form pyroxene. This may have occurred before garnet formation.

7) Retrograde reaction of large garnet porphryroblasts with hornblende to form plagioclase and sodic hornblende.

The garnet at the Old Hooper Mine appears to have followed a course of development identical to the Gore Mountain garnet amphibolite. The Noth River Mine appears to have originated through virtually anhydrous metamorphism of gabbroic anorthosite.

In conclusion, the following can be identified as critical factors in determining which garnet forming reaction occurs; PH_2O, and the amount of metamorphic recrystallization and deformation. Whole-rock chemistry and mineral chemistry do not appear to be major factors as evidenced by the occurrence of the same basic garnet-forming reaction in olivine gabbro, gabbroic anorthosite, and iron-rich gabbroic cumulates. Whole-rock chemistry, however, may apparently affect the composition of the product garnet.

Bibliography

Ashwal, L.D., 1982; Mineralogy of mafic and Fe-Ti oxide-rich differentiates of the Marcy anorthosite massif, Adirondacks, New York, Am. Mineral. 67, 14-27.

_____, and Seifert, K.E., 1980; Rare earth element geochemistry of anorthosite and related rocks from the Adirondacks, New York, and other massif type complexes, Geol. Soc. Am. Bull. 91, 659-684.

Balk, R., 1930; Structural survey of the Adirondack anorthosite, J. Geol. 38, 289-302.

Bartholeme, P., 1960; Genesis of the Gore Mountain garnet deposit, New York. Econ. Geol. 55, 255-277.

Bence, A.E., and Albee, A.L., 1968; Emperical correction factors for the electron microanalysis of silicates and oxides. Jour. Geol. 76, 382-403.

Binns, R.A., 1964; Zones of progressive regional metamorphism in the Willyama complex, Broken Hill district, New South Wales. Geol. Soc. Australia Jour. 11, 283-330.

_____, 1965; The mineralogy of metamorphosed basic rocks from the Willyama complex, Broken Hill district, New South Wales. Part 1. Hornblendes. Mineral. Mag. 35, 306-326.

Bohlen, S.R. and Essene, E.J., 1977; Feldspar and oxide thermometry of granulites in the Adirondack Highlands. Contrib. Mineral. Petrol. 62, 153-169.

_____, 1978; Igneous pyroxenes from metamorphosed anorthosite massifs. Contrib. Mineral. Petrol. 65, 433-442.

Buddington, A.F., 1939; Adirondack Igneous Rocks and their Metamorphism. Geol. Soc. Am. Mem. 7.

_____, 1952; Chemical petrology of some metamorphosed Adirondack gabbroic, syenitic, and quartz syenitic rocks (N.Y.). Am. Jour. Sci., Bowen Volume, pt. 1, 37-84.

_____, 1963; Isograds and the role of H_2O in metamorphic facies of orthogneisses of the NW Adirondack area, N.Y.. Geol. Soc. Am. Bull. 74, 1155-1182.

_____, 1965; The origin of three garnet isograds in Adirondack gneisses. Mineral. Mag. 34, 71-81.

_____, 1966; The occurrence of garnet in the granulite-facies terrane of the Adirondack Highlands: a discussion. J. Petrol. 7, 331-335.

_____, 1969; Adirondack anorthosite series. In Origin of Anorthosites and Related Rocks, Y. Isachsen, ed. N.Y. State Mus. and Sci. Serv. Mem. 18, 215-231.

Davis, B.T.C., 1969; Anorthositic and quartz syenitic series of the St. Regis Quadrangle, New York. In Origin of Anorthosites and related Rocks, Y. Isachsen, ed. N.Y. State Mus. and Sci. Serv. Mem. 18, 281-288.

DeWaard, D., 1965a; The occurrence of garnet in the granulite-facies terrane of the Adirondack Highlands. J. Petrol. 6, 165-191.

_____, 1965b; A proposed subdivision of the granulite facies. Am. Jour. Sci. 263, 455-461.

_____, 1967; The occurrence of garnet in the granulite facies terrane of the Adirondack Highlands and elsewhere, an amplification and reply. J. Petrol. 8, 210-232.

_____, 1969; The anorthosite problem: the problem of the anorthosite-charnockite suite of rocks. In Origin of Anorthosite and Related Rocks, Y. Isachsen, ed. N.Y. State Mus. and Sci. Serv. Mem. 18, 71-92.

_____ and Romey, W.D., 1969; Chemical and petrologic trends in the anorthosite-charnockite series in the Snowy Mountain massif, Adirondack Highlands. Am. Mineral. 54, 529-538.

Ellis, D.J. and Green, D.H., 1979; An experimental study of the effect of Ca upon garnet-clinopyroxene exchange equilibria. Contrib. Mineral. Petrol. 71, 13-22.

Engel, A. and Engel C., 1962; Progressive metamorphism of amphibolite, NW Adirondack Mts. Geol. Soc. Am. Buddington Volume, 37-82.

Gasparik, T. and Lindsley, D.H., 1980; Phase equilibria at high pressure of pyroxenes containing monovalent and trivalent ions. In: Pyroxenes, C.T. Prewitt, ed., Mineral. Soc. Am. Reviews in Mineralogy, 7, 309-340.

Gilbert, M.C., Helz, R.T., Popp, R.K. and Spear, F.S., 1982; Experimental studies of amphibole stability. In Amphiboles: Petrology and Phase Relations, D.R. Veblen and P.H. Ribbe, eds., Mineral. Soc. Am. Reviews in Mineralogy, 9b, 229-354.

Griffin, W.L., 1971; Genesis of coronas in anorthosites of the Upper Jotun Nappe, Indre Sogn, Norway. J. Petrol. 12, 219-243.

_____ and Heier, K.S., 1969; Parageneses of garnet in granulite-facies rocks, Lofoten-Vesteraalen, Norway. Contrib. Mineral. Petrol. 23, 89-116.

Hollister, L.S., 1966; Garnet zoning: an interpretation based on the Rayleigh fractionation model. Science, 154, 1647-1650.

Husch, J., Kleinspehn, K. and McLelland, J., 1975; Anorthositic rocks in the southern Adirondacks; basement or non-basement. Geol. Soc. Am. NE sec. mtg., Abstracts with Programs 7, 78.

Isachsen, Y. and Fisher, D., 1970; Geologic map of N.Y. - Adirondack sheet; compiled and edited by Y. Isachsen and D. Fisher: N.Y. State Mus. and Sci. Ser., State Ed. Dept., Albany, N.Y.

Jarosewich, E., Nelson, J.A. and Norberg, J.A., 1979; Electron microprobe reference samples for mineral analysis. In: Mineral Sciences Investigations, 1976-1977, R.F. Fudali, ed. Smithsonian Contributions to Earth Sciences, no. 22, 68-72.

Johannsen, A., 1938; A Descriptive Petrography of the Igneous Rocks. vol. 1, ed. 2, U. of Chicago Press.

Johnson, C.A. and Essene, E.J., 1982; The formation of garnet in olivine-bearing metagabbros from the Adirondacks. Contrib. Mineral. Petrol. 81, 240-251.

Kretz, R., 1963; Kinetics of crystallization of garnet at two localities near Yellowknife. Can. Mineral. 12, 1-25.

Krieger, M.H., 1937, Geology of the Thirteenth Lake Quadrangle. N.Y. State Mus. Bull. 301.

Letteny, C.D., 1969; The anorthosite-norite-charnockite series of the Thirteenth Lake Dome, South-central Adirondacks. In Origin of Anorthosite and Related Rocks, Y. Isachsen, ed. N.Y. State Mus. and Sci. Serv. Mem. 18, 329-342.

Levin, S., 1950; Genesis of some Adirondack deposits. Geol. Soc. Am. Bull. 61, 519-565.

Luther, F.R., 1976; Petrological Evolution of the Garnet Deposit at Gore Mountain, Warren County, New York. Unpublished Ph.D. Dissertation, Lehigh University.

Martignole, J. and Schrijver, K., 1971; Association of (hornblende) garnet-clinopyroxene subfacies of metamorphism and anorthosite masses. Can. Jour. Earth Sci. 10, 698-704.

McLelland, J. and Isachsen, Y., 1980; Structural synthesis of the southern and central Adirondacks: a model for the Adirondacks as a whole and plate-tectonics interpretations. Geol. Soc. Am. Bull. pt. 1, 91, 208-292.

_____ and Whitney, P.R., 1977; The origin of garnet in the anorthosite-charnockite suite of the Adirondacks. Contrib. Mineral. Petrol., 60, 161-181.

_____, 1980; A generalized garnet-forming reaction for metaigneous rocks in the Adirondacks. Contrib. Mineral. Petrol. 72, 111-122.

Miller, W.J., 1912; The garnet deposits of Warren County, New York. Econ. Geol. 7, 493-501.

_____, 1938; Genesis of certain Adirondack garnet deposits. Am. Mineral. 23, 399-408.

Novillo, M.M., 1981; Petrological Evolution of the Ruby Mountain Garnetiferous Gneiss, Southeastern Adirondack Mountains, New York. Unpublished M.S. thesis, Lehigh University.

Rast, N., 1965; Nucleation and growth of metamorphic minerals. In: Controls of Metamorphism, W. Pitcher and G. Flinn, eds., Oliver and Boyd, Edinburgh, 73-102.

Raheim, A. and Green, D.H., 1974; Experimental determination of the temperature and pressure dependence of the Fe-Mg partition coefficient for coexisting garnet and clinopyroxene. Contrib. Mineral. Petrol. 48, 179-203.

Reitmeijer, F.J.M., 1983; Chemical distinction between igneous and metamorphic orthopyroxenes those co-existing with Ca-rich clinopyroxenes: a re-evaluation. Mineral. Mag. 47, 143-151.

Robinson, P., Spear, F.S., Schumacher, J.C., Laird, J., Klein, C., Evans, B.W. and Doolan, B.L., 1982; Phase relations of metamorphic amphiboles: natural occurrence and theory. In: Amphiboles: Petrology and Experimental Phase Relations, D.R. Veblen and P.H. Ribbe, eds., Mineral. Soc. Am. Reviews in Mineralogy, 9b, 1-228.

Silver,L.T., 1969; A geochronologic investigation of the Adirondack Complex, Adirondack Mountains, New York. In Origin of Anorthosite and related Rocks, Y. Isachsen, ed. N.Y. State Mus. and Sci. Serv. Mem. 18, 233-252.

Spry, A., 1969; Metamorphic Textures, Pergamon Press, New York.

Turner, F.J., 1981; Metamorphic Petrology, Mineralological, Field, and Tectonic Aspects, 2nd ed., McGraw-Hill, New York.

Wager, L.R. and Brown, G.M., 1967; Layered Igneous Rocks, Freeman, San Francisco.

Walton, M. and DeWaard, D., 1967; Precambrian geology of the Adirondack Highlands, a reinterpretation, Geol. Rundshau 56, 596-629.

Whitney, P.R. and McLelland, J.M., 1973; Origin of coronas in metagabbros of the Adirondack Mountains, New York. Contrib. Mineral. Petrol. 39, 81-98.

_____, 1983; Origin of biotite-hornblende-garnet coronas between oxides and plagioclase in olivine metagabbros, Adirondack region, New York. Contrib. Mineral. Petrol. 82, 34-41.

Winkler, H.G.F., 1979; Petrogenesis of Metamorphic Rocks. 5th ed. Springer Verlag, New York.

Appendices

Additional Microprobe Data Not Included in Previous Tables

Pyroxenes, Ruby Mountain

	RM1-2	RM1-3	RM1-4	RM1-5	RM29-2	RM29-3	RM13-2
SiO_2	50.38	49.34	50.16	50.32	50.78	50.84	49.91
TiO_2	0.23	0.24	0.11	0.24	0.33	0.21	0.00
Al_2O_3	2.22	2.31	2.10	1.76	1.94	2.29	2.36
FeO	13.41	15.54	13.16	13.28	13.07	12.81	24.93
MnO	0.00	0.00	0.00	0.00	0.00	0.00	0.00
MgO	11.84	11.66	11.58	11.63	12.34	11.96	19.88
CaO	19.60	18.79	19.80	20.29	19.96	19.94	1.42
Na_2O	1.05	0.91	1.09	0.85	0.96	1.11	0.06
K_2O	0.00	0.00	0.00	0.00	0.00	0.00	0.00
total	98.72	98.79	98.00	98.37	99.38	98.96	98.56

	RM24-2	RM24-3	RM7-3	RM7-4	RM7-5	RM13-4
SiO_2	50.76	50.68	50.01	50.29	50.27	50.31
TiO_2	0.17	0.33	0.54	0.33	0.30	0.14
Al_2O_3	2.48	2.87	3.26	2.57	2.51	1.77
FeO	10.70	10.94	12.56	13.37	13.03	26.70
MnO	0.00	0.00	0.00	0.00	0.00	0.00
MgO	14.04	12.99	11.54	11.75	11.91	19.70
CaO	19.12	19.69	19.49	19.76	18.69	0.34
Na_2O	1.35	1.26	1.43	1.37	1.48	0.04
K_2O	0.00	0.00	0.00	0.00	0.00	0.00
total	98.62	98.77	98.83	99.44	98.19	99.00

(Appendices, Continued)

Number of Cations per 6 Oxygens

Si	1.938	1.915	1.944	1.946	1.938	1.945	1.918
Ti	.006	.006	.003	.006	.009	.006	0.0
Al	.100	.105	.095	.080	.087	.103	.107
Fe	.431	.504	.426	.429	.417	.409	.801
Mg	.679	.675	.669	.670	.702	.682	1.139
Ca	.808	.781	.822	.840	.816	.809	.058
Na	.078	.068	.081	.063	.070	.082	.004

Si	1.929	1.927	1.916	1.924	1.939
Ti	.005	.009	.015	.009	.008
Al	.111	.128	.147	.115	.114
Fe	.304	.347	.402	.427	.420
Mg	.795	.736	.659	.670	.684
Ca	.778	.802	.800	.809	.772
Na	.099	.092	.106	.101	.110

(Appendices, Continued)
Hornblendes, Ruby Mountain Metagabbro

	RM13-1	Rm13-2	RM13-3	RM1-4	RM1-5	RM1-7	RM13-8
SiO_2	40.99	40.83	40.91	41.02	41.24	41.68	41.22
TiO_2	2.23	2.11	2.03	2.77	2.74	2.63	2.22
Al_2O_3	13.38	13.55	14.02	12.38	12.83	12.86	13.53
FeO	16.57	16.50	15.96	20.65	19.37	19.28	16.08
MnO	0.00	0.00	0.00	0.00	0.00	0.00	0.00
MgO	10.10	9.75	10.52	8.89	8.99	9.05	10.29
CaO	11.01	11.52	11.29	11.43	10.78	10.84	11.14
Na_2O	1.88	1.93	1.93	1.73	1.64	1.63	1.91
K_2O	1.41	1.31	1.40	1.63	1.73	1.69	1.38
total	97.56	97.48	98.06	100.52	99.33	99.57	97.78

	RM13-13	RM1-16	RM1-17	RM1-18	RM1-19
SiO_2	40.84	41.24	40.36	39.87	40.46
TiO_2	2.15	2.23	2.01	2.26	2.31
Al_2O_3	13.93	13.86	12.23	12.25	12.87
FeO	15.64	16.42	22.00	21.76	21.83
MnO	0.00	0.00	0.00	0.00	0.00
MgO	10.56	9.92	8.70	8.54	8.09
CaO	11.16	11.27	10.71	10.67	10.58
Na_2O	1.91	1.90	1.50	1.67	1.62
K_2O	1.31	1.38	1.64	1.59	1.66
total	97.50	98.22	99.15	98.61	99.43

(Appendices, Continued)
Number of Cations per 23 Oxygens

Si		6.101	6.121	6.042	6.044	6.090	6.132	6.115
Ti		.249	.237	.226	.304	.309	.291	.248
Al		2.346	2.394	2.440	2.150	2.233	2.230	2.365
Fe	3+	.572	.339	.577	.673	.696	.652	.501
Fe	2+	1.489	1.729	1.393	1.871	1.695	1.707	1.493
Mg		2.241	2.178	2.316	1.952	1.980	1.986	2.275
Ca		1.779	1.865	1.865	1.834	1.735	1.736	1.792
Na		.550	.566	.561	.503	.478	.473	.557
K		.271	.251	.266	.311	.332	.323	.263

Si		6.054	6.107	5.986	5.962	5.998
Ti		.239	.248	.223	.253	.257
Al		2.433	2.419	2.138	2.159	2.249
Fe	3+	.576	.440	1.026	1.089	.996
Fe	2+	1.362	1.593	1.703	1.632	1.709
Mg		2.333	2.190	1.923	1.903	1.788
Ca		1.797	1.808	1.751	1.754	1.721
Na		.556	.550	.444	.497	.558
K		.251	.262	.319	.563	.322

(Appendices, Continued)
Garnets, Ruby Mountain Metagabbro

RM1

SiO_2	35.52	34.67	35.86	36.14	36.77
Al_2O_3	20.85	20.52	21.51	21.55	21.51
FeO	29.61	29.20	28.27	28.72	29.40
MnO	1.93	1.94	1.82	1.68	1.84
MgO	3.19	3.26	3.26	3.29	3.31
CaO	8.91	9.23	9.37	9.46	8.87
total	100.00	98.81	100.09	100.84	101.70

Number of cations per 12 Oxygens

Si	2.868	2.841	2.871	2.874	2.900
Al	1.984	1.982	2.030	2.020	1.998
Fe	1.999	2.000	1.893	1.910	1.939
Mn	.131	.134	.123	.113	.123
Mg	.383	.397	.389	.390	.388
Ca	.770	.810	.803	.806	.749

SiO_2	37.54	38.56	38.22	38.72	37.95	37.92	38.52
Al_2O_3	21.92	21.71	22.07	21.89	22.16	21.93	21.90
FeO	25.35	24.36	24.41	24.84	25.19	24.49	23.81
MnO	1.65	1.25	1.14	1.15	1.11	1.16	1.21
MgO	5.59	6.58	6.38	6.33	6.51	6.40	6.31
CaO	7.81	8.15	8.19	8.28	8.43	8.05	8.35
total	99.87	100.60	100.40	101.21	101.34	99.94	100.11

SiO_2	37.80	38.25	38.21
Al_2O_3	21.96	21.85	22.10
FeO	25.14	24.17	25.13
MnO	1.50	1.30	1.43
MgO	5.84	6.20	6.12
CaO	8.23	8.48	7.99
total	100.46	100.23	100.97

Number of Cations per 12 Oxygens

Si	2.941	2.976	2.956	2.974	2.922	2.950	2.981
Al	2.024	1.974	2.012	1.981	2.010	2.010	1.997
Fe	1.661	1.572	1.579	1.596	1.622	1.593	1.540
Mn	.109	.081	.074	.074	.072	.076	.079
Mg	.652	.756	.735	.725	.747	.742	.728
Ca	.655	.674	.678	.681	.695	.670	.692

Si	2.940	2.965	2.950
Al	2.013	1.996	2.011
Fe	1.635	1.567	1.622
Mn	.099	.085	.093
Mg	.677	.716	.704
Ca	.685	.704	.660

(Appendices, Continued)

	RM11a	RM11-1	RM29a				
SiO_2	36.81	36.35	37.34	37.14	37.49	37.27	37.50
Al_2O_3	21.45	20.54	21.79	22.03	21.38	21.84	21.44
FeO	28.60	28.60	28.47	29.25	29.39	29.36	29.01
MnO	3.31	3.01	1.73	1.69	1.75	1.81	1.67
MgO	2.50	2.56	3.17	2.55	2.98	3.04	3.10
CaO	8.81	8.28	8.38	8.74	8.53	8.62	8.57
total	101.48	99.34	100.88	101.41	101.52	101.95	101.30

Number of Cations per 12 Oxygens

Si	2.916	2.944	2.944	2.926	2.951	2.923	2.953
Al	2.003	1.960	2.024	2.046	1.983	2.018	1.989
Fe	1.895	1.936	1.877	1.927	1.934	1.925	1.909
Mn	.221	.206	.115	.113	.116	.120	.111
Mg	.295	.309	.372	.299	.350	.356	.364
Ca	.748	.718	.707	.737	.719	.724	.723

(Appendices, Continued)

Microprbe Analyses of Pyroxenes, Speculator Metagabbro

	S28-2	S38-2	S38-4	S38-5	S38-6	S38-7	S38-9
SiO_2	52.50	52.80	53.23	52.77	52.48	52.80	53.21
TiO_2	0.35	0.13	0.10	0.13	0.04	0.44	0.13
Al_2O_3	3.64	2.64	1.21	1.45	1.45	3.27	1.75
FeO	5.16	9.32	26.14	25.94	27.28	9.36	10.56
MnO	0.00	0.00	0.00	0.00	0.00	0.00	0.00
MgO	14.43	13.14	20.11	20.18	19.46	12.66	12.78
CaO	23.47	22.78	0.00	0.00	0.49	22.11	22.23
Na_2O	1.08	1.01	0.00	0.18	0.00	0.86	1.08
K_2O	0.00	0.00	0.00	0.00	0.00	0.00	0.00
total	100.63	101.83	100.78	100.65	101.20	101.50	101.74

	S42-1	S42-2	S42-3	S42-6	S42-7	S42-8	S42-9
SiO_2	51.99	52.27	50.68	50.56	51.40	51.65	52.62
TiO_2	0.10	0.40	0.13	0.49	0.48	0.47	0.16
Al_2O_3	1.27	2.69	2.08	3.65	3.59	3.50	1.64
FeO	28.00	10.95	29.88	10.53	10.86	10.78	10.47
MnO	0.00	0.00	0.00	0.00	0.00	0.00	0.00
MgO	18.85	12.42	15.94	12.04	12.26	12.25	12.49
CaO	0.46	21.05	2.31	20.86	21.15	21.63	21.52
Na_2O	0.00	0.94	0.88	1.21	1.19	1.11	0.90
K_2O	0.00	0.00	0.00	0.00	0.00	0.00	0.00
total	100.66	100.71	101.88	99.35	100.93	101.38	99.81

(Appendices, Continued)

	S42-12	S42-13	S42-14	S28-3	S28-4	S28-5	S28-6
SiO_2	51.05	51.14	51.66	50.09	51.42	50.40	52.12
TiO_2	0.49	0.79	0.48	0.76	0.68	0.50	0.39
Al_2O_3	2.66	3.39	3.71	5.67	4.69	5.23	4.42
FeO	12.99	10.45	10.37	5.63	5.67	5.26	5.51
MnO	0.00	0.00	0.00	0.00	0.00	0.00	0.00
MgO	13.13	12.29	12.41	14.82	15.25	14.15	15.39
CaO	19.91	22.26	21.76	22.58	22.86	22.99	22.09
Na_2O	1.00	1.18	1.15	0.65	0.76	0.48	0.57
K_2O	0.00	0.00	0.00	0.00	0.00	0.00	0.00
total	101.22	101.49	101.55	100.20	101.33	99.01	100.49

	S28-7	S28-8	S28-9	S28-10	S56-1	S56-2	S56-3
SiO_2	51.22	51.45	50.02	50.08	50.77	51.72	51.50
TiO_2	0.86	0.47	0.69	0.50	0.22	0.37	0.16
Al_2O_3	5.75	4.51	6.43	5.32	5.97	5.51	5.34
FeO	5.44	5.88	6.15	5.86	7.10	6.87	5.32
MnO	0.00	0.00	0.00	0.00	0.00	0.00	0.00
MgO	15.64	14.88	14.56	14.88	13.47	14.32	14.42
CaO	22.48	22.76	21.62	21.93	21.81	21.50	23.33
Na_2O	0.46	0.53	0.62	0.52	1.09	1.47	1.21
K_2O	0.00	0.00	0.00	0.00	0.00	0.00	0.00
total	101.86	100.48	100.09	99.10	100.43	101.76	101.40

(Appendices, Continued)

	S23-2	S10-2	S10-5	S10-6	S23-3
SiO_2	50.81	52.08	52.60	51.35	51.35
TiO_2	0.24	0.19	0.46	0.47	0.00
Al_2O_3	0.96	2.47	3.25	3.52	0.98
FeO	30.55	10.73	10.12	11.62	31.37
MnO	0.00	0.02	0.04	0.04	0.18
MgO	16.72	13.14	12.27	11.46	16.51
CaO	0.54	21.00	21.92	20.63	0.51
Na_2O	0.24	1.02	0.94	1.04	0.00
K_2O	0.00	0.00	0.00	0.00	0.00
total	100.06	100.66	101.60	100.12	100.89

(Appendices, Continued)
Number of Cations per 12 Oxygens

	S28-2	S38-2	S38-4	S38-5	S38-6	S38-7	S38-9
Si	1.921	1.940	1.988	1.975	1.968	1.940	1.965
Ti	.009	.003	.002	.003	.001	.012	.003
Al	.156	.114	.053	.064	.064	.141	.076
Fe	.157	.286	.816	.812	.855	.287	.326
Mg	.787	.720	1.120	1.126	1.088	.693	.703
Ca	.920	.897	0.0	0.0	.019	.870	.879
Na	.076	.071	0.0	0.0	0.0	.061	.077

	S42-1	S42-2	S42-3	S42-6	S42-7	S42-8	S42-9
Si	1.969	1.947	1.933	1.912	1.915	1.916	1.977
Ti	.002	.011	.003	.013	.013	.013	.004
Al	.056	.117	.093	.162	.157	.153	.072
Fe	.886	.341	.953	.333	.338	.334	.329
Mg	1.064	.689	.906	.678	.681	.677	.699
Ca	.018	.840	.094	.845	.844	.859	.866
Na	0.0	.067	.064	.089	.086	.079	.065

	S42-12	S42-13	S42-14	S28-3	S28-4	S28-5	S28-6
Si	1.911	1.899	1.910	1.844	1.871	1.873	1.901
Ti	.013	.022	.013	.020	.018	.014	.010
Al	.117	.148	.161	.246	.201	.229	.190
Fe	.406	.324	.320	.173	.172	.163	.168
Mg	.732	.680	.684	.813	.827	.784	.837
Ca	.798	.885	.862	.890	.891	.915	.863
Na	.072	.085	.082	.046	.053	.034	.040

(Appendices, Continued)

	S28-7	S28-8	S28-9	S28-10	S56-1	S56-2	S56-3
Si	1.847	1.887	1.840	1.861	1.870	1.877	1.873
Ti	.023	.013	.017	.014	.006	.010	.004
Al	.244	.194	.278	.233	.259	.235	.229
Fe	.164	.180	.189	.182	.218	.208	.161
Mg	.841	.813	.799	.824	.739	.774	.787
Ca	.869	.894	.852	.873	.860	.836	.909
Na	.032	.037	.049	.037	.077	.103	.085

	S23-2	S10-2	S10-5	S10-6	S23-3
Si	1.967	1.942	1.938	1.930	1.975
Ti	.006	.005	.012	.013	0.0
Al	.043	.108	.141	.155	.044
Fe	.989	.334	.311	.365	1.008
Mg	.965	.730	.674	.642	.947
Ca	.022	.839	.865	.831	.020
Na	.017	.073	.075	.075	0.0

(Appendices, Continued)

Microprobe Analyses of Garnet, Speculator Metagabbro

S10

SiO_2	38.74	37.48	38.22	38.21	38.01	38.58	38.70
Al_2O_3	22.23	22.47	22.84	22.39	22.48	22.16	22.19
FeO	27.27	24.01	25.66	26.13	25.57	25.74	25.68
MnO	0.86	0.79	0.84	0.78	0.75	0.32	0.89
MgO	4.90	5.01	5.52	5.90	5.52	5.55	5.44
CaO	7.39	11.82	8.53	8.47	8.73	9.01	8.83
total	101.38	101.59	101.61	101.89	101.06	101.36	101.73

Number of Cations per 12 Oxygens

Si	2.988	2.891	2.932	2.931	2.935	2.966	2.968
Al	2.021	2.043	2.066	2.042	2.046	2.008	2.006
Fe	1.759	1.548	1.646	1.676	1.651	1.655	1.647
Mn	.055	.051	.054	.050	.049	.0211	.057
Mg	.564	.575	.631	.675	.636	.635	.622
Ca	.611	.976	.701	.696	.722	.742	.725

(Appendices, Continued)

	S42b			S38			
SiO_2	37.40	38.46	38.26	37.81	38.05	39.27	38.95
Al_2O_3	22.14	22.14	22.05	22.15	22.42	22.45	22.18
FeO	28.05	27.12	27.38	28.23	28.00	26.69	26.75
MnO	0.96	0.85	0.85	0.98	1.02	0.82	0.76
MgO	4.41	4.44	4.73	4.21	4.15	4.78	4.98
CaO	8.56	8.16	7.86	7.80	8.16	7.77	7.95
total	101.41	101.16	101.14	101.17	101.81	101.79	101.57

Number of Cations per 12 Oxygens

	S42b			S38			
Si	2.911	2.980	2.969	2.949	2.946	3.007	2.994
Al	2.036	2.022	2.016	2.035	2.046	2.025	2.010
Fe	1.830	1.757	1.777	1.841	1.813	1.709	1.719
Mn	.063	.055	.056	.064	.067	.053	.049
Mg	.512	.512	.547	.489	.479	.546	.570
Ca	.715	.677	.653	.651	.677	.637	.654

(Appendices, Continued)
Sample descriptions

RM refers to Ruby Mountain metagabbro, S refers to Speculator metagabbro. First number is the sample number, as shown on the sample location maps (except for Ruby Mountain hornblendes, where the first number is the number identifying the analyses), the second number is the identification number of the analyses.

Pyroxene Sample Locations, Ruby Mountain Metagabbro

RM1-2, 3, 4, 5 Large inequant clinopyroxenes containing inclusions of hornblende, from a thin section with a large amount of biotite, lower part of main metagabbro.

RM7-3 Twinned clinopyroxene partly surrounded by hornblende, main metagabbro.

RM7-4, 5 Equant untwinned clinopyroxene, same thin section asRM7-3.

RM13-2, 4 Equant xenoblastic orthopyroxenes from garnet hornblendite layer, near a large garnet porphyroblast, center of main metagabbro.

RM24-2, 3 Inequant clinopyroxenes rimmed by hornblende, upper part of main metagabbro.

RM29-2, 3 Clinopyroxenes from plagioclase-clinopyroxene symplectite, main metagabbro. Thin section contains abundant biotite.

Hornblende Sample Locations, Ruby Mountain Metagabbro

RM-1, 2, 3 Hornblendes from garnet hornblendite near large garnet porphyroblast, center of main metagabbro. Same thin section as pyroxenes RM13-2, 4.

RM-4, 5, 7 Hornblendes adjacent to clinopyroxenes, lower part of main metagabbro layer.

RM-16 Hornblende from same garnet hornblendite layer, not associated with garnet porphyroblast, center of main metagabbro.

RM-17, 18, 19, 20 Discrete Hornblende grains adjacent to clinopyroxenes which contain hornblende inclusions.

(Appendices, Continued)
Garnet Sample Locations, Ruby Mountain Metagabbro

RM1 Small garnet, .1 cm in diameter, located within an antiperthitic plagioclase, lower part of main metagabbro.

RM-11 Small garnet, .16 cm in diameter, from a mafic foliation band, containing inclusions of clinopyroxene and hornblende.

RM11a Small garnet, .14 cm in diameter, surrounded by plagioclase, lower part of main metagabbro.

RM29a Small garnet, .6 cm in diameter, surrounded by plagioclase, center of main metagabbro.

RM51 Large garnet porphyroblast, 1.5 cm in diameter, from garnet hornblendite in upper metagabbro layer.

Pyroxene Sample Locations, Speculator Metagabbro

S10-2 Equant pyroxene from granular pyroxene rim around large inequant clinopyroxene, normal metagabbro south of large-garnet zone.

S10-5,6 Equant clinopyroxenes with embayed contacts where adjacent to garnet porphyroblast, normal metagabbro.

S23-2, 3 Orthopyroxenes from northern margin of metagabbro, occurring in a thin section containing no clinopyroxene and abundant green pleochroic hornblende, magnetite and ilmenite.

S28-1, 2 Large clinopyroxenes containing hornblende lamellae, large-garnet zone.

S28-3, 6, 9 Twinned clinopyroxenes, not associated with hornblende, large-garnet zone.

S28-4, 5, 7, 8 Twin lamellae from twinned clinopyroxenes, same thin section as S28-3, 6, 9, large-garnet zone.

S38-2 Inequant clinopyroxene, from thin section containing brown hornblende in normal metagabbro a few cm above a mafic layer.

S38-4, 5 Orthopyroxene fingers adjacent to hornblende, same thin section as S38-2, normal metagabbro.

S38-6 Inequant clinopyroxene adjacent to small garnet porphyroblast, same thin section as S38-2, normal metagabbro.

S38-7 Inequant clinopyroxene adjacent to hornblende, same thin section as S38-2, normal metagabbro.

S38-9 Equant, metamorphic clinopyroxene from a lensoid aggregate of clinopyroxene, from a hornblende-free part of same thin section as S38-2, normal metagabbro.

S42-1, 2 Inequant clinopyroxenes partly rimmed by hornblende, normal metagabbro.

S42-3, 13 Twinned clinopyroxenes, same thin section as S42-1, 2, normal metagabbro.

S42-6, 7, 8, 9, 14 Twin lamellae within clinopyroxenes, same thin section as S42-1, 2, normal metagabbro.

S42-12 Equant, metamorphic clinopyroxene from a granular rim around inequant clinopyroxene. Hornblende grain embays outer rim of this grain.

S56-1, 3 Twinned clinopyroxene occurring as a large embayed inclusion within garnet porphyroblast, large-garnet zone.

S56-2 Twin lamallae, same grain as S56-1, 2.

Garnet sample locations, Speculator Metagabbro

S10 Small porphyroblast, .6 cm in diameter, exhibiting embayed contacts with orthopyroxene, clinopyroxene, and plagioclase, normal metagabbro.

S38 Small, .12 cm diameter, inequant grain in mafic foliation band, associated with brown hornblende, normal metagabbro.

S42b Small, .16 cm diameter, inequant grain containing embayed inclusions of clinopyroxene and hornblende.

Vita

John Herbert Weakliem was born on April 13, 1958, in Ithaca, NY to Mr. and Mrs. Herbert Weakliem. He graduated from Hopewell Valley Central High School in June, 1976. After working for a year in a plastics factory, he entered Allegheny College, Meadville, PA, in September, 1977. He graduated Cum Laude in June, 1981, with a B.S. in Geology, Geology Department Honors, and was co-holder of the Walter M. Small Prize for the best senior thesis in Geology. In August, 1981, he began his graduate career in the Department of Geological Sciences , Lehigh University. He held a University Fellowship from 1981 to 1982, and was a Teaching Assistant from 1982 to 1983. He recieved his Master of Science degree in Geology from Lehigh University in June, 1984. Mr. Weakliem is a member of the Mineralogical Society of America, the American Geophysical Union, and Sigma Xi.